Programa de Doctorado en Biociencias Moleculares

DESIGN OF ROBUST IMMOBILIZED Xys1Δ XYLANASE BIOCATALYSTS: PROCESS INTENSIFICATION FOR XOS PRODUCTION FROM LIGNOCELLULOSIC RESIDUES

María Romero Fernández

Madrid, 2018

Agradecimientos

En primer lugar me gustaría agradecer al Ministerío de Economía y Competitividad la ayuda financiera que ha hecho posible esta Tesis Doctoral, y a todas las instituciones que han ayudado a su desarrollo. A todo el personal del Instituto de Catálisis y Petroleoquímica, por todos los servicios prestados, especialmente al Servicio de Mantenimiento y al Servicio de Limpieza.

A mi director, José Manuel Guisán por esta oportunidad, por ayudarme, por su entusiasmo y su optimismo, y por demostrar que siempre hay lugar para la generosidad. A mi co-director, Javier Rocha, por su paciencia en el día a día, por enseñarme y ayudarme, por confirar en mí y por ser ejemplo continuo de auto-exigencia y superación. A mi tutora María Fernández Lobato por su inintermitente disponibilidad, su ayuda y su trato cercano. A Blanca de las Rivas, y todo el grupo del Biotecnología Bacteriana, por enseñarme, por ayudarme y haberme hecho sentir una más.

A mis compañeros Lara, Sonia, Alejandro, Sandro, Janaina, y también Chiara y Cristina, por toda vuestra ayuda, por aguantarme y hacerme aprender, por todos los momentos compartidos y los kilómetros recorridos, por abrirme las puertas de otros lugares, y de vuestras casas.

A mis amigos, por estar siempre ahí, por escucharme y por tantas y tantas risas. Por demostrarme que no hay amistad que se suscriba al radio de ningún perímetro. Muy especialmente, a mis amigas Cristina, Mercedes y Ángela, por vuestra inestimable ayuda, vuestra empatía y vuestra generosisdad. Por haberme ayudado a mejorar, y por tener siempre algo bueno que decir y una sonrisa que ofrecer.

A mi más antigua compañera, mi hermana, por su incalculable capacidad de animar, de agradar y ayudar. A mi abuela, por ayudarme y por ofrecerme siempre una palabra amiga. A Teresa, por su ayuda constante y por demostrar que una sonrisa puede más que cualqueir situación. A mis padres, por enseñarme y animarme a hacer lo que me gusta, a no rendirme nunca, y a no aceptar un “no” por respuesta; por ayudarme siempre, y habérmelo dado todo. A Carlos, por ser único, por su apoyo, su energía y hacer que cualquier día sea mejor.

Resumen

Los xilo-oligosacáridos han sido clasificados como prebióticos por sus efectos beneficiosos sobre la salud humana. La xilanasa Xys1Δ de *Streptomyces halstedii* JM8 fue inmovilizada en glioxil-agarosa mediante unión covalente multipuntual. El biocatalizador de Xys1Δ resultante presentó un incremento de termo-estabilidad de 62 veces con respecto a la enzima soluble, y se utilizó para catalizar la reacción de hidrólisis del xilano para la producción de XOS. Con el fin de incrementar su termo-estabilidad, se desarrolló una estrategia basada en el recubrimiento de la superficie del mismo con capas de polímeros. La modificación óptima consistía en una bicapa formada por una capa de polímero derivado de dextrano y otra de polímero polietilenimina. El biocatalizador óptimo resultante era 550 veces más estable que la enzima soluble (a pH 7 y 70 ºC). Con este biocatalizador se realizó la reacción de hidrólisis de xilanos de diferente procedencia para la producción de XOS, en modo discontinuo. El rendimiento total de reacción de hidrólisis de xilano de haya, trigo y maíz fue del 93% en 4 h; 44% en 5 h; y del 100% en 1 h, respectivamente. A estos tiempos, la conversión de estos tres xilanos en XOS fue del 65 %; 31% y 76%, respectivamente. Este biocatalizador fue reutilizado durante 15 ciclos de reacción de hidrólisis del xilano de haya sin verse comprometida su actividad catalítica.

Con el objetivo de incrementar de nuevo la estabilidad del biocatalizador de Xys1Δ inmovilizado, se desarrolló una estrategia basada en la intensificación de la rigidificación del área de superficie de la enzima implicada en la unión covalente multipuntual. Para ello, se introdujeron 1 – 4 residuos de lisina por sustitución de residuos de arginina, con el fin de establecer 1 – 4 enlaces covalentes adicionales entre la enzima y el soporte. Estos enlaces, si se establecieron, no promovieron ningún incremento de termo-estabilidad debido probablemente a que esto no supuso un aumento extra de la rigidificación de esta área de superficie.

La reacción de hidrólisis del xilano de maíz para producir XOS en flujo continuo se desarrolló con un reactor empaquetado de lecho fijo. Para ello, la xilanasa Xys1Δ fue inmovilizada por unión covalente multipuntual sobre soportes basados en polímeros de metacrilato, funcionalizados con grupos glioxil, con el objetivo de evitar pérdida enzimática y permitir mayores flujos, ya que estos soportes presentan mejores propiedades mecánicas. El soporte óptimo presentó un valor de área BET de 69,5 m^2/g y una distribución de tamaño de poro estrecha (tamaño de diámetro de poro de 80 nm). El biocatalizador de Xys1Δ inmovilizado sobre este soporte mostró una capacidad máxima de carga proteica de 20 mg/g, y un grado de termo-estabilidad elevado. Con este biocatalizador se catalizó la reacción en continuo de hidrólisis de este xilano a diferentes flujos. El mayor valor de productividad específica para XOS, 3.277 $g_{XOS}\ g_{enzyme}^{-1}\ h^{-1}$, con mínima producción de xilosa, se obtuvo a 10 mL/min.

Abstract

Xylo-oligosaccharides (XOS) have been described as prebiotics and display beneficial effects upon human health. The xylanase Xys1Δ, from *Streptomyces halstedii* JM8, was immobilized on glyoxyl-agarose beads by multipoint covalent attachment. The resulting immobilized Xys1Δ biocatalyst was 62-fold more thermo-stable than its soluble counterpart, and was used to catalyse the hydrolysis reaction of xylan for XOS production. A strategy based on surface coating with layers of polymers was developed to further increase the thermo-stability of this biocatalyst. The optimal modification consisted of surface coating with a bilayer formed by a layer of derived dextran polymer and a layer of polyethylenimine. The optimised biocatalyst was 550-fold more stable than the soluble Xys1Δ enzyme (at 70 ºC, pH 7). This optimised biocatalyst was used for production of xylo-oligosaccharides from soluble xylans of various sources in batch mode. Total reaction yields for beechwood, wheat and corncob xylan were 93% in 4 h, 44% in 5 h and 100% in 1 h, respectively. At these time points, xylan conversion yields to XOS were 65 % for beechwood xylan; 31% for wheat arabinoxylan; and 76% for corncob xylan. The optimised biocatalyst was reused for 15 reaction cycles of beechwood xylan hydrolysis without affecting its catalytic activity.

To further increase the thermo-stability of the immobilized Xys1Δ biocatalyst, a strategy based on intensification of rigidification of the enzyme surface region involved in multipoint covalent attachment was developed. For this purpose, 1 – 4 additional lysine residues were introduced by substitution of native arginine residues to form 1 – 4 additional covalent bonds between enzyme and immobilization support. These covalent bonds, if formed, did not promote increased thermo-stabilizing effects, as they did not probably provide more intense rigidification of this enzyme surface area.

Continuous flow reaction of corncob xylan hydrolysis for XOS production has been developed with an optimised packed-bed reactor (PBR). For this purpose, the xylanase Xys1Δ was immobilized by multipoint covalent immobilization on supports consisting of methacrylic polymer matrices previously functionalized with glyoxyl groups. The aim was to avoid enzyme leaching and to allow high flow rates since these supports display enhanced mechanical properties. The optimal support presented an area BET value of 69.5 m^2/g and a narrow pore-size distribution (80 nm pore size diameter). The resulting immobilized Xys1Δ biocatalyst onto this support displayed a maximum protein loading of 20 mg/g support, and high thermo-stability. A PBR was developed with this biocatalyst and used for continuous xylan hydrolysis at different flow rates. The specific volumetric productivity for XOS, 3,277 $g_{XOS}\ g_{enzyme}^{-1}\ h^{-1}$, was achieved at 10 mL/min flow rate with minimum production of xylose.

Index

Abbreviations

XOS: xylo-oligosaccharides

Xys1Δ: recombinant xylanase from *Streptomyces halstedii* JM8 which has been modified at its carboxy terminus with a hexa-His tag

DNS: dinitrosalicylic acid

PEG6000: 6000 Da polyethylene glycol

PEI: polyethylenimine

Ag-CB: agarose activate activated with cyanogen bromide groups

Ag-G: agarose highly activated with glyoxyl groups

Dex100: dextran (40 KDa) oxidised up to 100%

Dex20: 40 KDa (40 KDa) dextran oxidised up to 20%

Dex20-80: dextran (40 KDa) polymer oxidised and then reduced to 80%, and finally oxidised up to 20%

MIP: Mercury Intrusion Porosimetry

AI: Adsorption Isotherm

DP: Degrees of polymerization

1. Introduction

1.1. Introduction

In today´s world, everyone prefers naturally occurring bioactive molecules rather than modern therapeutic agents for their health and well-being. The mechanism of action of these bioactive molecules is based on the principle "Prevention is better than cure", and so, they display their benefits by enhancing quality of human life. Moreover, following this principle, consumers also prefer foods with additional attributes along with routine nutritional qualities (Samanta et al., 2015). The term "Functional food" was first used in Japan, in the 1980s, for food products containing special constituents that have advantageous physiological effects. Currently, functional foods can be considered as basic nutrition foods which have demonstrated physiological effects, and include food with natural bioactive molecules, derived food and bioactive molecules added to food as supplement e.g. probiotics, antioxidant, prebiotics, etc. (Singh et al., 2015).

Among all these biologically active compounds, prebiotics seem to be preferred as they show positive effects over human physiology: selective growth stimulation of beneficial gut microflora; enhanced mineral absorption; cholesterol lowering; immune modulation; antioxidant and anti-carcinogenic properties; etc. (Samanta et al., 2015).

1.2. Prebiotics

1.2.1. Definition

The concept of "prebiotic" came into light in the year 1995. They were defined as "Non-digestible food ingredients which beneficially affect the host by selectively stimulating the growth and/or activity of a limited number of bacteria in the colon" (Gibson and Roberfroid, 1995). Then, its definition passes through several steps of modifications from 1995 to the present. In 2007, the Food and Agricultural Organization (FAO) constituted a technical committee to revisit the definition of prebiotic: "A prebiotic is a non-viable food component that confers health benefit on the host associated with modulation of microbiota". Next attempts to qualify a prebiotic were made to broaden their sites of action such as skin, oral cavity and female genital tract (Pineiro et al., 2008). However, recently, the proposers of prebiotic concept wanted to restrict it again to gastrointestinal microflora: "A prebiotic is a selectively fermented

ingredient that results in specific changes in the composition and/or activity of gastrointestinal microbiota thus conferring benefit(s) upon host health" (Gibson et al., 2010). In line with this, the prebiotic concept is associated with selective stimulation of growth and activity of single or multiple gut microflora in order to demonstrate quantifiable health benefits following its consumption. However, apart from changes in the definition over time, an ideal prebiotic should follow these criteria (Samanta et al., 2015): selective fermentation by beneficial gut microflora (evident from in vitro or in vivo experiments); modulation of gut microflora homeostasis towards beneficial sides resulting into increase of population or metabolic activities; ensures host health and well-being (enhances productivity or product quality in animals); originated from plants or synthesized by microorganisms or their enzymes; maintain structural integrity while passing through different parts of the gastrointestinal tract; no residue problems; ideally to be used as food/feed additive; compatibility with other food/feed ingredients.

1.2.2. Benefits of prebiotics upon human health

Current research on prebiotics has demonstrated their potential as health promoters including gut health maintenance, colitis prevention, cancer inhibition, immune stimulation, cholesterol removal, reduction of cardiovascular disease, prevention of obesity and constipation, restoration of vaginal ecosystem and bacteriocin production (Samanta et al., 2015).

1.2.3. Types of prebiotics

Nowadays, the majority of prebiotics sold in the market are non-digestible oligosaccharides (Samanta et al., 2015). Fructooligosaccharides, inulin, lactulose and galatooligosaccharides are well established ones in Europe, Japan and United States. However, a wider range of emergent prebiotics exists including soyoligosaccharides, xilooligosaccharides (XOS), isomaltooligosaccharides, gentiooligosaccharides, lactosucrose, glucooligosaccharides and pecticoligosaccharides (Lam and Chi-Keung Cheung, 2013). In recent years, the use of XOS as prebiotics is gaining an increasing interest, since they influence many aspects of human health and potentially work against gastrointestinal disorders. However, their popularity is mainly due to the fact that they are sourced from lignocellulosic materials which compose agricultural crop residues. These residues are inexpensive, abundant and renewable in nature (Samanta et al., 2015), although, they are also found in fruits, vegetables, bamboo, honey and milk (Singh et al., 2015).

1.3. Xylo-oligosaccharides

1.3.1. Definition and physicochemical properties

According to IUP-IUPAC, oligosaccharides are defined as oligomers composed of 2-10 monosaccharide residues. They have low molecular weight carbohydrate residues and are classified into two groups: digestible and non-digestible. While the ones containing α-linkages are digestible by human enzymes, the others containing β-linkages located in anomeric carbons are non-digestible, and so, they are resistant to hydrolysis by human enzymes, except for some cases such as galactosides (e.g. lactose). Xylo-olygosaccharides are non-digestible oligosaccharides as they are oligomers of β-(1→4)-linked xylose units with various substituents including acetyl, phenolic, and uronic acid (Singh et al., 2015). They are available in market as a white powder and contain from 2 to 6 molecules of xylose: xylobiose (2 monomers), xylotriose (3 monomers), xylotetrose (4 monomers), xylopentose (5 monomers), and xylohexose (6 monomers) (Samanta et al., 2015). However, some other researchers consider molecules with higher number of xylose residues (≤20) as XOS (Singh et al., 2015). XOS are stable over a wide range of pH values (2.5 – 8.0), even at the relatively low gastric pH, and at temperatures up to 100ºC, which means an advantage compared with other prebiotics such as FOS and inulin (Lam and Chi-Keung Cheung, 2013). For this reason, XOS display a good thermal stability during pasteurization and autoclave sterilization procedures at low pH value as compared to FOS. Also, xylo-oligosaccharides containing from 3 to 5 xylose residues are more sensitive to alkaline decomposition in comparison to longer chain ones (Singh et al., 2015).

1.4. Xylo-oligosaccharides production

1.4.1. Source of XOS in nature

Xylo-oligosaccharides (XOS) are the hydrolysis product of xylan, which is available in abundance in nature as a major constituent of hemicellulose. The latter is a component of lignocellulosic biomass (Singh et al., 2015). Lignocellulosic materials are the most abundant organic residue in the world (Lam and Chi-Keung Cheung, 2013). Accounting only for sugar for ethanol production in Brazil, the production of sugar cane for the season 2012/13 was estimated to be 596.6 billion tons. At 135 kg of dried bagasse per ton of crushed cane, the total bagasse generated in this season was approximately 80.5 billion tons (Lam and Chi-Keung Cheung, 2013).

1.4.2. Composition of lignocellulosic biomass

Lignocellulosic biomass is composed of: cellulose, a linear polymer of (1→4)-linked β-glucose residues; hemicelluloses, a heteropolysaccharide comprising of pentose and hexose units; and lignin. Hemicellulose is the second most abundant polymer (25 – 35 %) after cellulose (45 – 55 %) in plant cell walls. This heteropolymer have β-(1→4)-linked backbone and include xyloglucans, xylans, mannans and glucomannans, and β-(1→3, 1→4)-glucans (Singh et al., 2015).

1.4.3. Composition of xylan

Xylan accounts for 25 - 35% of dried biomass of woody tissues of dicots and lignified tissues of monocots. Also, it comprises up to 50% in some grasses and tissues of cereal grains (Samanta et al., 2015). Most xylans are made up of a main backbone of β-(1→4)-linked xylose residues, and substituted with arabinofuranosyl, glucopyranosil and uronic acid derivatives, ferulic and coumaric acid, acetyl and phenolic acids which are either ether or ester substituted to the hydroxyl groups of xylose units (Lam and Chi-Keung Cheung, 2013, Singh et al., 2015). Depending on xylan source (plants and different tissues of the same plant,) it would vary its structure and composition (Singh et al., 2015).

XOS are reported to be found in fruits, vegetables, bamboo, honey and milk, but its concentration is too low to exhibit prebiotic effects (Samanta et al., 2015). Besides, tons of lignocellulosic biomass generated from post-harvest and processing activities of grains, fruits and vegetables, such as corn stover, sugarcane bagasse, rice and wheat straw, pomace, peel, etc., are discarded annually (Singh et al., 2015). This drives to a reduction in the nutritional value of food, as well as to an increment of residue generation with its associated costs, and so, becoming a major concern to farmers, industrialists, environmentalist and civil authorities (Samanta et al., 2015). For these reasons, it is required a smart mechanism to translate overproduced lignocellulosic biomass into value added products, such as XOS, for the subsequent improvement of both human and livestock health, and economic well-being.

1.4.4. Mechanisms of XOS production from lignocellulosic materials

Several agricultural residues or by-products have been analyzed to extract xylan by different mechanisms (Samanta et al., 2015) including autohydrolysis, chemical and enzymatic treatments, or a combination of them (Lam and Chi-Keung Cheung, 2013).

1.4.4.1. Autohydrolysis

The autohydrolysis treatment is carried out in the presence of water in specialized equipment where the mixture is exposed to a particular temperature and pressure. Xylan molecules are broken down into smaller ones, such as xylo-oligosaccharides, due to the catalytic depolymerisation caused by hydronium ions. These ions are derived from autoionization of water molecules and the further cleavage of acetyl groups to acetic acid (Samanta et al., 2015). In order to obtain XOS, the autohydrolysis treatment can be used alone or in combination with acid or enzymatic processes (Lam and Chi-Keung Cheung, 2013). This treatment leaves cellulose and lignin in the solid phase of the reaction mixture (Samanta et al., 2015). When autohydrolysis has been applied to XOS production, the maximum yield could be achieved under mild operating conditions (Lam and Chi-Keung Cheung, 2013). Increasing the severity factor is translated into decreased degree of polymerization and increasing decomposition of XOS into xylose (Samanta et al., 2015). For this reason, to obtain XOS with a degree of polymerization of 2 – 6 xylose units, the products released from this process must be exposed to extra treatment such as enzymatic or acid hydrolysis (Lam and Chi-Keung Cheung, 2013). Apart from extra processing, other disadvantages of this process in XOS generation are the requirement for specialized equipment and the production of undesirable components such as xylose, furfural, etc. (Lam and Chi-Keung Cheung, 2013).

1.4.4.2. Chemical treatment: acid hydrolysis

Chemical treatments for XOS production can be acid or alkali (Lam and Chi-Keung Cheung, 2013). Acid hydrolysis method can be used as a process to obtain XOS from lignocellulosic biomass or as pretreatment for xylan extraction from these materials to make it accessible to enzymatic treatment. The acid treatment itself to obtain XOS has been extensively reported (Lam and Chi-Keung Cheung, 2013). The effect of different acid concentrations (1.22% - 4.90% H_2SO_4) on XOS productions from xylan polymers contained in different plants was evaluated (Akpinar et al., 2009). The degree of XOS depolymerization increased with time and acid concentration, being 2.45% H_2SO_4 in 30 min of reaction time at 100ºC the best conditions for acid hydrolysis. However, even under these conditions, the XOS yield was low (7.5% - 13%). In another study (Otieno and Ahring, 2012), they obtained high yield of XOS production (64.9% - 92.2%) using a rapid thermo-acid process (0.1% H_2SO_4 at 145ºC for 1h). In this case, the content (19.7%) and the quality of XOS (70% of XOS ranging from 2 to 4 xylose units) were promising, along with the low content of xylose (5.9%). Although acid hydrolysis used as unique method for XOS production is simpler, the major problem is associated with the

generation of toxic components such as furfural and hydroxyl-methyl-furfural (Lam and Chi-Keung Cheung, 2013).

1.4.4.3. Chemical treatment: Alkali hydrolysis

On the contrary to acid hydrolysis, alkali hydrolysis method has only been reported as a pretreatment for xylan extraction and it is used in combination to an acid or enzymatic treatment to obtain XOS (Lam and Chi-Keung Cheung, 2013). A xylan extraction process was developed to evaluate both, type of alkali treatment and alkali concentration (Samanta et al., 2012). Xylan recovery was 12.5% and 63.2% for 2% and 12% NaOH, respectively; and 14.4% and 83.5% for 2% and 12% KOH, respectively. This shows an increased xylan recovery with higher alkali concentration. Xylan obtained by this method was used as substrate for XOS production by acid hydrolysis (0.25M sulfuric acid at 90ºC). XOS yields were 86.6%, 82.4% and 68.5% in 15, 30 and 60 min. Moreover, in another study, an alkali pretreatment was compared with an acid one to extract xylan and then, the hydrolysis product was evaluated for XOS generation by using a commercial xylanase (Aachary and Prapulla, 2009). Xylan extraction yields were similar (approximately 40%), although the best pretreatment was alkaline hydrolysis in terms of XOS yields. On the contrary, in another study, the XOS yield obtained from enzymatic hydrolysis using xylan extracted by alkali pretreatment was slightly lower than from acid hydrolysis pretreatment (Akpinar et al., 2010). However, the acid hydrolysis pretreatment has two of the major disadvantages, which are considerably high amounts of monosaccharides and formation of furfural (Lam and Chi-Keung Cheung, 2013).

1.4.4.4. Enzymatic treatment of pre-hydrolyzed lignocellulosic biomass

Basing on these results, the best method to obtain xylo-oligosaccharides from lignocellulosic materials seems to be the combination of an alkali chemical pretreatment to extract xylan from this residue and the subsequent enzymatic hydrolysis of the extracted xylan to produce XOS (Lam and Chi-Keung Cheung, 2013). Production of XOS by enzymatic means is carried out by xylanases hydrolysing β-(1→4) xylan bonds.

1.5. Xylanase enzymes

1.5.1. Enzymatic complexes degrading hemicellulose in nature

In nature, hemicellulose can be completely hydrolyzed by a pull of hemicellulase enzymes. These enzymes include xylanase (β-1,4-xylanase; E.C.3.2.1.8), β-xylosidase (β-1,4-xylosidase;

E.C.3.2.1.37), α-glucuronidase (α-glucuronidase; E.C.3.2.1.139), α-arabinofuranosidase (α-L-arabinofuranosidase; E.C.3.2.1.55) and acetylxylan esterase (E.C.3.2.1.1.72). Among them, xylanases and β-xylosidases are the two key enzymes responsible for the hydrolysis of xylan, the major component of hemicellulose. Xylanases act on the β-(1→4)-linked xylose homopolymeric backbone producing xylo-oligosaccharides, while β-xylosidases act on them releasing xylose. In order to produce XOS for the industry, the enzymatic complex used must have a low activity, or none activity at all, of β-xylosidases to avoid the production of xylose which not only inhibits XOS production, but also, is not desirable as xylose would have to be further eliminated. So, enzymatic hydrolysis of xylan is accomplished by xylanase (β-1,4-xylanase; E.C.3.2.1.8) (Juturu and Wu, 2012).

1.5.2. General characteristics and applications of xylanases

Xylanases are produced by many microorganisms including bacteria, marine algae, plants, protozoans, insects, snails and crustaceans. Most of microbial xylanases are extracellular since the large sized substrates cannot easily penetrate the cell wall. Apart from XOS production, these enzymes have wide applications in the industry. They are used for production of bulk chemicals, enzymatic treatment of animal feeds to release pentose sugars, bio-bleaching of wood pulps, as food additives in baking industry, ingredients in laundry detergents, or fabric care compositions (Anné et al., 2014).

1.5.3. Xylanase enzymes classification

Xylanases belong to glycoside hydrolases (GH) enzyme class and enzymes from this class are further classified into families (Juturu and Wu, 2012). At present, 130 glycoside hydrolases families exist under the CAZy database. Although xylanases are found in different GH families (5, 7, 8 10, 11, 16, 26, 30, 43, 52, 62), most of them are generally classified into two major families: 10 (F) and 11 (G) basing on primary and three dimensional structures (Anné et al., 2014).

1.5.3.1. Structure of xylanases belonging to family 10 glycoside hydrolases

Family 10 glycoside hydrolases consist of β-1,4-xylanases; β-1,3-xylanases (E.C.3.2.1.32) and cellobiohydrolases (E.C.3.2.1.91), the majority being β-1,4-xylanases (Anné et al., 2014). Family 10 β-1,4-xylanases are high molecular weight enzymes structurally composed of a cellulose-binding domain and a catalytic domain connected by a linker peptide (Juturu and Wu, 2012). Xylanases belonging to this family display a $(\beta/\alpha)_8$ fold TIM barrel structure (Juturu and

Wu, 2012). Two glutamate moieties have been reported to act as catalytic residues of the enzyme reaction which proceeds by a double displacement mechanism. GH10 xylanases are found to be less selective and so, able to attack several polysaccharides with different side chain modifications (Anné et al., 2014). In addition, these enzymes are highly specific for small xylo-oligosaccharides (Lam and Chi-Keung Cheung, 2013). Family 11 glycoside hydrolases are low molecular weight enzymes which have a β-jelly roll structure (Juturu and Wu, 2012). These enzymes are only active on substrates containing D-xylose and long chain xylo-oligosaccharides (Lam and Chi-Keung Cheung, 2013). So, they have low catalytic versatility (Lam and Chi-Keung Cheung, 2013). Xylo-oligosaccharides with more than 5 xylose units are more abundantly produced by family 11 xylanases (Techapun et al., 2003) (Lam and Chi-Keung Cheung, 2013).

Among all xylanase enzymes belonging to family 10, a xylanase enzyme from *Streptomyces halstedii* JM8 (Xys1Δ) has been selected for the present doctoral thesis to improve their catalytic properties in order to further optimise xylan hydrolysis reaction for xylo-oligosaccharides production. This bacteria, which was isolated from straw, secretes into the culture supernatant at least two proteins of 45 kDa (Xys1L) and 33 kDa (Xys1S), respectively, which show hydrolytic activity against xylan. Being both proteins encoded by the same gene, XYSA, the smaller form originates from the larger one by proteolytic cleavage at the C-terminus. The 3D structure of the *S. halstedii* xylanase catalytic domain devoid of the glycine-rich region (Xys1Δ) has been resolved (PDB code 1NQ6) (Díaz et al., 2004).

1.5.3.2. Molecular catalytic mechanism of xylanases belonging to family 10 glycoside hydrolases

Family 10 xylanases molecular architecture consists of an elliptical TIM-barrel scaffold, whose top is composed by loops arranged to form a long groove. This cleft is extended across the shorter diameter of the barrel and is lined by aromatic and hydrophilic residues. It is generally accepted to constitute the binding site for the substrate xylan polymer. A pair of acidic residues from disparate parts of the enzyme is found on opposite sides of this groove and acts as catalytic acid and base, respectively. One of these two catalytic residues is acting as a nucleophile and the other one as an acid-base catalyst (Schmidt et al., 1999).

For family 10 xylanase members, the map of xylose subunits binding sites within this binding site cleft, and the details of the interactions between these subunits and the xylanase enzyme, have been reported. These interactions will determine specific aspects of the enzyme function (e.g., endo or exo, minimum size of xylo-oligomer which can be cleaved, reactivity toward

branched substrates, etc.). In order to describe the mapping of xylose subunit binding sites, it is worth mentioning that according to the established convention, xylan monomers binding subsites are numbered negatively (-I, -II, etc.) from the cleavage site (i.e., the location of the two catalytic residues) toward the non-reducing end of the bound xylan molecule. Binding subsites in the opposite direction beyond the cleavage site will be denoted by positive roman capitals (+I, +II, etc.) (Schmidt et al., 1999).

Moreover, it is generally accepted that the substrate binding cleft is divided into two areas separated by the site of catalytic cleavage: an area consisting of subsites –I to –III, with strong and specific substrate interactions; and a section of the cleft consisting of subsites +I and +II, where substrate interactions seem to be much weaker and less specific. So, the former part of the binding cleft is referred to as "substrate recognition area", and the latter, as "product release area" (Schmidt et al., 1999).

In order to determine the mapping of xylose subunit binding sites around the catalytic center of the famility 10 xylanase from *Penicillium simplicissimum,* crystallographic substrate diffusion experiments with xylo-oligomer substrates of 1-5 xylose units were performed. They showed that xylose molecules bound to the binding site cleft at positions –II and –III, as well as a location intermediate between +I and +II. In contrast to all other compounds, the monomeric xylose did not form an hydrogen bond to the proton donor Glu132, due to the lack of occupancy of subsite –I. Both rings of the xylobiose molecule bind at subsites -I and -II, while the full xylotriose molecule occupies subsites -I to -III. In contrast, larger oligomers (xylotetraose and xylopentose) appear to have been cleaved between the third and the fourth sugar ring from the non-reducing end. For xylotetraose, three rings bind to subsites -I to -III, but the fourth ring is located after the cleavage site, detached from the other three rings, occupying a position intermediate between subsites +I and +II. Similarly, three rings of xylopentose bind to subsites –I to –III and the other two rings bind to +I and +II positions of the binding site cleft. According to catalytic results, the observed minimum substrate length is xylotetraose, and it is due to the stronger binding of the first 3-4 xylose units to subsites of the substrate recognition area as compared to the product release area (Schmidt et al., 1999).

In addition, crystallographic studies of the catalytic domain of another xylanase belonging to famility 10 $(\beta/\alpha)_8$ barrel folded xylanases, from *Thermoanaerobacterium saccharolyticum* JW/SL-YS485 (TsXylA), and the ligands-bound TsXylA complexes along with ligands-bound E146A and E251A mutants (catalytic residues mutants) were performed. Analysis from these studies showed the mapping of xylobiose, xylotriose and xylotetraose ligands in the substrate binding groove, and the interactions between xylose subunits and active site residues.

Xylobiose, xylotriose and xylotetraose were found to occupy subsites -II to -I, -III to -I, and -IV to -I, respectively. At the –IV subsite, xylose units sugars hang loosely, at the open end of the groove, while at -I, -II, and -III positions, monomers are tightly fixed deep in the tunnel (Han et al., 2013).

1.6. Optimization of enzymatic xylan hydrolysis for XOS production by biocatalyst engineering

The XOS production from xylan by enzymatic means is influenced by some critical parameters. The yield, productivity and type of oligosaccharide produced depend on several factors: the composition of xylan suspension which will be the substrate for enzymatic hydrolysis (substrate engineering); the reactor system to carry out the hydrolysis reaction and process conditions (reaction engineering) and specificity, activity and stability of the xylanase enzyme used as biocatalyst (biocatalyst engineering). Focusing on biocatalyst engineering, the output of XOS production processes depends not only on the type of xylanase but also depends on its microorganism source, the expression system used, its stability and activity displayed at different temperatures and pH values. In order to meet industrial requirements of yield, productivity and XOS polymerization degree for XOS production, some research has been developed: to find in nature xylanase enzyme variants displaying good stability and activity; to develop efficient protein expression systems which allow production of active xylanase enzyme and easy downstream processing; and to engineer xylanase enzyme variants or conjugants with enhanced thermostability and activity by different technologies, such as immobilization and post-immobilization methodologies (Techapun et al., 2003, Juturu and Wu, 2012, Lam and Chi-Keung Cheung, 2013, Anne et al., 2014).

1.6.1. Biocatalyst optimization by the selection of proper microorganism source and expression systems for heterologous xylanase production

Taking into account the microorganism source of xylanases, they are produced by a wide range of microorganisms including bacteria (*Bacillus* sp., *Streptomyces* sp., *Clostridium absonum*), fungi (*Aspergillus* sp., *Fusarium oxysporum*, *Thermoascus aurantiacus*, *Trichoderma reesei*) and yeast (*Thermomyces* sp.) (Techapun et al., 2003). Reasons to select a specific host are plentiful: development and running costs, yield, downstream processing requirements, time to market, necessity of correct glycosylation, and available infrastructure (Anné et al., 2014).

Among bacterial expression systems, *Escherichia coli* is an ideal platform for expressing recombinant proteins. This is due to multiple factors such as rapid growth, inexpensive media, simple techniques required for transformation, and easy purification of expressed proteins (Juturu and Wu, 2012). As an example, a xylanase from *A. niger* US368 has been expressed in *E. coli* and activated with copper (Elgharbi et al., 2015). *Streptomyces lividans* is another heterologous protein expression host which could provide a solution to some of the problems related to protein expression in *E. coli* (Anné et al., 2014). Bacteria belonging to the genus *Streptomyces* do not have an outer membrane, and so, proteins can be directly secreted into the culture medium. In addition, various *Streptomyces* efficiently secrete native proteins in high amounts. Concerning this, both the Sec-dependent and the twin-arginine translocation (tat) pathways have been demonstrated to be very useful. Among *Streptomyces* bacteria, *S. coelicolor* is the model organism for genetic and morphological analysis, but for cloning purposes, *S. lividans* is the host of choice. The reason behind is its low endogenous protease activity (Anné et al., 2014)

1.6.2. Biocatalyst optimization by engineering highly thermostable xylanase enzymes via immobilization and post-immobilization technologies

Thermal stability is a key factor for the efficient and economical use of enzymes as biocatalysts (Mateo et al., 2007b). The use of high temperatures in XOS production processes may be useful to increase reaction rates, to dissolve high concentrations of xylan and to prevent microbial contaminations. In recent years, many strategies have been proposed and evaluated to improve thermal stability of enzymes: search by new enzymes in thermophilic microorganisms, modification of enzyme structure by rational protein engineering, directed evolution methods, use of immobilization techniques and chemical modifications (Cabrera et al., 2010, Milessi et al., 2016).

1.6.2.1. Engineering highly thermostable xylanase enzymes by immobilization technology

On the one hand, the immobilization of an enzyme can increase its thermal stability by rigidification of enzyme structure (Martinek et al., 1977, Klibanov, 1983, Gianfreda and Scarfi, 1991, Gupta, 1991, Mateo et al., 2007b); or prevention of subunits dissociation in multimeric enzymes (Mateo et al., 2007b). In addition, it can improve some other properties such as activity (Yu et al., 2004, Mateo et al., 2007b, Palomo, 2008); specificity (Palomo et al., 2003, Mateo et al., 2007b); selectivity (Palomo et al., 2003, Yu et al., 2004, Chaubey et al., 2006, Mateo et al., 2007b, Palomo, 2008); or resistance to inhibitors (Mateo et al., 2007b, Rocha-Martin et al.,

2014). Moreover, enzyme immobilzation allows enzymes to be reused for several cycles, thus increasing reaction productivity (Mateo et al., 2007b).

Focusing on the application of immobilization technology to increase thermal stability of monomeric enzymes by rigidification of their structure, research has been developed for several decades with respect to xylanase immobilization. Some researchers have increased thermo-stability of xylanases from very different sources by immobilization onto a wide range of supports, and using an important variety of immobilization techniques, with the aim to meet industrial requirements within a broad spectrum of applications:

- Xylanases immobilization on commercially available supports

In the 1990's, two xylanase enzymes from *Aspergillus* sp. 5 and *Aspergillus* sp. 44, respectively were non-covalently immobilized on Eudragit S-100, retaining 70 and 80% of strain 5 and strain 44 xylanase activities, respectively. Due to immobilization, half-life at 60°C was improved from 15 to 30 min and 10 to 25 min of strain 5 and strain 44 xylanases, respectively (Gawande and Kamat, 1998). A 47 kDa xylanase (FXYN) from *Streptomyces olivaceoviridis* E-86 was also immobilized on Eudragit S-100 with 90% yield. The half-life of the enzyme at 60 ºC was prolonged from 39 to 64 min due to immobilization (Ai et al., 2005). In addition, a xylanase from *Bacillus pumilus* strain MK001 was immobilized on different matrices following different immobilization methods. Entrapment using gelatin (GE), physical adsorption on chitin (CH), ionic binding with Q-sepharose (Q-S), and covalent binding with HP-20 beads showed the maximum xylanase immobilization efficiencies (40%; 35%; 45% and 42%, respectively). The free xylanase retained 50.0% activity, whereas xylanase immobilized on HP-20, Q-S, CH, and GE retained 68.0, 64.0, 58.0, and 57.0% residual activity, respectively, after 3 h of incubation at 80.0 °C (Kapoor and Kuhad, 2007). *Penicillium occitanis* xylanase 2 was expressed with a His-tag in *Pichia pastoris* (PoXyn2) and then immobilized on nickel-chelate Eupergit C by covalent coupling reaction with a high immobilization yield (93.49 %). Immobilization increased thermo-stability when compared with the free enzyme too. The relative activity after 30 min incubation at 60ºC of immobilized PoXyn2 was 85 % while that of free PoXyn2 was only 15 % (Driss et al., 2014a).

- Xylanase immobilization on agarose-based supports

A xylanase from *Aspergillus niveus* was successfully expressed in *Aspergillus nidulans* (XAN). The thermal stability of this enzyme was extremely improved by covalent immobilization on glyoxyl-agarose with 91.4% of residual activity after 180 min at 60 ◦C, while the free xylanase showed a half-life of 9.9 min at the same temperature (Damásio et al., 2011). The commercial

xylanase NS50014 from Novozymes was also immobilized on glyoxyl-agarose, glutaraldehyde-agarose, and amino-epoxy-agarose supports, and on differently activated chitosan supports: glutaraldehyde-chitosan, glyoxyl-chitosan, and epoxy-chitosan. The best chitosan support was epoxy-chitosan, which allowed 100% immobilization yield and 64% recovered activity, but no significant increase in thermal stability was observed. Immobilization on glyoxyl-agarose showed low immobilization yield and stabilization degree due to the low concentration of lysine groups in the enzyme molecule. However, when protein was chemically modified with ethylenediamine before glyoxyl-agarose immobilization, this new enzyme were 40-fold more stable than free enzyme (Manrich et al., 2010). Similarly, a xylanase from *Aspergillus versicolor* was immobilized on agarose based supports activated with different groups: glyoxyl, PEI, MANAE, and glutaraldehyde. Anionic exchange supports, PEI-agarose and MANAE-agarose, displayed low yields (lower than 34%). After incubation at 60◦C, half-life values of free xylanase, xylanase immobilized on glutaraldehyde–agarose, and xylanase immobilized on glyoxyl–agarose, were 17 min, 25 min and 2h, respectively. Thus, glyoxyl-agarose immobilization allowed the highest stabilizing factor and preserved 85% of catalytic activity (Aragon et al., 2013b). Furthermore, XynA, a recombinant enzyme from *Bacillus subtilis*, was immobilized on three different supports activated with glyoxyl and glutaraldehyde groups. A great increase in the thermal stability of the enzyme at 56◦C was achieved with immobilization on glyoxyl activated supports: 75-fold for chitosan and 8600-fold for agarose (Milessi et al., 2016). Another xylanase, produced by *Aspergillus tamarii* Kita, was immobilized on CM-cellulose, glyoxyl-agarose and CNBr-agarose. The best support in terms of increased thermo-stability was considered to be glyoxyl-agarose. At 80◦C, the stability factor obtained for immobilization on glyoxyl-agarose was 7.6 compared to CNBr-agarose (Heinen et al., 2017).

- Xlanases immobilization on chitosan-based supports

Aspergillus niger xylanase A (XylA) was immobilized onto Fe_3O_4-coated chitosan magnetic nanoparticles prepared by the layer-by-layer self-assembly approach. Immobilization was achieved by covalent bonds formed between the aldehyde group of glutaraldehyde and the amino group of enzyme. The Fe_3O_4-coated chitosan magnetic nanoparticles showed a recovery activity of 56.5% and improved thermostability compared with free XylA. When treated at 70 °C and pH 6.0 for 4 min, the residual activities of immobilized and free XylA were 84.6% and 56.2%, respectively (Liu et al., 2014). Also, *Penicillium occitanis* xylanase 3 was expressed in *Pichia pastoris* (PoXyn3) and immobilized on chitosan activated with glutaraldehyde by covalent coupling reaction. The immobilization yield and the xylanase recovered activity were 98.8±2.5% and 94.45±3.5%, respectively. Immobilization increased thermo-stability when compared with the free enzyme. The relative activity after 30 min incubation at 80 ºC of

immobilized PoXyn3 was 85% while that of free PoXyn3 was only 15% (Driss et al., 2014b). Likewise, a bifunctional enzyme possessing xylanase and cellulose activity was constructed (ATXX) and covalently immobilized on a novel support based on carbon coated chitosan nanoparticle which was also prepared by layer-by-layer self-assemble approach. The immobilized ATXX showed improved thermo-stability compared with the free enzyme. When treated at 70 ºC and pH 6.0 for 2 min, the residual xylanase activities of the immobilized and free ATXX were 79.8% and 54.1%, respectively (Liu et al., 2015). Another xylanase (xynTF16) from a thermophilic bacterium *Geobacillus* sp. TF16, was covalently immobilized on chitosan with 85.6% yield. Free enzyme preserved 50% of its activity when incubated 2h at 55◦C, while immobilized enzyme retained 45% of its activity after 6 h incubation at 55◦C (Cakmak and Saglam Ertunga, 2017). Besides, the mature peptide of *Thermomonospora fusca* TF xylanase A (TfxA), was high-level expressed in *Escherichia coli* BL21 (DE3), reETfxA, and immobilized on a novel mesoporous SiO_2 microsphere (MSM)-coated chitosan support via covalent bonds between aldehyde group of glutaraldehyde and amine group of the enzyme. When treated at 70 °C and pH 6.0 for 15 min, the residual activities of free and immobilized reETfxA were 84.2 and 100.2%, respectively (Liu et al., 2017).

- Xylanases immobilization on other types of supports

A cellulase-free and alkali-stable xylanase from *Bacillus pumilus* SV-85S (MTCC 9861) was immobilized on a polymethyl methacrylate (PMMA) nanofiber membrane (NFM) which was synthesized by an electrospinning technique. PMMA NFM was initially derivatized with an amine group using phenylenediamine. The amine derivatized membrane was functionalized with an aldehyde group using glutaraldehyde to obtain reactive arm chains on the support surface. Thermostability of the immobilized enzyme was better when compared to the free enzyme. After 1h incubation at 60 ◦C, the residual activity of free and immobilized xylanase was 28% and 72%, respectively (Kumar et al., 2013). In another study, an extracellular xylanase produced from *Bacillus pumilus* VLK-1 was immobilized on glutaraldehyde-activated aluminum oxide pellets. Free xylanase retained 45 % and 30 % of initial activity after incubation at 55 and 65 °C for 2 h, whereas the residual activity of covalently immobilized enzyme at these temperatures was 50 % and 35 % respectively (Kumar et al., 2014). Other researchers reported the immobilization of a xylanase from *Thermomyces lanuginosus* on two types of aluminum hydroxide particles (gibbsite and amorphous $Al(OH)_3$) through adsorption, retaining 75% and 64% of the original catalytic activities after adsorption to these two types of particles, respectively. Free xylanase was stable at 45°C-70°C, whereas the adsorbed xylanases were stable at 45°C-80°C, indicating an enhanced thermal stability of xylanase after adsorption to the particles (Jiang et al., 2015). In addition, a purified xylanase from *Bacillus licheniformis*

Alk-1 was immobilized within glutaraldehyde activated calcium alginate beads. The activity retention of calcium-alginate immobilized beads (entrapped) and glutaraldehyde-activated beads (cross-linked) was 42% and 94%, respectively. At 60 ºC, free, entrapped and cross-linked enzymes retained 16%, 34% and 50% of their original activity after 240 min incubation, respectively (Kumar et al., 2017). And finally, maghemite (- Fe_2O_3), a recently sought after nanoparticle, was silanized with (3-aminopropyl) triethoxysilane (APTES) for use in the preparation of cross-linked enzyme aggregates of a recombinant xylanase from *Trichoderma reesei* (resulting in Xyl-CLEA-silanized maghemite). The maghemite surfaces were modified by APTES, at which this organosilane binds to a metal oxide of the maghemite by adsorption or covalent bonding. In addition, through the active amino group in the APTES structure, it is able to further bind the enzyme. Temperature stability was enhanced. After 30 min at 60 ◦C, the Xyl-CLEA-silanized maghemite still retained approximately 50% of its activity, compared to the free enzyme, which only retained 20% (Shaarani et al., 2016).

Despite all these immobilization methods and supports described for immobilization of xylanase enzymes in literature, glyoxyl-agarose based supports have been reported to yield very high thermo-stabilizing effects since they allow multipoint covalent attachment of enzymes. This type of immobilization strategy is established via short spacer arms and involves many residues of enzyme surface, driving to rigidification of enzyme structure. Consequently, relative distances among all residues involved in multipoint covalent immobilization would be maintained unaltered during conformational changes induced by any distorting agent (heat, organic solvents, extreme pH values), thus, resulting in a reduction of conformational changes involved in enzyme inactivation and in a great increase of enzyme stability (Mateo et al., 2007b).

A xylanase enzyme variant, which consists of the catalytic domain devoid of the linker region of a xylanase from *Streptomyces halstedii* JM8 (Xys1Δ), has been also immobilized by multipoint covalent immobilization attachment on glyoxyl-agarose support in a previous work, allowing a stabilization factor of 200-fold while retaining 65% of initial catalytic activity.

1.6.2.2. Engineering highly thermostable xylanase enzymes by post-immobilization technology

Together with immobilization technology, several post-immobilization techniques can complement it in order to achieve a better biocatalyst in terms of high activity, stability and selectivity (Bolivar et al., 2012). These techniques mainly consist of enzyme surface coating with polymers via either covalent binding or ionic exchange.

Among polymers used for covalent coating of enzyme surfaces, aldehyde-dextran polymers have been extensively used. These polymers have been applied to increase immobilized enzyme thermo-stability (Fernandez-Lafuente et al., 1999, Gutarra et al., 2011); stability against organic solvents (Fernandez-Lafuente et al., 1999, Rodrigues et al., 2009, Godoy et al., 2010); to prevent subunit dissociation of multimeric enzymes (Bolivar et al., 2012, Pessela et al., 2008); and to modulate different catalytic properties such as activity or selectivity (Godoy et al., 2010, Gutarra et al., 2011).

Similarly, polyethylenimine (PEI) polymers have been commonly used for enzyme surface coating via ion exchange. These polymers have been applied to adsorb many different proteins at neutral pH (Mateo et al., 2000); to stabilize multimeric enzymes by preventing subunit dissociation (Bolivar et al., 2009); to increase stability against organic solvents (Guisan et al., 2001, Abian et al., 2001); to increase stability against air bubbles (Betancor et al., 2004); to improve thermo-stability of immobilized enzymes (Cabrera et al., 2010); and to modulate catalytic properties such as activity or selectivity (Fernández-Lorente et al., 2011).

Among all these catalytic properties, thermo-stability is perhaps one of the most interesting to target since it is essential for industrial applicability of biocatalysts (Mateo et al., 2007b). In this respect, derived dextran polymers and polyethylenimine polymers have been extensively used due to their chemical structures.

Dextran is a very hydrophilic commercial polymer composed by a main backbone of glucose molecules (α(1→6)-linked D-glucopyranosyl units). This polymer can undergo simple chemical reactions to substitute some groups of glucose monomers. Oxidation with $NaIO_4$ allows transformation of dextran into a poly-aldehyde containing macromolecule which is able to react with enzyme surface amino groups. This reaction can be easily controlled so as to determine to which extent this dextran molecule is transformed into a poly-aldehyde containing molecule (e.g. 100%; 20%, etc.). After reduction with $NaBH_4$, it becomes a poly-hydroxyl harboring structure. Dextran has been reported, together with its derivatives, to modify enzyme surfaces for generation of hydrophilic environments (Fernandez-Lafuente et al., 1999, Rodrigues et al., 2009). This is due to the fact that the poly-aldehyde region of the dextran molecule will react with enzyme surface amino groups, thus anchoring the macromolecule, while the hydrophilic region composed by poly-hydroxyl will be surrounding enzyme surface, which could potentially drive to thermo-stabilizing effects.

Polyethylenimine is a polymer with high density of ionized tertiary, secondary and primary amino groups. This fact allows chemical modification of enzyme surface through strong ionic

exchange of this cationic polymer on any area of enzyme surface containing anionic groups (Cabrera et al., 2010). As a consequence, it also generates hydrophilic conditions around enzyme molecule potentially driving to thermo-stabilization effects (Velasco-Lozano et al., 2014, Padilla-Martinez et al., 2015).

1.6.2.3. Engineering highly thermostable xylanase enzymes by intensification of multipoint covalent immobilization

Multipoint covalent attachment on glyoxyl-agarose based supports allows high values of stabilization against distortion agents such as high temperatures due to rigidification of the enzyme structure. So, another strategy to further increase these thermo-stabilization effects would be to intensify rigidification of the enzyme surface region involved in multipoint covalent attachment. For this purpose, additional lysine residues could be introduced, thus providing this enzyme surface region with more points to form covalent bonds with the immobilization support. These additional lysine residues could be introduced via conservative site-directed mutagenesis, thus, substituting native arginine residues by lysine ones; or via non-conservative mutagenesis, such as replacing acidic residues (glutamic or aspartic acids) with lysine ones (Abian et al., 2004). This approach has been successfully developed for other enzymes in literature.

Three point mutations were performed on the surface of a penicillin G acylase (PGA) from *E. coli*. These mutations consisted of Aspβ13, Gluβ272, and Argβ276 residues replacement by lysine residues, and they were located on a region just opposite to the active centre which was rich in native lysine residues. After immobilization on glyoxyl-agarose, the enzyme variant displaying these three point mutations showed improved stability under all tested conditions, with stabilization factors ranging from 2 to 11 compared with the native enzyme immobilized on the same support (Abian et al., 2004).

This strategy has been also applied to engineer mutants of lipase 2 from *Geobacillus thermocatenulatus* (BTL2) to reinforce rigidification on two regions which were shown to be especially susceptible to trigger deactivation under denaturing conditions. One of these regions is close to residue 334 and is relatively rich in native lysine residues; while the other one is close to residue 40 and is poor in those residues. Accordingly, additional lysine residues were introduced via conservative site-directed mutagenesis in these two regions. For the first region, arginine residues 336, 331, 388 and 313 were replaced resulting in the "+4Lys" mutant, and the previous ones plus arginine residues 135 and 107 resulting in the "+6Lys" mutant. For poorly lysine enriched region, arginine residues 374, 379, 22 and 48 were replaced to engineer the

"+4Lys" mutant, while for the"+6Lys" mutant, the previous plus arginine residues 35 and 5 were selected. After multipoint covalent immobilization of these four enzyme variants, thermo-stabilization factors were higher than the ones obtained for their unmodified enzyme counterparts (Godoy et al., 2014).

1.7. Optimization of enzymatic xylan hydrolysis for XOS production by reaction engineering

Together with biocatalyst engineering, optimization of xylan hydrolysis reaction for XOS production could be also achieved by selection of bioreactor system and configuration of its mechanical and operational design. According to their mode of operation, bioreactor can be classified into batch, fed-batch and continuous (Sen et al., 2016). Biochemical reactions are mostly conducted in batch reactors, such as stirred tanked reactors. Major constraints of batch reactors are low productivity, high operation costs, loss of enzymatic activity and low purity of the desired product (Sen et al., 2016).

Compared to stirred tank reactors, continuous flow reactors offer significant processing advantages: improved temperature control; increased mixing efficiency; application of extreme conditions; controlled scaling factors; improved safety ratings; in-line control; easy product recovery, etc. (Wiles and Watts, 2012, Dall'Oglio et al., 2017). In addition, continuous processing is required to develop sustainable manufacturing since it has been reported to meet some of the twelve principles of green chemistry (Wiles and Watts, 2012). Besides flow reactor technology, biocatalysis is considered a technology intrinsically compatible with green chemistry (Wiles and Watts, 2012). However, despite the effectiveness of their combination, the potential of biocatalysis in flow reactors is far from being fully exploited (Zambelli et al., 2016).

As described above, enzyme immobilization reduces the cost contribution problem associated with enzyme biocatalysts since it allows enzyme re-use (Mateo et al., 2007b); and may also enhance different catalytic properties (Mateo et al., 2007b). Enzyme immobilization also allows the use of enzyme biocatalysts in continuous flow reactors (Itabaiana Jr et al., 2013). Several methods have been described to incorporate heterogeneous catalysts, such as immobilized enzyme biocatalysts, in flow reactors including packed-beds reactors (PBRs); monoliths, and wall-coated systems (Wiles and Watts, 2012). In most cases, PBRs are the choice for biocatalyzed continuous processes. A PBR consists of a column packed with the specific heterogeneous catalyst, where the reaction media is pumped throughout the column under a

flow rate. The most suitable performance for PBRs is to convert substrates into products in just one cycle (Itabaiana Jr et al., 2013).

With this respect, an ideal enzyme immobilization support to develop immobilized enzyme biocatalysts for continuously operating PBRs should meet two important criteria: high enzyme loading onto its surface, to avoid recycling operations; and good mechanical properties in order to allow operations at high flow rates. Concerning the immobilization protocol, it should avoid enzyme leaching and preserve enzyme catalytic activity, while allowing high thermo-stability.

Continuous flow operations at high flow rates should be expected to increase reaction productivity. To operate at high flow rates, the pressure drop produced by the bed is required to be very low. With this concern, immobilization supports consisting of methacrylic polymer matrices could be a good choice for PBRs since the pressure drop produced by the bed is very low. There are a few examples in literature of these methacrylic polymer matrices used as enzyme immobilization supports with high values of protein loading (Neto et al., 2015, Basso et al., 2016, Tacias-Pascacio et al., 2016). Respecting immobilization protocol, multipoint covalent immobilization on glyoxyl-functionalized agarose supports have been extensively described to enable high enzyme loading while providing optimised enzyme catalytic properties such as thermo-stability (Mateo et al., 2007b), and hindering enzyme leaching.

2. Objectives

The aim of this doctoral thesis is to enhance several enzymatic properties of a recombinant xylanase by the application of different enzyme technology techniques, to optimise the hydrolysis reaction of xylan to produce XOS, which have important prebiotic effects upon human health. This enzyme consists of the catalytic domain devoid of the linker region of the xylanase from *Streptomyces halstedii* JM8, Xys1Δ.

To achieve this global aim, different objectives have been targeted:

2.1. Increasing thermo-stability of immobilized Xys1Δ biocatalyst by post-immobilization techniques. A strategy based on chemical modifications by surface coating with a multilayer of polymers has been developed.

2.2. Increasing operational stability of this optimised immobilized Xys1Δ biocatalyst (obtained by previous strategy) for production of XOS from soluble xylans of various sources. These hydrolysis reactions have been carried out in batch mode at high temperatures.

2.3. Increasing thermo-stability of immobilized Xys1Δ biocatalyst by enhancement of multipoint covalent attachment. Site-directed mutagenesis has been applied to introduce additional lysine residues on Xys1Δ surface to provide a higher number of covalent bonds with immobilization support.

2.4. Increasing process productivity of continuous flow reaction of xylan hydrolysis to produce XOS by using an optimised immobilized Xys1Δ biocatalyst. This biocatalyst has been obtained by multipoint covalent immobilization of Xys1Δ enzyme onto different methacrylic polymeric based supports, and the resulting optimal biocatalyst in terms of more adequate area BET, pore size distribution, maximum protein loading and thermo-stability, has been applied to a PBR for continuous synthesis of XOS from xylan.

3. Materials

Supplier	Enzymes
IBFG-CSIC, donated from Prof. Ramón Santamaría	Xys1Δ xylanase from *Streptomyces halstedii* JM8
CBMSO-UAM, produced by Fermentation Service, CBMSO-UAM	Xys1Δ xylanase from *Streptomyces halstedii* JM8

Supplier	Enzyme immobilization supports
Agarose Bead Technologies	10% cross-linked agarose beads (10 BCL) 6% cross-linked agarose beads (6 BCL)
General Electric Healthcare	Cyanogen bromide-activated-Sepharose
Purolite	Purolite® ECR8204F Purolite® ECR8215F
Resindion	Relizyme™ EP403/S

Supplier	Substrates
Megazyme	Beechwood xylan Wheat arabinoxylan low viscosity
Carbosynth	Xylan from corncob

Supplier	Chemical reagents
Sigma-Aldrich Chem. Co	Sodium borohydride Sodium periodate Sodium hydroxide Dinitrosalicylic acid Sodium acetate Sodium chloride Sodium phosphate Glycidol Glycerol

	Trehalose Polyethyleneglycol, 6 KDa (PEG6000) Polyethylenimine (PEI) (1,300; 10,000; 25,000 and 70,000 Da) Dextran (40,000 Da)
Thermo Fisher Scientific	Pierce™ BCA Protein Assay Kit
Megazyme	Purified standards: xylobiose, xylotriose, xylotetraose, xylopentaose, and xylohexaose

Supplier	Molecular biology reagents
Takara	PrimeSTAR™ HS DNA Polymerase dNTP Mixture
Favorgen	FavorPrep Plasmid Extraction Mini Kit
Fermentas	NdeI restriction enzyme
Roche	HindIII restriction enzyme

Supplier	Others
Sartorius Stedim Biotech	0.2 µm cellulose acetate filters
Agarose Beads Technologies	8 mL empty FPLC columns

4. Methods

4.1. General methods

4.1.1. Enzyme production

The gen (XYSA) coding the catalytic domain without the linker region of a xylanase from *Streptomyces halstedii* JM8, Xys1Δ (GenBank Accession Number: U41627 from 938 nucleotide to 1975; PDB code: 1NQ6), was cloned into pNX4 (**Table 1**) (Rodríguez et al., 2005) or pTX4 (**Table 1**). The *Streptomyces* expression plasmid pTX4 was obtained by cloning the 2,1 Kb BglII fragment from plasmid pXHis1 (Adham et al., 2002) into the BglII site of *Streptomyces* multicopy vector pIJ702 (Katz et al., 1983). This BglII fragment contained the XYSA gene under the control of its own promoter (xysAp) between the mmrt (T1) and fdt (T2) transcriptional terminators.

S. lividans 1326 derivatives were grown on solid MSA medium for sporulation, on R2YE medium for transformation (Kieser T, 2000), and in liquid YES medium (1 % yeast extract, 10.3 % sucrose, 5 mM MgCl2) for protein expression. Protoplasts, for DNA transformation, were obtained from cell grown in liquid YES medium supplemented with 0.5 % glucose and 0.5 % glycine. *Streptomyces* manipulations were done as reported by Kieser et al. (Kieser T, 2000).

Protein concentration of the culture supernatant containing Xys1Δ was determined according to Pierce™ BCA Protein Assay Kit protocol and using bovine serum albumin as standard.

4.1.1.1. Enzyme production in flasks

Plasmid DNA derived from pNX4 was transformed into *S. lividans* 1326 under neomycin (15 µg/mL) selection. The obtained colonies were used to inoculate 10ml of YES medium supplemented with 1% xylose and 15 µg/mL neomycin, and developed in 50 mL three-baffled flasks. They were incubated at 28ºC and 200 rpm for 8 days. Supernatants were collected by centrifugation at 10,000 g for 10 min and used as the source of protein.

4.1.1.2. Enzyme production in bench-top STR

Plasmid DNA derived from pTX4 was transformed into *S. lividans* 1326 under neomycin (15 µg/mL) selection. Transformants were used to inoculate 200 mL YES medium supplemented with 1% (w/v) xylose and 15 µg/mL neomycin in 250 mL baffled flasks. Incubation was carried out for 48 h at 28 ºC and at 220 rpm in an orbital shaker. This culture was then used to inoculate the fermenter medium. Batch fermentation was carried out in 4 L working volume using a

Biostat® Aplus autoclavable bioreactor. Fermentation medium with the same composition was sterilized inside the reactor prior to inoculation. Fermentation was developed for 166 h at 28 ºC under constant agitation provided by two standardized Rushton impellers placed at axial position over the height of the tank. No pH control was carried out. 2 mL of antifoam (2000 Da polyethylene glycol) was initially added. Dissolved oxygen was maintained at 25% - 75% of saturation by supplementing air at 1 v/v/min as needed. Culture medium containing Xys1Δ protein was separated from grown cells by filtration, and used as source of this enzyme.

4.1.2. Xylanase enzymatic activity assay

Xylanase activity was colorimetrically measured by DNS method (Miller, 1959), using xylose as standard. A mixture of 4% (w/v) beechwood xylan in 50 mM sodium acetate buffer at pH 5.0 was stirred for 1h at 25 ºC and then centrifuged for 1h at 3,750 rpm. The soluble fraction was diluted to 1% (w/v) for xylanase activity assay. The conditions for xylanase activity assay were 10 min at 25 ºC under constant agitation in 50 mM sodium acetate buffer pH 5.0, containing 100 µL of xylanase solution and 900 µl of 1% xylan substrate. One unit of enzyme activity was defined as the amount of enzyme required to release 1 µmol of reducing sugars (xylose equivalents) in 1 min.

4.1.3. XOS analysis

The XOS content of product from different xylan hrydrolysis reactions was analyzed by high-performance anion exchange chromatography coupled with pulsed amperometric detection (HPAEC-PAD). This analysis was carried out in an ICS3000 Dionex system consisting on a SP gradient pump, an AS-HV autosampler and an electrochemical detector with a gold working electrode and Ag/AgCl as reference electrode. An anion-exchange 3 × 250 mm Carbo-Pack PA-200 column (Dionex) was used at 30 °C. The initial mobile phase was 15 mM NaOH at 0.5 mL/min for 12 min. Then, an 8 min-gradient from 15 mM to 75 mM NaOH and from 0 mM to 80 mM sodium acetate was applied. Next, the mobile phase composition varied from 75 mM to 100 mM NaOH and from 80 mM to 320 mM sodium actetate for 10 min. A final 15 min-gradient was programmed to return to the initial conditions (15 mM NaOH and 0 mM sodium acetate). Resulting peaks were analyzed using the Chromeleon software. The identification and quantification of linear XOS was done using commercial standards. All samples were previously filtrated through 0.2 µm cellulose acetate filters and conveniently diluted with H2O (d). All analyses were carried out in duplicate, and data were expressed as the mean value. Standard deviation was never higher than 5%.

4.2. Methods for increasing thermo-stability of the immobilized Xys1Δ biocatalyst by post-immobilization techniques

4.2.1. Immobilization of the Xys1Δ enzyme on agarose beads activated with cyanogen bromide groups

An aliquot of 1 g of hydrated Ag-CB was added to 25 mM sodium phosphate buffer at pH 7.0 with a fraction of extracellular culture medium, from enzyme production in flasks, containing 10 mg of protein. The suspension was gently stirred at 4 ºC for 15 min. Then, the resulting immobilized biocatalyst (Ag-CB-Xys1Δ) was filtered and suspended into 1 M ethanolamine solution at pH 8.0 for 2 h to block any remaining reactive group.

4.2.2. Evaluation of enzyme preservation with different additives at immobilization conditions

Some additives were firstly evaluated for Xys1Δ enzyme preservation at immobilization conditions, pH 10. A fraction of extracellular culture medium, from enzyme production in flasks, containing 1.2 mg of protein was suspended in 20%, 40% and 50% (w/v) of glycerol, trehalose and PEG6000 in 100 mM sodium carbonate buffer pH 10 and incubated at 25 ºC, along with the enzyme diluted in the same buffer, used as control. Samples were withdrawn at different time points and xylanase activity was determined. Residual activity was calculated at the ratio of xylanase activity at different time points to initial xylanase activity.

4.2.3. Immobilization of Xys1Δ enzyme on agarose beads activated with glyoxyl groups

6% and 10% cross-linked agarose beads were fully activated with glyoxyl groups (Ag-G) as previously described (Guisán, 1988).

The immobilization procedure of this enzyme was developed by two different approaches to obtain two immobilized Xys1Δ biocatalysts with low (10 mg protein/g on 6% Ag-G support, resulting in immobilized Ag-G-Xys1Δ-L biocatalyst) and high (20 mg protein/g on 10% Ag-G support, resulting in immobilized Ag-G-Xys1Δ-H biocatalyst) protein loading, respectively.

4.2.3.1. Immobilization of Xys1Δ enzyme on Ag-G with low protein loading to obtain immobilized A-G-Xys1Δ-L biocatalyst

To obtain the immobilized A-G-Xys1Δ-L biocatalyst, the immobilization process was performed by diluting a volume of extracellular culture medium from enzyme production in

flasks, containing 10 mg of protein, with 5 g of glycerol and 1.3 mL of 900 mM sodium carbonate buffer pH 10 . This enzyme solution, with a final volume of 10 mL, was added to 1 g of 6% Ag-G support. The suspension was gently stirred at 4 ºC for 4 h, and then incubated at 20 ºC for 16 h.

A fraction of this enzyme solution before being offered to the support was taken and used as control. Periodically, samples of the supernatant, the suspension and the control were withdrawn and xylanase activity was determined. When immobilization was completed, the mixture was reduced for 30 min in the presence of 1% (w/v) substrate with 1 mg/mL $NaBH_4$. Then, the resulting Ag-G-Xys1Δ-L biocatalyst (**Table 3**) was washed with distilled water and stored at 4 ºC. The immobilized activity is defined as the difference between the control activity and the supernatant activity at given conditions. The immobilization yield is defined as the ratio of the immobilized activity at one-time point to the initial activity. Expressed activity is defined as the ratio of recovered activity on the solid support after the immobilization process to the initial activity.

4.2.3.2. Immobilization of the Xys1Δ enzyme on Ag-G with high protein loading to obtain immobilized Ag-G-Xys1Δ-H biocatalyst

To obtain the immobilized Ag-G-Xys1Δ-H biocatalyst, the immobilization procedure was performed by mixing a volume of extracellular culture medium from enzyme production in bench-top STR, containing 20 mg of protein, with 10 g of glycerol and 2.6 mL of 900 mM sodium carbonate buffer pH 10. This enzyme solution with a final volume of 20 mL was added to 1g of 10% Ag-G support. This suspension was incubated under mild agitation at 4 ºC for 120 h.

A fraction of this enzyme solution before being offered to the support was taken and used as a control. Periodically, samples from the supernatant, the suspension and the control were withdrawn and xylanase activity was determined. When immobilization was completed, the mixture was reduced for 30 min in the presence of 1% substrate with 1 mg/mL $NaBH_4$. Then, the resulting Ag-G-Xys1Δ-H biocatalyst (**Table 3**) was washed with distilled water and stored at 4 ºC.

4.2.4. Preparation of a derived dextran polymer: 100% modified to poly-aldehyde (Dex100)

10.02 g of dextran (40,000 Da molecular weight) was diluted in 300 ml of distilled water and oxidised up to 100% by the addition of 26.16 g of $NaIO_4$. After 90 min of mild agitation, the

mixture was dialyzed against water and 300 mL of 100 mM sodium phosphate buffer pH 7 were added. The pH value was adjusted to 7 and this dextran preparation (Dex100) was stored at 4ºC.

4.2.5. Preparation of a derived dextran polymer: 20% modified to poly-aldehyde (Dex20)

10.02 g of dextran (40,000 Da molecular weight) was diluted in 300 ml of distilled water and oxidised up to 20% by the addition of 5.232 g of $NaIO_4$. After 90 min of mild agitation, the mixture was dialyzed against water and 300 mL of 100 mM sodium phosphate buffer pH 7 were added. The pH value was adjusted to 7 and this dextran preparation (Dex20) was stored at 4ºC.

4.2.6. Preparation of a derived dextran polymer: 80% modified to poly-hydroxyl and 20% modified to poly-aldehyde (Dex20-80)

10.02 g of dextran (40,000 Da molecular weight) was diluted in 300 ml of distilled water and oxidised up to 80% by the addition of 20.928 g of $NaIO_4$. After 90 min of gentle agitation at 25 ºC, the dextran preparation was dialyzed against an excess of distilled water and pH value was adjusted to 8.5 with 900 mM sodium carbonate buffer at pH 8.5. Then, the dextran preparation was reduced with 10 mg/mL $NaBH_4$ for 2 hours under constant agitation at 25 ºC. Once reduction was completed, the pH value was adjusted to 7 and the mixture was dialyzed again against distilled water. Finally, this dextran preparation was oxidised to the 20% by adding 5.232 g of $NaIO_4$. After 90 min of mild agitation, the mixture was dialyzed against water and 300 mL of 100 mM sodium phosphate buffer pH 7 were added. The pH value was adjusted to 7 and this dextran preparation (Dex20-80) was stored at 4ºC.

4.2.7. Surface coating of immobilized Ag-G-Xys1Δ-L and Ag-G-Xys1Δ-H biocatalysts with different derived dextran polymers by chemical modifications via covalent binding

1 g of Ag-G-Xys1Δ-L was added to 10 mL, 50 mL and 250 mL of each dextran preparation in order to get low, medium and high surface coating degrees, respectively. After 16 h of gentle agitation at 25 ºC, the pH value was adjusted to 8.5 with 900 mM sodium carbonate buffer at pH 8.5. Then, different modified immobilized A-G-Xys1Δ-L biocatalysts were reduced in the presence of 1% (w/v) of beechwood xylan in distilled water with 1 mg/mL $NaBH_4$ for 30 min at 25 ºC. Finally, they were vacuum-filtered, washed with distilled water and stored at 4 ºC.

1 g of Ag-G-Xys1Δ-H was added to 10 mL, 50 mL and 250 mL of Dex20-80 preparation in order to get low, medium and high surface coating degrees, respectively. The same procedure was applied.

4.2.8. Surface coating of immobilized Ag-G-Xys1Δ-L and Ag-G-Xys1Δ-H biocatalysts with PEI by chemical modification via ionic exchange

Different PEI solutions were prepared by adding different quantities (0.01 g; 0.1 g; 1 g; 2 g and 10 g) of 1,300 Da PEI to 20 mL of 25 mM sodium phosphate buffer pH 8. After being adjusted to pH 8, each of these PEI solutions were added to 1 g of Ag-G-Xys1Δ-L and incubated at 25 ºC for 90 min under mild agitation. Finally, they were vacuum-filtered, and the resulting modified Ag-G-Xys1Δ-L biocatalysts with PEI were washed with an excess of distilled water, and stored at 4 ºC. Then, other four different solutions of PEI were prepared by applying the same procedure with 1 g of PEI with different molecular weights (10,000 Da; 25,000 Da and 70,000 Da), and afterward, with different quantities (0.1 g, 1g and 2 g) of 25,000 Da PEI. Each of these PEI solutions were added to 1 g of Ag-G-Xys1Δ-L, and the same procedure was applied.

Different PEI solutions were prepared by adding different quantities (0.01 g; 0.1 g; 1 g; 2 g and 10 g) of 25,000 Da PEI to 20 mL of 25 mM sodium phosphate buffer pH 8. After being adjusted to pH 8, each of these PEI solutions were added to 1 g of Ag-G-Xys1Δ-H, and the same procedure was followed. Resulting modified Ag-G-Xys1Δ-H biocatalysts with PEI were washed with distilled water, and stored at 4 ºC.

4.2.9. Surface coating of immobilized Ag-G-Xys1Δ-L+PEI and Ag-G-Xys1Δ-H+PEI biocatalysts with a derived dextran polymer by chemical modification via covalent binding

1 g of Ag-G-Xys1Δ-L+PEI or Ag-G-Xys1Δ-H+PEI biocatalysts (**Table 3**), was added to 10 mL of Dex20-80 dextran preparation. After 16 h of gentle agitation at 25 ºC, the pH value was adjusted to 8.5 with 900 mM sodium carbonate buffer at pH 8.5. Then, these two preparations were reduced in the presence of 1% (w/v) of substrate with 10 mg/mL $NaBH_4$ for 2 h at 25 ºC. Finally, they were vacuum-filtered, and the resulting modified Ag-G-Xys1Δ-L+PEI+DEx20-80 and Ag-G-Xys1Δ-H+PEI+Dex20-80 biocatalysts (**Table 3**) were washed with distilled water and stored at 4 ºC.

4.2.10. Surface coating of immobilized Ag-GXys1Δ-L+Dex20-80 and Ag-G-Xys1Δ-H+Dex20-80 biocatalysts with PEI by chemical modification via ionic exchange

1 g of Ag-G-Xys1Δ-L+Dex20-80 biocatalyst (**Table 3**) was added to 20 mL of a PEI solution. This PEI solution consisted of 0.1 g of a 25,000 Da PEI polymer diluted in 20 mL of 25 mM sodium phosphate buffer pH 8. In addition, 1 g of Ag-G-Xys1Δ-H+Dex20-80 biocatalyst (**Table 3**), was added to 20 ml of a PEI solution consisting of 1 g of a 25,000 Da PEI polymer diluted in 20 ml of 25 mM sodium phosphate buffer pH 8. After adjusting the pH value of these preparations to 8, they were incubated at 25 ºC for 90 min under gently agitation. Finally, they were vacuum-filtered and the resulting modified Ag-G-Xys1Δ-L+Dex20-80+PEI and Ag-G-Xys1Δ-H+Dex20-80+PEI biocatalysts (**Table 3**) were washed with distilled water, and stored at 4 ºC.

4.2.11. Thermal-stability of different chemically modified immobilized Xys1Δ-L and Xys1Δ-H biocatalysts by surface coating with polymers via covalent and ionic binding

0.1 g of different modified Ag-G-Xys1Δ biocatalysts were suspended in a 1 mL solution of 25 mM sodium phosphate buffer at pH 7 and then, incubated at 70 ºC. Samples were withdrawn at different time points and xylanase activity was determined. Unmodified Ag-CB-Xys1Δ, Ag-G-Xys1Δ-L or Ag-G-Xys1Δ-H were suspended in the same buffer and used as controls by incubating them along with chemically modified immobilized biocatalysts. Residual activity was calculated at the ratio of xylanase activity at different time points to initial xylanase activity. Inactivation parameters were determined from the best-fit model of the experimental data, which was the one based on two-stage series inactivation mechanism with no residual activity, as previously reported (Romero et al., 2012). Stabilization factors were calculated by dividing $t_{1/2}$ of each modified biocatalyst by $t_{1/2}$ of the control.

4.3. Methods for increasing operational stability of the optimised immobilized Ag-G-Xys1Δ-H biocatalyst of xylan hydrolysis reaction for XOS production in batch mode at high temperatures

4.3.1. Substrate solutions preparations

Beechwood xylan, corncob xylan and wheat arabinoxylan were used as hydrolysis reaction substrates. Three mixtures of 4% (w/v) beechwood xylan, corncob xylan and wheat arabinoxylan in 50 mM sodium acetate buffer at pH 5.0 were stirred for 1h at 25 ºC and then centrifuged for 1h at 3,750 rpm. The obtained supernatants were considered to be the soluble fractions, and were used as substrates for hydrolysis reactions.

The soluble fraction from the 4% (w/v) suspension of beechwood xylan in 50 mM sodium acetate buffer pH 5 contained 85.4% of starting material, basing on dry weight; while soluble fractions obtained for corncob xylan and wheat arabinoxylan suspensions were 100% of their starting materials, respectively.

4.3.2. Hydrolysis of xylan by the unmodified immobilized Ag-G-Xys1Δ-H biocatalyst and by the immobilized Ag-G-Xys1Δ-H+Dex20-80+PEI biocatalyst

0.2 g of unmodified Ag-G-Xys1Δ-H and Ag-G-Xys1Δ-H+Dex20-80+PEI (**Table 3**) were suspended in 20 mL of beechwood xylan, corncob xylan or wheat arabinoxylan hydrolysis substrate solutions. Hydrolysis reactions were conducted at 50 ºC and pH 5, under orbital agitation. At different time points of reaction course, samples were withdrawn and XOS content was analyzed as described in *XOS analysis* section.

4.3.3. Operational stability of the unmodified immobilized Ag-G-Xys1Δ-H biocatalyst and the immobilized Ag-G-Xys1Δ-H+Dex20-80+PEI biocatalyst

0.1 g of unmodified Ag-G-Xys1Δ-H and Ag-G-Xys1Δ-H+Dex20-80+PEI biocatalysts (**Table 3**) were suspended in 10 mL of beechwood xylan substrate solution. Hydrolysis reactions were conducted at 50 ºC and pH 5 under orbital agitation. At 3 h of the reaction course, the reaction mixture was vacuum-filtered and XOS content was analyzed. Afterwards, immobilized biocatalysts were washed and offered again to 10 mL of fresh substrate solution to carry out a new reaction cycle.

4.4. Methods for increasing thermo-stability of the immobilized Xys1Δ biocatalyst by enhancement of multipoint covalent attachment via site-directed mutagenesis

4.4.1. Bacterial strains and DNA manipulation

Plasmid pXHis1 (Adham et al., 2002) (**Table 1**) was the source of XYSAΔ gene. *E.coli* DH10B strain was used as host for genetic manipulation of plasmids. All molecular biology protocols were performed using standard methods (Sambrook et al., 1989). All plasmids and primers used are listed in **Table 1** and **Table 2**, respectively.

4.4.2. Construction of XYSAΔ gene mutants in *E. coli*

Plasmid pXHis1 (Adham et al., 2002) (**Table 1**), carrying the XYSAΔ gene, was used as template for site-directed mutagenesis reactions. For the first round of mutagenesis, two reactions were assembled, each one containing a different pair of primers (**Table 2**): Arg58Lys5 - Arg58Lys3; and Arg201204Lys5 - Arg201204Lys3, respectively. The mutagenic reactions were carried out in a Masterpersonal thermocycler, with PrimeSTAR^{TM} HS DNA Polymerase, 0.2 mM of the four deoxynucleotides (dNTP Mixture) and 0.3 µM of each primer. Cycling conditions were: 30 cycles of 10 seconds at 95 ºC, 5 seconds at 55 ºC and 1 min 20 seconds at 72 ºC; final extension at 72 ºC for 10 min. After treatment with 10 U of *DpnI* at 37 ºC for 16 h, the reactions mixtures were transformed into *E. coli* DH10B, which was grown under ampicillin (100 µg/mL) selection. Both transformants were collected and plasmid DNA, carrying the constructions from the two mutagenic reactions (called pXHis1-R58K and pXHis1-R201K-R204K, respectively; **Table 1**), was isolated using FavorPrep Plasmid Extraction Mini Kit.

For the second round of mutagenesis, one reaction was carried out at the same conditions using plasmid DNA pXHis1-R201K-R204K as template and Arg239Lys5 - Arg239Lys3 pair of primers (**Table 2**). The same procedure was applied and resulting construction was called pXHis1-R201K-R204K-R239K (**Table 1**). This construction was used as template for the third round of mutagenesis, following the same procedure as before and using Arg58Lys5 - Arg58Lys3 pair of primers (**Table 2**). The resulting construction was called pXHis1- R58K-R201K-R204K-R239K (**Table 1**).

Different plasmid DNA, each carrying one construction with a different number of point mutations (pXHis1-R58K; pXHis1-R201K-R204K; pXHis1-R201K-R204K-R239K and

pXHis1-R58K-R201K-R204K-R239K; **Table 1**), was digested with *NdeI* and *HindIII* , and the resulting 1.5 Kb fragments were purified by agarose gel electrophoresis a nd cloned into pNX4 plasmid (Rodríguez et al., 2005) (**Table 1**) digested with the same enzymes. *E. coli* DH10B was transformed with these four constructions and grown, under kanamycin (50 µg/mL) selection. Transformants were collected and plasmid DNA was isolated (pNX4-R58K, pNX4-R201K-R204K, pNX4-R201K-R204K-R239K and pNX4-R58K-R201K-R204K-R239K; **Table 1**).

4.4.3. Purification of Xys1Δ enzyme variants

S. lividans JI66 was used as the host for derivatives of the multicopy plasmid pNX4 (Rodríguez et al., 2005). Production of different Xys1Δ variants was carried out in flasks as described above. Culture supernatants were obtained after 6 days of growth and were used as source of different enzyme variants for affinity purification.

Highly activated Ni-IDA-agarose gels were prepared as previously described (Armisén et al., 1999) and used as support for affinity chromatography. A fraction of each culture supernatant containing 3.5 mg of total protein was added to 50 mM sodium phosphate buffer containing 150 mM NaCl and 5 mM of imidazole and adjusted to pH 7.0 (input fraction) resulting in 10 mL total volume. Then, these 10 mL fractions were added to 1 mL of highly activated Ni-IDA-agarose gel, which was previously equilibrated with the same buffer, and incubated at 4 ºC for 18 h under mild agitation. Afterwards, these suspensions were packed into columns by gravity (flowthrough fraction) and washed with 10 mL of 50 mM sodium phosphate buffer pH 7.0 containing 150 mM NaCl and 10 mM of imidazole (washing fraction). Finally, adsorbed protein was eluted by adding 10 mL of 50 mM sodium phosphate buffer pH 7.0 containing 150 mM NaCl and 500 mM imidazole after incubation at 4 ºC for 2 h under mild agitation (elution fraction). Obtained fractions were dialyzed against distilled water containing 10 mM $MgCl_2$ (dialysis fraction). The resulting purified Xys1Δ variants were respectively termed Xys1Δ-WT; Xys1Δ-R58K; Xys1Δ-R201K-R204K; Xys1Δ-R201K-R204K-R239K; and Xys1Δ-R58K-R201K-R204K-R239K.

4.4.4. Specific activity and kinetic analysis of Xys1Δ enzyme variants

Apparent Michaelis–Menten constants were determined using the soluble fraction of bechwood xylan as substrate. Hydrolysis conditions were: 10 min at 25 ºC in 50 mM sodium acetate buffer, pH 5, containing 0.001 mg of purified Xys1Δ variants and xylan concentrations varying from 0.25 to 20 mg/mL, with 1 mL total volume. The release of reducing sugars was measured by the DNS method, as described above.

The specific activity of purified mutant xylanases was evaluated in presence of 15 mg/mL beechwood xylan (soluble fraction) at 25 ºC.

4.4.5. Immobilization of Xys1Δ enzyme variants on 10% glyoxil-agarose beads

10% cross-linked agarose beads were activated with glyoxyl groups as previously described (Guisán, 1988). The immobilization of different Xys1Δ enzyme variants on this support was performed by adding 0.5 mg of each Xys1Δ enzyme variant to 10 mL solution containing 50% (w/v) glycerol and 100 mM sodium carbonate buffer pH 10. This enzyme solution was added to 1g of support and the suspension was mildly agitated at 4ºC for 48 h, before Schiff bases reduction (Guisán, 1988). A fraction of the enzyme solution before being offered to the support was taken and used as control. Periodically, samples from supernatant, suspension and control were withdrawn and xylanase activity was determined. The resulting immobilized Xys1Δ variants biocatalysts (respectively termed Ag-G-Xys1Δ-WT; Ag-G-Xys1Δ-R58K; Ag-G-Xys1Δ-R201K-R204K; Ag-G-Xys1Δ-R201K-R204K-R239K; and Ag-G-Xys1Δ-R58K-R201K-R204K-R239K) were washed with distilled water and finally, stored at 4ºC.

4.4.6. Thermal-stability of Xys1Δ enzyme variants and immobilized Xys1Δ variants biocatalysts

A solution consisting of 0.025 mg/mL of each purified Xys1Δ enzyme variant in 50 mM in sodium acetate buffer pH 5 was incubated at 50 ºC. Samples were withdrawn at different time points and xylanase activity was determined. Xys1Δ-WT enzyme was suspended in the same buffer and used as control. Residual activity was calculated at the ratio of xylanase activity at different time points to initial xylanase activity.

Besides, 0.1 g of different immobilized Xys1Δ variants biocatalysts (Ag-G-Xys1Δ-R58K; Ag-G-Xys1Δ-R201K-R204K; Ag-G-Xys1Δ-R201K-R204K-R239K; and Ag-G-Xys1Δ-R58K-R201K-R204K-R239K) were suspended in a 1 ml solution of 50 mM sodium acetate buffer pH 5 and then, incubated at 65 ºC. Samples were withdrawn at different time points and xylanase activity was determined. Immobilized Ag-G-Xys1Δ-WT biocatalyst was suspended in the same buffer and used as control. Residual activity was calculated at the ratio of xylanase activity at different time points to initial xylanase activity.

4.5. Methods for increasing process productivity of continuous flow reaction of xylan hydrolysis to produce XOS by multipoint covalent immobilization of the Xys1Δ enzyme onto different methacrylic polymeric based supports

4.5.1. Synthesis of glyoxyl-functionalized methacrylic supports

Relizyme™ EP403/S (R403S), Purolite® ECR8204F (P8204F) and Purolite® ECR8215F (P8215F) were functionalized with glyoxyl groups: epoxy groups were firstly hydrolyzed with 0.5 M H_2SO_4; and resulting glyceryl groups were oxidised with 100 mM $NaIO_4$. Both reactions were developed for 2 h at room temperature under constant agitation. Finally, glyoxyl-functionalized methacrylic supports (termed R403S-G, P8204F-G and P8215F-G, respectively) were washed with abundant distilled water and stored at 4 ºC. The Relizyme™ EP403/S (R403S) support was also oxidised with a lower $NaIO_4$ concentration after H_2SO_4 hydrolysis. The resulting support was termed R403S-G-25.

4.5.2. Morphological characterization of glyoxyl-functionalized methacrylic supports

Physical characterization of these enzyme supports based on methacrylic polymer functionalized with glyoxyl groups was carried out by Mercury Intrusion Porosimetry (MIP) and Adsorption Isotherm (AI). MIP was developed following standardized protocol with mercury intrusion-extrusion equipment, Micromeritics AutoPore IV 9510. Resolution in terms of pore size was 7 nm to 360 µm (3.6 x 105 nm). Data analysis was carried out with AutoPore IV 9500 V1.09 software. AI was carried out following standardized procedure with Asap2420 Micromeritics equipment using N_2 as analysis adsorptive. This technique allowed determination of materials containing a pore size range from 0.5 to 500 nm. Analysis of resulting data was conducted with MicroActive 4.02 software.

4.5.3. Immobilization of the Xys1Δ enzyme on glyoxyl-functionalized methacrylic supports

4.5.3.1. Determination of optimal immobilization condition for each glyoxyl-functionalized methacrylic support

Four fractions of extracellular culture medium from enzyme production in bench-top STR, containing 0.5 mg of total protein, were suspended in either 10 mL of 50% (w/v) glycerol 100 mM sodium carbonate buffer pH 10, or 10 mL of 100 mM sodium carbonate buffer pH 10.

Then, the four enzyme solutions were offered to 1 g of each support (Ag-G, R403S-G, P8204F-G and P8215F-G) and resulting suspensions were incubated at either 4 ºC or 25 ºC. A fraction of these enzyme solutions before being offered to different supports was taken and used as control. Periodically, samples from supernatant and control were withdrawn, and xylanase activity was determined.

4.5.3.2. Determination of maximum loading capacity for the Xys1Δ enzyme of each glyoxyl-functionalized methacrylic support

A fraction of extracellular culture medium from enzyme production in bench-top STR, containing either 80 mg or 40 mg of total protein was suspended in either 27.5 mL or 15 mL of 100 mM sodium carbonate buffer pH 10 and respectively added to 1 g of Ag-G, or to 1g of glyoxyl-functionalized methacrylic supports: R403S-G, P8204F-G and P8215F-G. The suspensions were incubated at 4 ºC for 96 h under mild agitation. A fraction of these enzyme solutions before being offered to the support were taken and used as control. Periodically, samples from the supernatant and the control were withdrawn and remaining protein concentration and remaining xylanase activity were determined. Remaining activity was calculated by dividing remaining activity in the supernatant at different time points into initial activity. Immobilized protein and activity were calculated as the difference between remaining protein or remaining activity at different time points, and initial protein or initial activity, respectively.

4.5.3.3. Immobilization of the Xys1Δ enzyme at maximum protein loading on each glyoxyl-functionalized methacrylic support

Four fractions of crude culture medium containing 40 mg; 20 mg; 20 mg; and 10 mg of total protein were suspended in 15 mL of 100 mM sodium carbonate buffer pH 10 and added to 1 g of Ag-G, R403S-G, P8204F-G, and P8215F-G, respectively. The four resulting suspensions were incubated at 4 ºC for 96 h under mild agitation. A fraction of these enzyme solutions before being offered to the support were taken and used as control. Periodically, samples from the supernatant and the control were withdrawn and xylanase activity was determined. When immobilization was completed, the suspensions were reduced for 30 min in the presence of 1% corncob xylan in distilled water with 1 mg/mL $NaBH_4$ for Schiff bases reduction (Guisán, 1988), and then, washed with distilled water. Finally, resulting biocatalysts (respectively termed Ag-G-Xys1Δ-40-HT; R403S-G-Xys1Δ-20-HT; P8204F-G-Xys1Δ-20-HT and P8215F-G-Xys1Δ-10-HT) were stored at 4 ºC.

4.5.3.4. Immobilization of the Xys1Δ enzyme with different protein loading on R403S-G

Four fractions of crude culture medium containing either, 15 mg, 10 mg, 5 mg or 1 mg of total protein were suspended in 15 mL of 100 mM sodium carbonate buffer pH 10 and respectively added to 1 g of R403S-G. The three resulting suspensions were incubated at 4ºC for 96 h under mild agitation. Onwards, the same procedure as described above was followed. The resulting biocatalysts were respectively termed R403S-G-Xys1Δ-15-HT; R403S-G-Xys1Δ-10-HT, R403S-G-Xys1Δ-5-HT and R403S-G-Xys1Δ-1-HT.

4.5.4. Thermal stability of different immobilized Xys1Δ biocatalysts

0.1 g of different immobilized Xys1Δ biocatalysts, Ag-G-Xys1Δ-40-HT; R403S-G-Xys1Δ-20-HT; P8204F-G-Xys1Δ-20-HT and P8215F-G-Xys1Δ-10-HT, were suspended in 50 mM sodium acetate buffer at pH 5 and then, incubated at 65 ºC. Samples were withdrawn at different time points and xylanase activity was determined. Residual activity was calculated at the ratio of xylanase activity at different time points to initial xylanase activity.

4.5.5. Continuous production of XOS in Packed-Bed Reactors (PBRs)

Different packed-bed reactors were set up by packing the obtained immobilized Xys1Δ biocatalysts into 8 mL FPLC columns (70 mm of height and 12 mm of inner diameter) by gravity. Substrate solution was pumped using a peristaltic pump at different flow rates (0.1 up to 10 mL/min) in order to obtain residence times from 0.8 min to 80 min. Substrate solution consisted of 4% corncob xylan (w/v) in 50 mM sodium acetate buffer at pH 5. The temperature was set to 30 ºC by a thermo-stated chamber. Different aliquots (150 µL) of the exiting flow stream were withdrawn at different time points of the reaction course, and XOS content was analyzed by the method described above. The volumetric productivities for XOS [r_p (g_{XOS} L^{-1} h^{-1}) = C x F/V, where C is XOS concentration at exit flow stream (g L^{-1}), F is the flow rate (L h^{-1}) and V is the reactor void volume (L)]; and the specific productivities [q_p (g_{XOS} g_{enzyme}^{-1} h^{-1}) = volumetric productivity (g_{XOS} L^{-1} h^{-1})/enzyme concentration (g_{enzyme} L^{-1})]; and residence times (h) [τ (h) = V/F where F is the flow rate (L h^{-1}) and V is the reactor void volume (L)] were evaluated for each reaction flow rate, according to literature (Nunes et al., 2015). The void volume for PBRs implemented with immobilized biocatalysts on R403S-G was considered to be 5.40 mL, and was calculated from the porosity value given by MIP (**Table 1**). The void volume for PBRs implemented with immobilized biocatalysts on Ag-G was considered to be 4.83 mL, and was calculated from data of dry agarose density (1.64 g/mL) (Pluen et al., 1999), and concentration of organic material in a fiber (0.65 g/mL) (Pluen et al., 1999).

5. Results

5.1. Increasing thermo-stability of the immobilized Xys1Δ biocatalyst by post-immobilization techniques

As previously described in *Introduction* section, post-immobilization techniques can complement enzyme immobilization to further modulate some enzyme catalytic properties such as activity, stability and selectivity, and consist of enzyme surface coating with polymers by either covalent binding or ionic exchange (Bolivar et al., 2012).

Among all these catalytic properties, thermo-stability is perhaps one of the most important ones to be improved since it is essential for industrial applicability of biocatalysts (Mateo et al., 2007b). With respect to this, derived dextran polymers and polyethylenimine polymers have been extensively used as their chemical structures allow the generation of hydrophilic conditions around the enzyme molecule surface. As a result, they create a protective layer against distortion agents such as temperature, thus, potentially driving to thermo-stabilization effects.

In a previous study, the recombinant xylanase Xys1Δ, from *Streptomyces halstedii* JM8, was overexpressed in *S. lividans* and immobilized on agarose beads activated with glyoxyl groups (Aragon et al., 2013a). In this section, to further thermo-stabilize the resulting immobilized Xys1Δ biocatalyst, a strategy based on surface coating with a multilayer of polymers was carried out. First of all, immobilization of this enzyme on agarose beads activated with glyoxyl groups was optimised. Then, the surface of the resulting immobilized Xys1Δ biocatalyst was modified by coating with a first layer of derived dextran and polyethylenimine polymers at different coating degrees. Afterwards, the optimal resulting biocatalysts in terms of thermo-stability, from each type of polymer modification, were modified with a second layer of the other polymer to get a bilayer of polymer. The effect of these chemical modifications on biocatalyst activity, biocatalyst thermo-stability, and operational stability were evaluated.

5.1.1. Optimization of immobilization of the Xys1Δ enzyme on glyoxyl-activated agarose beads

The immobilization procedure was optimised to obtain an immobilized Xys1Δ biocatalyst with higher recovered activity. To achieve it, some additives were evaluated to preserve remaining enzyme activity at immobilization conditions. For this purpose, Xys1Δ soluble enzyme was

incubated with different additives at different concentrations (20%-50% (w/v)) at pH 10 and 25 ºC, as this enzyme was fairly unstable at these conditions (Aragon et al., 2013a): glycerol, trehalose and PEG6000. Results from thermal-inactivation of this biocatalyst at 25 ºC and pH 10 in the presence of these additives showed that glycerol at 50% (w/v) allowed the highest thermo-stabilization factor with respect to the soluble enzyme at specified conditions (**Figure 1**). Therefore, the Xys1Δ immobilization procedure was carried out in 50% glycerol at pH 10 by a two-step process: 4 h at 4 ºC, and 17.5 h at 20 ºC, before Schiff´s bases reduction (Guisán, 1988). The immobilization yield was 25% after first step, and the final immobilization yield was 92%. The expressed activity of the resulting biocatalyst, Ag-G-Xys1Δ-L (**Table 3**), was 28.24 U/g support, being 81.54% of total offered activity.

Figure 1. Thermal inactivation course of soluble Xys1 Δ at 25ºC pH 10 in the presence of additives. Symbols: soluble Xys1Δ in 100mM sodium carbonate buffer pH 10 (closed circle); 20% glicerol 100 mM sodium carbonate buffer pH 10 (closed square); 40% glicerol 100 mM sodium carbonate buffer pH 10 (closed triangle); 50% glycerol 100 mM sodium carbonate buffer pH 10 (open triangle); 20% PEG6000 100 mM sodium carbonate buffer pH 10 (closed diamond); 40% PEG6000 100 mM sodium carbonate buffer pH 10 (open circle); and 20% trehalose 100 mM sodium carbonate buffer pH 10 (star).

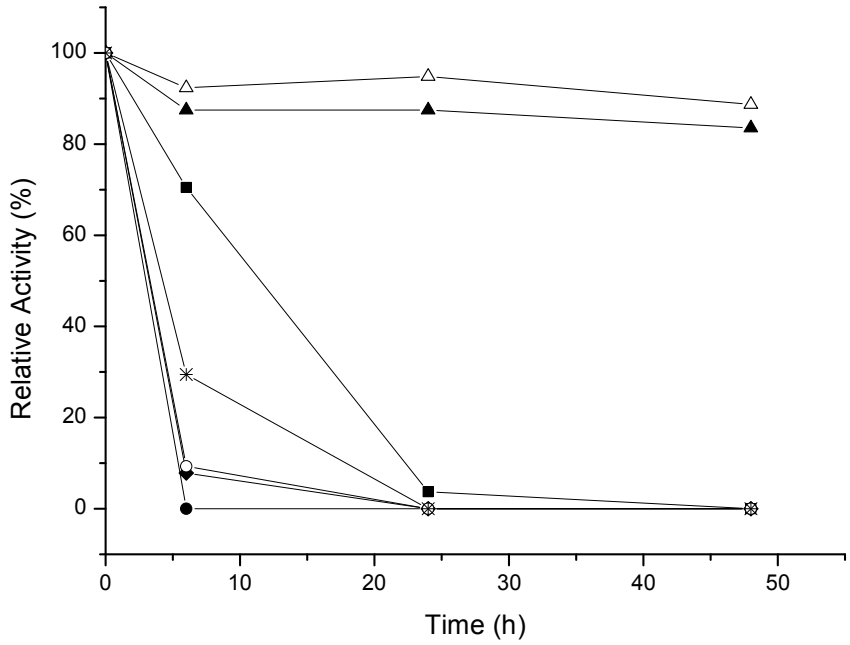

Besides Xys1Δ enzyme immobilization on Ag-G, the same enzyme was immobilized on Ag-CB. This immobilization protocol promotes covalent immobilization by only one point between the reactive groups of the support and the N-terminus of the protein. This biocatalyst is expected to exhibit similar properties to those of the native enzyme, thus preventing artifacts that may

occur with soluble proteins (interaction with hydrophobic interfaces, aggregation with other proteins, etc.) (Bolivar et al., 2012). For this reason, the resulting biocatalyst from the immobilization of this enzyme on Ag-CB with a protein loading value of 10 mg/g support, Ag-CB-Xys1Δ-L (**Table 3**), was used as control for further thermal inactivation studies. These thermal inactivation studies aimed to evaluate thermo-stabilizing properties of different modifications by surface coating with polymers, together with the Ag-G-Xys1Δ-L biocatalyst.

5.1.2. Surface coating of the immobilized Ag-G-Xys1Δ-L biocatalyst with a first layer of different derived dextran polymers by chemical modification via covalent binding

The surface of this biocatalyst was chemically modified, via covalent binding, with three derived dextran polymers, each one harboring a different pattern of chemical groups (**Figure 2**), and at different coating degrees. Each derived dextran polymer consisted of one size dextran polymer (40,000 Da molecular weight) which was oxidised up to 100% to yield poly-aldehyde (Dex100); oxidised up to 80% and then reduced to yield poly-hydrolxyl, and then, oxidised up to 20% to yield poly-aldehyde (Dex20-80); or oxidised up to 20% to yield poly-aldehyde (Dex20); (see *Introduction* section; **Figure 2**). Aldehyde groups would react with enzyme surface amino groups to form a covalent bond. Each derived dextran polymer was covalently bound to the immobilized enzyme surface at three different coating degrees: 0.15 g dextran/g biocatalyst (low coating degree); 0.8 g dextran/g biocatalyst (medium coating degree); and 4 g dextran/g biocatalyst (high coating degree).

When the surface of immobilized Ag-G-Xys1Δ-L biocatalyst was coated with a first layer of Dex100, the degree of recovered activity was very low (25%). The effect was the same regardless surface coating degree. On the contrary, when the surface was coated with a first layer of Dex20 or Dex20-80 (62% - 100%), almost all the immobilized activity was retained with all degrees of surface coating.

Figure 2. Schematic representation of one size dextran polymer (40,000 Da molecular weight) with different chemical modifications: an unmodified dextran molecule which consists of α-1,6 glycosidic linkages between glucose molecules (A); an oxidised dextran molecule (by the addition of $NaIO_4$) which harbours aldehyde groups (B); and a reduced dextran molecule (by the addition of $NaIO_4$, firstly, and $NaBH_4$, secondly), which harbours hydroxyl groups.

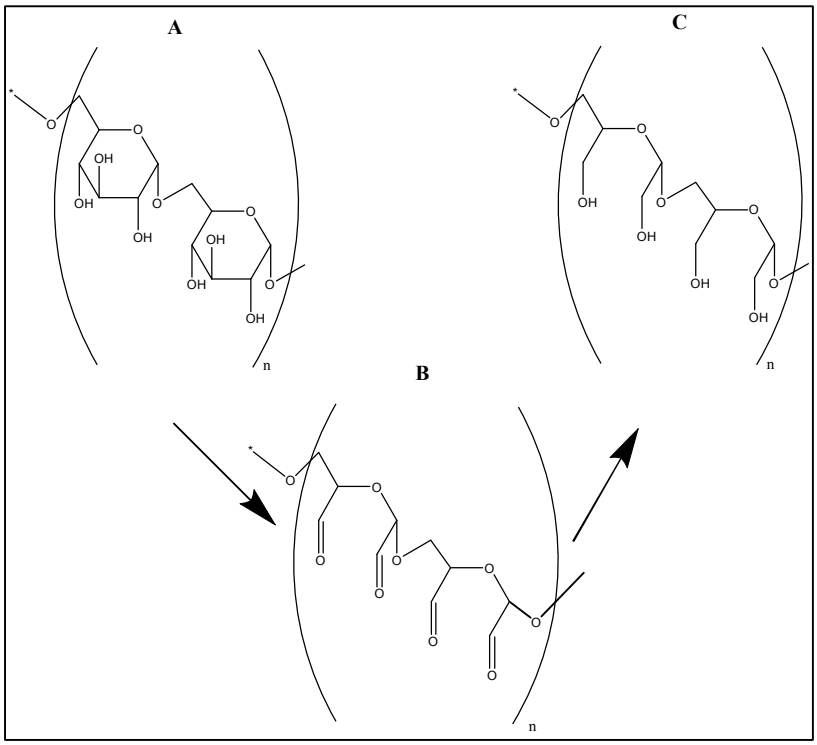

With the aim to evaluate if surface coating with a first layer of these derived dextran polymers exerted a protection effect against high temperature, all these chemically modified Ag-G-Xys1Δ-L biocatalysts were incubated at pH 7 and 70ºC along with the unmodified Ag-G-Xys1Δ-L and Ag-CB-Xys1Δ-L biocatalysts, which were used as control. Under these inactivation conditions, the Xys1Δ enzyme immobilized on Ag-CB (Ag-CB-Xys1Δ-L) was inactivated immediately. At a lower temperature, 50 ºC (and pH 7), Ag-CB-Xys1Δ-L was 62-fold less stable than Ag-G-Xys1Δ-L. At 50ºC and pH 5, this difference in thermal-stability was still more evident; Ag-CB-Xys1Δ-L was 150-fold less stable than Ag-G-Xys1Δ-L.

Results from thermal inactivation of all these chemically modified biocatalysts are shown in **Table 4**. Only when the surface of Ag-G-Xys1Δ-L biocatalyst was coated with Dex20-80, there was a thermo-stabilization effect (stabilization factor of 5 with respect to Ag-G-Xys1Δ-L and 305 with respect to Ag-CB- Xys1Δ-L, at pH 7 and 70ºC) with the lowest coating degree (0.15 g dextran/g biocatalyst). In this case, higher degrees of polymer coating did not cause any further stabilizing effect. Therefore, this modified biocatalyst (termed Ag-G-Xys1ΔL+Dex20-80

biocatalyst; **Table 3**) was selected to carry out coating with a second layer of PEI via ionic exchange.

5.1.3. Surface coating of the immobilized Ag-G-Xys1Δ-L biocatalyst with a first layer of a cationic polymer, polyethylenimine (PEI), by chemical modification via ionic exchange

Besides, the surface of this biocatalyst was chemically modified, via ionic binding, with a first layer of PEI with molecular weight ranging from 1,300 to 70,000 Da, and at different coating degrees (0.01-10 g/g immobilized Xys1Δ biocatalyst). No loss of activity of this biocatalyst was observed after all these surface modifications.

To evaluate if surface coating with a first layer of this cationic polymer exerted a protection effect against temperature, all these chemically modified Ag-G-Xys1Δ-L biocatalysts were incubated at pH 7 and 70ºC along with the unmodified Ag-G-Xys1Δ-L biocatalyst.

Results from thermal inactivation of all these chemically modified biocatalysts are shown in **Table 4**. All surface modifications of Ag-G-Xys1Δ-L biocatalyst with PEI polymer of different molecular weight at different coating degrees, promoted stabilizing effects. However, the highest thermo-stabilization factor (stabilization factor of 4.5 with respect to the unmodified Ag-G-Xys1Δ-L biocatalyst, and at least 285 with respect to the Ag-CB-Xys1Δ-L biocatalyst at pH 7 and 70ºC) was obtained by surface coating with PEI of 25,000 Da molecular weight and at 0.1 g/g biocatalyst. Higher molecular weights or coating degrees did not promote higher stabilization factors. Therefore, this modified Ag-G-Xys1Δ-L biocatalyst (termed Ag-G-Xys1Δ-L+PEI biocatalyst; **Table 3**) was selected to carry out coating with a second layer of derived dextran polymer via covalent binding.

5.1.4. Surface coating of the immobilized Ag-G-Xys1Δ-L biocatalyst with a second layer of derived dextran and PEI polymers via covalent and ionic binding, respectively

To further increase the thermo-stability of these two modified Ag-G-Xys1Δ-L biocatalysts, Ag-G-Xys1Δ-L+Dex20-80 and Ag-G-Xys1Δ-L+PEI, their surfaces were chemically modified by surface coating with a second layer of the other polymer, thus allowing the formation of a bilayer of polymers. So, the surface of Ag-G-Xys1Δ-L+Dex20-80 biocatalyst was modified

with a second layer of PEI of 25,000 Da molecular weight at a ratio of 0.1 g/g biocatalyst (resulting in Ag-G-Xys1Δ-L+Dex20-80+PEI biocatalyst; **Table 3**). In addition, the surface of Ag-G-Xys1Δ-L+PEI biocatalyst was modified with a second layer of Dex20-80 at a ratio of 0.15 g dextran/g biocatalyst (resulting in Ag-G-Xys1Δ-L+PEI+Dex20-80 biocatalyst; **Table 3**).

Figure 3.Time-courses of thermal inactivation at 70 ºC pH 7 of **A)** Xys1Δ-L immobilized on Ag-G (Ag-G-Xys1Δ-L; *closed square*); Ag-G-Xys1Δ-L biocatalyst modified by coating with 25 kDa PEI (Ag-G-Xys1Δ-L+PEI; *closed circle*); Ag-G-Xys1Δ-L modified by coating with a bilayer of 25 kDa PEI and Dex20-80 (Ag-G-Xys1Δ-L+PEI+Dex20-80; *closed diamond*); Ag-G-Xys1Δ-L modified by coating with Dex20-80 (Ag-G-Xys1Δ-L+Dex20-80; *closed traingle*); Ag-G-Xys1Δ-L modified by coating with a bilayer of Dex20-80 and 25 kDa PEI (Ag-G-Xys1Δ-L+Dex20-80+PEI; *open square*); **B)** Xys1Δ-H immobilized on Ag-G (Ag-G-Xys1Δ-H; *closed square*); Ag-G-Xys1Δ-H biocatalyst modified by coating with 25 kDa PEI (Ag-G-Xys1Δ-H+PEI*; closed circle*); Ag-G-Xys1Δ-H biocatalyst modified by coating with Dex20-80 (Ag-G-Xys1Δ-H+Dex20-80; *closed triangle*); and Ag-G-Xys1Δ-H modified by coating with a bilayer of Dex20-80 and 25 kDa PEI (Ag-G-Xys1Δ-H+Dex20-80+PEI; *open square*).

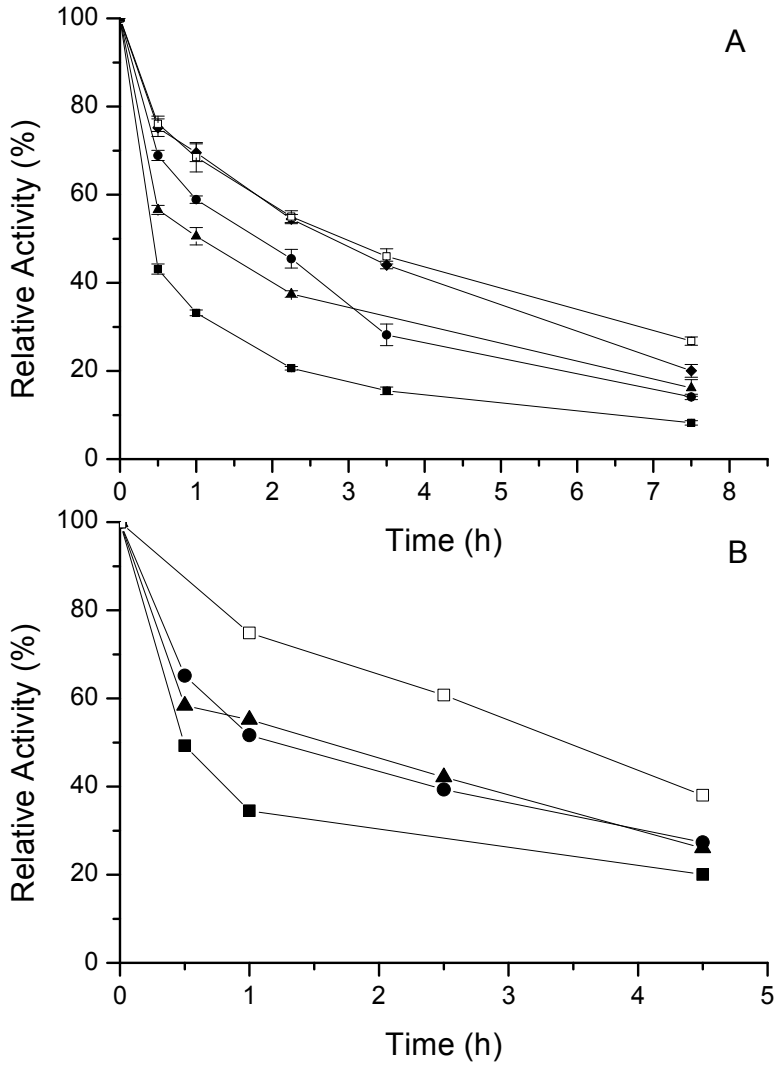

Results from thermal inactivation of these chemically modified biocatalysts (**Figure 3A**), indicated that when the surface of the Ag-G-Xys1Δ-L biocatalyst was modified by coating with a first layer through either, covalent binding with Dex20-80, or through ionic binding with PEI, there was a stabilizing effect, of 5 and 4.5, respectively, in reference to the unmodified Ag-G-Xys1Δ-L biocatalyst at 70ºC and pH 7, and at least 305 and 285, respectively, in regard to the Ag-CB-Xys1Δ-L biocatalyst (**Table 4**). Furthermore, when the surface of these two modified biocatalysts, were respectively modified by coating with a second layer through ionic binding with PEI (Ag-G-Xys1Δ-L+Dex20-80+PEI), or covalent binding with Dex20-80 (Ag-G-Xys1Δ-L+PEI+Dex20-80), considerably higher stabilization factors, of 8.1 and 7.5, were achieved, with respect to the stabilization factors obtained for the unmodified Ag-G-Xys1Δ-L biocatalyst (and at least 506 and 471 in respect to the Ag-CB-Xys1Δ-L biocatalyst; **Table 7**). In addition, surface coating with a bilayer formed by a first layer of Dex20-80 and a second layer of PEI seemed to promote a slightly higher stabilization effect. Therefore, in terms of thermo-stability, the optimised immobilized Ag-G-Xys1Δ-L biocatalyst by surface coating with a multilayer of polymers was the Ag-G-Xys1Δ-L+Dex20-80+PEI biocatalyst (**Table 3**).

5.1.5. Immobilization of the Xys1Δ enzyme on glyoxyl-activated agarose beads with high protein loading and surface coating with optimal chemical modifications with a monolayer and a bilayer of polymers

It should be also taken into account that a biocatalyst with high protein loading is expected to considerably increase reaction yield while proccess costs are maintained. So, with the aim to increase the yield of xylan hydrolysis reaction for XOS production in batch mode, an immobilized Xys1Δ biocatalyst with high protein loading was carried out. The immobilization procedure to obtain an immobilized Xys1Δ biocatalyst with high protein loading (termed Ag-G-Xys1Δ-H biocatalyst; **Table 3**) was developed in 50% glycerol at pH 10 and at 4 ºC for 120 h, before imine bonds reduction (Guisán, 1988). Immobilization yield was 92% and expressed activity was 78.6 U/g support.

Thermo-stability of the resulting immobilized biocatalyst with high protein loading, Ag-G-Xys1Δ-H biocatalyst (**Table 3**), was increased by surface coating with a layer and a bilayer of polymers. For this purpose, the same optimal chemical modifications as the ones obtained for the immobilized biocatalyst with low protein loading (Ag-G-Xys1Δ-L biocatalyst; **Table 3**) were applied to the Ag-G-Xys1Δ-H biocatalyst. Coating degrees for each of them were evaluated for this biocatalyst.

Thermal inactivation results indicated that coating by covalent binding with Dex20-80 polymer also promoted stabilization effects on this immobilized biocatalyst with high protein loading at the lowest coating degree (stabilization factor of 2.9; **Table 7**). Higher coating degrees did not allow significantly higher stabilization factors.

When the surface of the unmodified Ag-G-Xys1Δ-H biocatalyst was coated with PEI of 25,000 Da molecular weight by ion exchange, the highest thermo-stabilization effect is obtained with a coating degree of 1 g/g biocatalyst (**Table 7**). So, the two optimal modifications by coating with a monolayer of these two polymers were surface coating with Dex20-80 at 0.15 g dextran/g biocatalyst (resulting in the Ag-G-Xys1Δ-H+Dex20-80 biocatalyst; **Table 3**) and with 25,000 Da PEI at 1 g/g biocatalyst (resulting in the Ag-G-Xys1Δ-H+PEI biocatalyst; **Table 3**).

Finally, to further increase the thermo-stability of the Ag-G-Xys1Δ-H+Dex20-80 biocatalyst, the surface of this biocatalyst was modified with a second layer of PEI of 25,000 Da molecular weight at a ratio of 1 g/g biocatalyst (resulting in the Ag-G-Xys1Δ-H+Dex20-80+PEI biocatalyst; **Table 3**). As shown by results from thermal inactivation of these chemically modified biocatalysts (**Figure 3B**), the highest thermo-stabilization factor (thermo-stabilization factor of 6.7 with respect to the Ag-G-Xys1Δ-H biocatalyst at pH 7 and 70 ºC; and at least 550 with respect to Ag-CB-Xys1Δ-L biocatalyst at pH 7 and 70 ºC ; **Table 7**) was achieved by surface coating with a bilayer of Dex20-80 and PEI (Ag-G-Xys1Δ-H+Dex20-80+PEI biocatalyst; **Table 3**). This optimised biocatalyst, in terms of thermo-stability, was then used for hydrolysis reactions of xylan from different sources to produce XOS in batch mode, and to develop consecutive cyles of this hydrolysis reaction.

5.2. Increasing operational stability of the optimised immobilized Ag-G-Xys1Δ-H biocatalyst for xylan hydrolysis reaction to produce XOS at high temperatures in batch mode

As described in literature, derived dextran polymers and polyethylenimine polymers have been extensively used to modify the surface of enzymes to potentially enhance their thermo-stability (among other catalytic properties). The reason behind is that their chemical structures allow the generation of hydrophilic conditions around the enzyme molecule surface, thus creating a protective layer against distortion agents such as temperature. Due to the fact that interactions between this hydrophilic layer and enzymatic surface residues could also modify the structure of the catalytic cleft of this enzyme, selectivity towards xylan may be affected. For this reason, in this section, hydrolysis reactions of xylan from different sources were accomplished in batch mode. This reactions were carried out with the optimised immobilized Xys1Δ-H biocatalyst which was modified by surface coating with a bilayer of polymers (Ag-G-Xys1Δ-H+Dex20-80+PEI; **Table 3**), along with the unmodified Ag-G-Xys1Δ-H biocatalyst, used as reference. In addition, the operational stability of this optimised biocatalyst for this reaction in batch mode was evaluated.

5.2.1. Hydrolysis reactions of different sourced xylan with the optimised immobilized Xys1Δ biocatalyst in batch mode

Together with the positive effect that surface coating with a bilayer of polymers had on the immobilized Xys1Δ biocatalyst thermo-stability, the effect of this chemical modification on the reaction yield of xylan conversion into different XOS was evaluated.

With this aim, hydrolysis reactions of different sourced xylan were carried out with the optimised obtained biocatalyst, Ag-G-Xys1Δ-H+Dex20-80+PEI, and with the unmodified Ag-G-Xys1Δ-H biocatalyst, used as reference. Beechwood xylan; corncob xylan and wheat arabinoxylan were used as reaction substrates. Basing on dry weight analysis of insoluble fractions, they were shown to display different degrees of solubility, probably indicating different structural compositions. In the case of beechwood xylan, soluble fraction accounted for

Figure 4. Time-courses of hydrolysis reaction of xylan from different sources (from beechwood (**A and B**), from wheat (**C and D**) and from corncob (**E and F**) at pH 5 and 50 ºC catalyzed by 1% (w/v) of unmodified Ag-G-Xys1Δ-H biocatalyst (**A, C and E**) or Ag-G-Xys1Δ-H+ PEI+Dex20-80+PEI (**B, D and F**). Xylo-oligosaccharides concentrations are determined by the method described above: xylose (white bars), xylobiose (gray bars), and xylotriose (black bars).

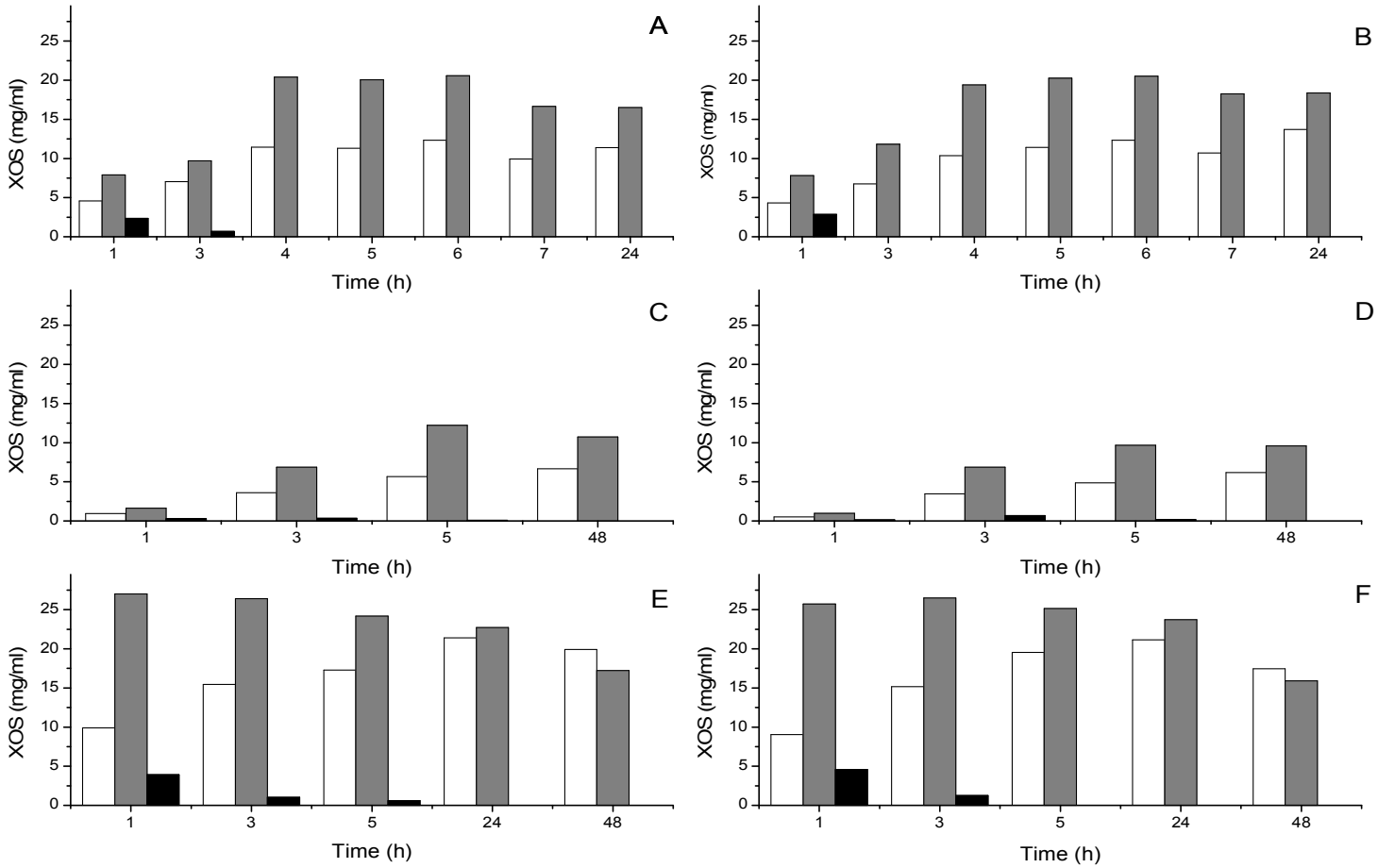

85.37% of the starting material; while soluble fractions obtained for corncob xylan and wheat arabinoxylan were 100% of their starting materials, respectively.

Hydrolysis reactions of each soluble xylan fraction at pH 5 were carried out with 1% (w/v) of the unmodified immobilized Ag-G-Xys1Δ-H biocatalyst, or the Ag-G-Xys1Δ-H+Dex20-80+PEI biocatalyst, at 50ºC under constant orbital agitation. Results from analysis of reaction products are shown in **Figure 4**. As observed, there was no significant difference between these two biocatalysts in terms of resulting xylan conversion yields into different XOS at any reaction time point for all studied xylan substrates. Xylobiose was observed to be the major reaction product when the three xylan types were used as reaction substrates (**Figure 4**). To confirm it, K_M and V_{max} kinetic parameters were calculated for these two biocatalysts using beechwood xylan as substrate. Values of Vmax were very similar; 10.62 U/ml and 13.62 U/ml for the unmodified and the modified biocatalysts, respectively. However, values of K_M were slightly different; 37.33 mg/ml and 53.25 mg/ml for the unmodified and the modified biocatalysts, respectively.

Focusing on the hydrolysis reaction of beechwood xylan with these two biocatalysts, the maximum total xylan conversion yield was 93%, and was reached at 4 h. It did not increase for 24 h of reaction. After 4 h of reaction, product mixture consisted only of xylose and xylobiose, with concentrations values of 11 mg/mL and 20 mg/mL, representing, respectively, the 35 % and the 64% of product mixture (**Figure 4A and 4B**).

Concerning the hydrolysis reaction of wheat arabinoxylan, the maximum total xylan conversion yield (44%) was achieved at 5 h of reaction course. However, XOS represented only 31% of total xylan.

In case of the hydrolysis reaction of corncob xylan, a maximum total xylan conversion yield of 100% was observed at 1 h of reaction course. At this time point, XOS mixture represented the 76%, with xylobiose concentration of 66%, while xylose and xylotriose accounted for 24% and 10%, respectively. However, at 24h of reaction course, only xylose (44%) and xylobiose (56%) were observed in the product mixture.

5.2.2. Consecutive cycles of hydrolysis reactions of xylan with the optimised immobilized Xys1Δ biocatalyst in batch mode

Afterwards, so as to evaluate the feasibility of reuse of the optimised Ag-G-Xys1Δ-H+Dex20-80+PEI biocatalyst, 15 cycles of hydrolysis reaction of beechwood xylan were carried out at the same conditions. Results are shown in **Figure 5**. As observed, xylan conversion yield to XOS was maintained for at least 15 consecutive hydrolysis reactions. This result means that not only thermo-stability of this immobilized biocatalyst was improved by surface coating with a bilayer of polymers, but also, its operational stability was increased accordingly.

Figure 5. Total xylan conversion yield (to xylose and to XOS) from consecutive cycles of soluble beechwood xylan hydrolysis reaction at pH 5 and 50 ºC catalyzed by 1% (w/v) of Ag-G-Xys1Δ-H +PEI+Dex20-80+PEI, in batch mode. Xylo-oligosaccharides concentrations are determined previously described.

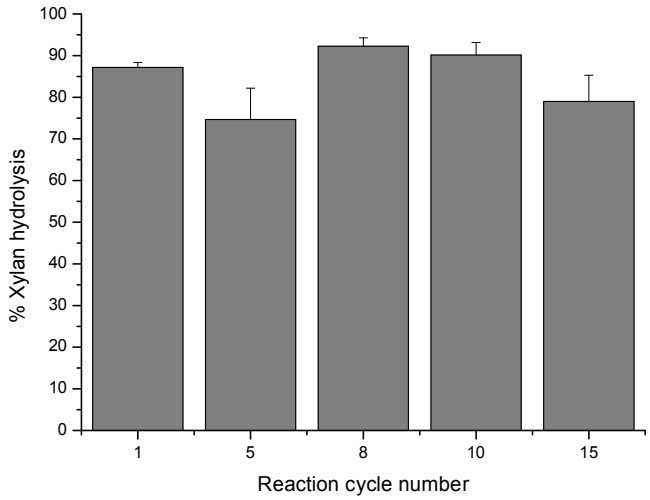

5.3. Increasing thermo-stability of the immobilized Xys1Δ biocatalyst by enhancement of multipoint covalent attachment via site-directed mutagenesis

As described in *Introduction* section, multipoint covalent attachment on glyoxyl-agarose based supports allows high values of stabilization against distortion agents such as high temperatures due to rigidification of the enzyme structure. Consequently, a strategy based on intensification of rigidification of the enzyme surface region involved in multipoint covalent attachment was developed to further increase these thermo-stabilization effects. For this purpose, additional lysine residues were introduced via conservative site-directed mutagenesis, thus, substituting native arginine residues by lysine ones, and so, providing this enzyme surface region with more points to potentially form covalent bonds with the immobilization support. Resulting enzyme variants were biochemically characterized and then immobilized on glyoxyl functionalized agarose support, along with wild type, which was used as reference. Finally, the thermo-stability of resulting biocatalysts was assessed.

5.3.1. Enzyme variants construction

The crystallographic structure of the Xys1Δ enzyme (PDB code: 1NQ6) was visualized with PyMOL (**Figure 6**). As a member of family 10 β-1,4-xylanases, this enzyme displays a typical $(\beta/\alpha)_8$ fold TIM barrel structure and presents two glutamic acid residues which take part in the double-displacement mechanism for hydrolysis of xylosidic bonds (Canals et al., 2003). One of these residues is glutamic acid residue 172, which acts as acid/base catalyst, and the other one is glutamic acid residue 280, which acts as nucleophile catalyst (**Figure 6A**). Fifteen different lysine residues were found all over this enzyme structure (**Figure 6B**), among which eight residues were observed to be almost located on the same plane (opposite to the active site) (**Figure 6C**), while the other six lysine residues seemed to be located on the same plane as the active site (**Figure 6D**). Accordingly, the region harbouring eight lysine residues was assumed to be susceptible to trigger stabilization via multipoint covalent attachment to the support. In this surface region, four additional arginine residues were located: 58 (**Figure 7A**), 201 (**Figure 7B**), 204 (**Figure 7C**), and 239 (**Figure 7D**), and so, they were selected to be replaced by lysine residues via conservative site-directed mutagenesis.

Figure 6. Schematic representation of crystallographic structure of Xys1Δ enzyme (PDB code: 1NQ6) visualized with PyMOL. As a member of family 10 β-1,4-xylanases, this enzyme displays a $(\beta/\alpha)_8$ fold TIM barrel structure: **A)** two glutamic acid residues which take part in the double-displacement mechanism for hydrolysis of xylosidic bonds are indicated, glutamic acid residue 172 (Glu172, green), which acts as acid/base catalyst acting as acid/base catalyst, and glutamic acid residue 280 (Glu280, yellow), which acts as nucleophile catalyst; **B)** 15 different lysine residues found all over this enzyme structure are indicated (red); **C)** 8 lysine residues which are observed to be almost located on the plane opposite to the active centre are indicated (red); and **D)** 6 lysine residues which are observed to be almost located on the same plane as the active centre are indicated (red).

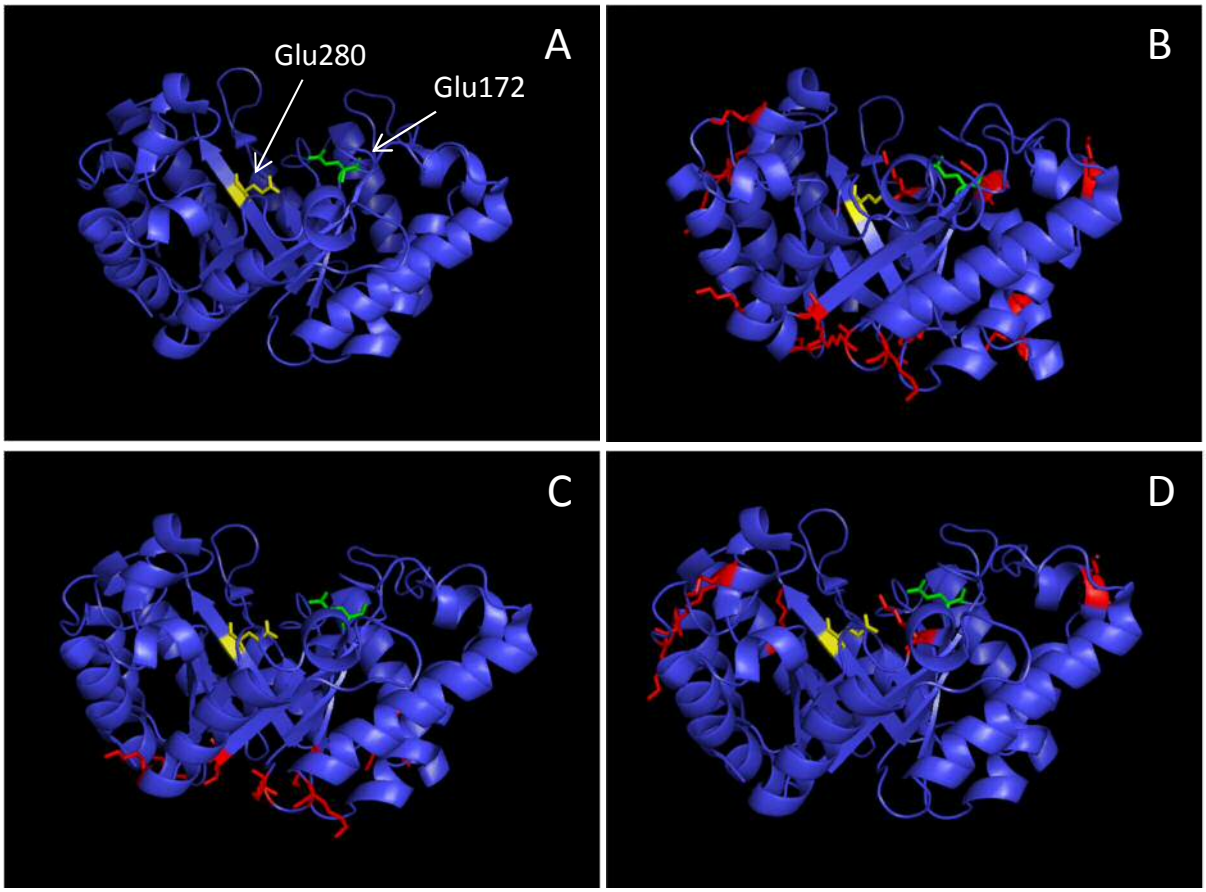

Therefore, four different Xys1Δ enzyme variants were constructed, each one displaying a different number of arginine residues replacements: arginine residue 58 by a lysine residue (resulting enzyme variant termed Xys1Δ-R58K); arginine residues 201 and 204 by lysine residues (resulting enzyme variant termed Xys1Δ-R201K-R204K); arginine residues 201, 204 and 239 by lysine residues (resulting enzyme variant termed Xys1Δ-R201K-R204K-R239K);

arginine residues 58, 201, 204, and 239 by lysine residues (resulting enzyme variant termed Xys1Δ-R58K-R201K-R204K-R239K).

Figure 7. Schematic representation of crystallographic structure of Xys1Δ enzyme (PDB code: 1NQ6) visualized with PyMOL, displaying a $(\beta/\alpha)_8$ fold TIM barrel structure. On the surface region located opposite to the active site where 8 lysine residues were found, four additional arginine residues were identified to be replaced by lysine residues: **A)** arginine residue 58 (Arg58, white); **B)** arginine residue 201 (Arg201, white); **C)** arginine residue 204 (Arg204, white); and **D)** arginine residue 239 (Arg239, white).

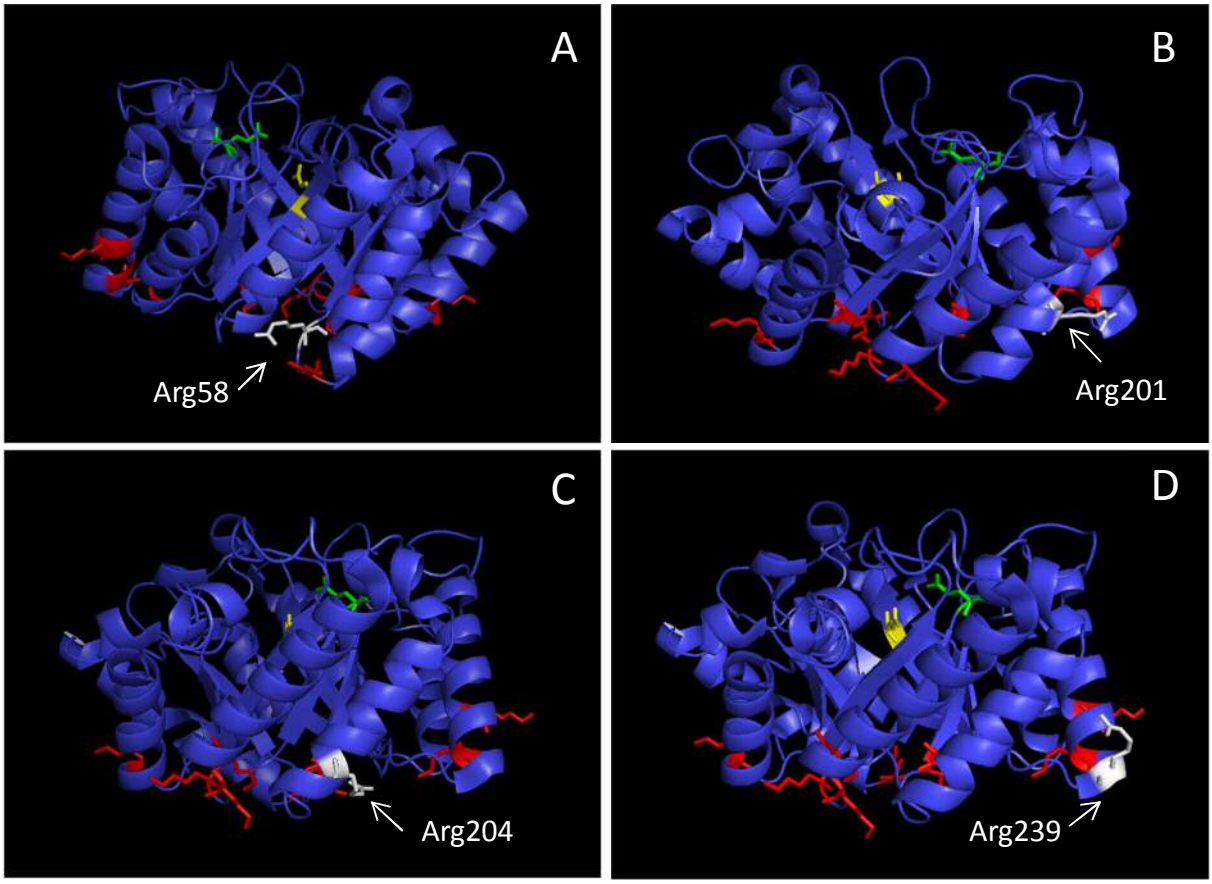

5.3.2. Enzyme variants purification and biochemical characterization

To evaluate if these residues replacements exerted any effect on kinetic properties of Xys1 enzyme, specific activity and kinetic parameters of purified Xys1Δ enzyme variants were evaluated at 25 ºC.

Beechwood xylan at different concentrations was used as substrate to compare kinetic parameters of resulting Xys1Δ enzyme variants to those of the wild type enzyme. Experimental data were subjected to linear fitting to the Michaelis–Menten model (Hanes-Woolf data calculation) and all correlation coefficients were above of 0.98. As shown in **Table 5**, the catalytic efficiency (K_{cat}/K_M) of different Xys1Δ variants was lower when compared to the wild type Xys1Δ. This decrease was principally due to the increase of the K_M, suggesting a negative contribution of all these residues replacements to the affinity towards this substrate.

5.3.3. Thermal inactivation of enzyme variants

Different purified Xys1Δ enzyme variants were immobilized on Ag-G (10BCL). Resulting immobilized Xys1Δ biocatalysts (Ag-G-Xys1Δ; Ag-Xys1Δ-R58K; Ag-G-Xys1Δ-R201K-R204K; Ag-G-Xys1Δ-R201K-R204K-R239K; and Ag-G-Xys1Δ-R58K-R201K-R204K-R239K) were evaluated for their thermo-stability so as to confirm if additional lysine residues, which were presumably forming more covalent bonds with the immobilization support, provided further thermo-stabilization effects.

According to results of thermal inactivation (**Figure 8B**), none of these immobilized enzyme variants biocatalysts displayed a higher degree of thermo-stability than their wild type counterparts. This should indicate that 1-4 additional covalent bonds formed between enzyme and immobilization support did not promote further thermo-stabilizing effects. This could probably lead to the conclusion that these additional covalent bonds did not provide more intense rigidification of the enzyme surface region involved in multipoint covalent attachment.

Figure 8. Time course of thermal inactivation, at 50 ºC pH 5 (**A**) or 65 ºC pH 5 (B), of different soluble (**A**) or immobilized (**B**) Xys1Δ biocatalysts: Xys1Δ-WT (closed square), Xys1Δ-R58K (closed circle), Xys1Δ-R201K-R204K (closed triangle), Xys1Δ-R201K-R204K-R239K (closed diamond) and Xys1Δ-R58K-R201K-R204K-R239K (closed star).

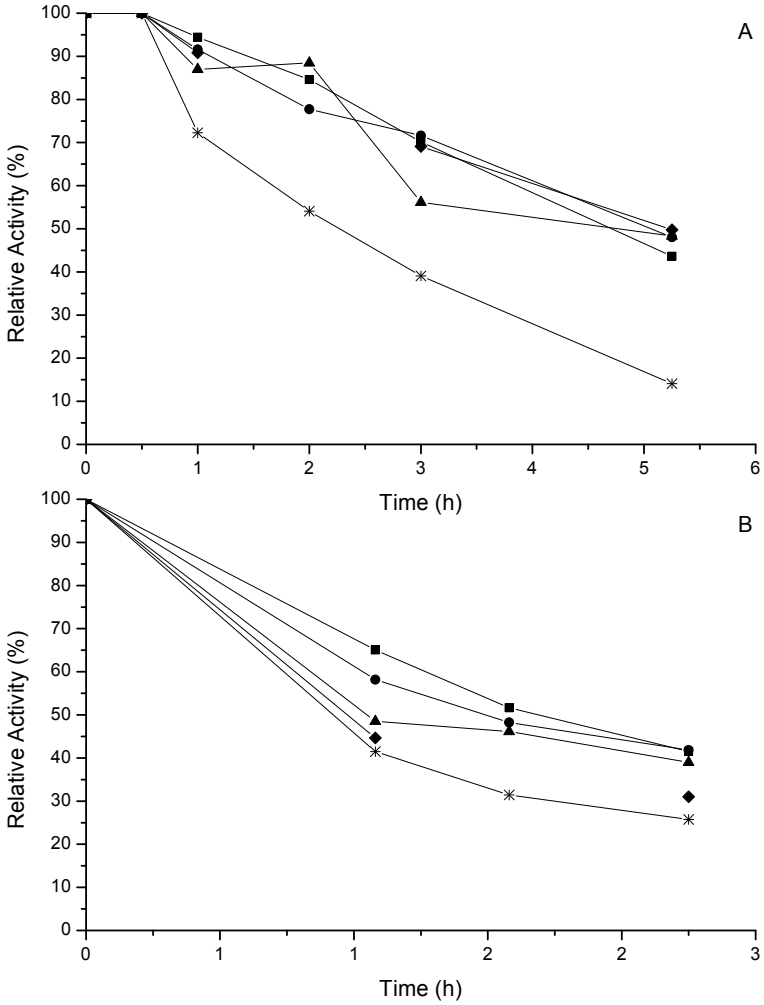

5.4. Increasing process productivity of continuous flow reaction of xylan hydrolysis to produce XOS by multipoint covalent immobilization of the Xys1Δ enzyme onto different methacrylic polymeric based supports

As described in the *Introduction* section, biocatalyzed processes could be also optimised by selection of the reactor system and by configuration of their mechanical and operational design. With this regard, continuous flow operated bioreactors will contribute to development of sustainable manufacturing while providing several operational advantages in comparison with batch reactors. Among these continuous flow operated reactors, PBRs are usually the choice for biocatalyzed processes.

An ideal immobilization support to develop immobilized enzyme biocatalysts for continuously operating PBRs should meet two important criteria: high enzyme loading onto its surface, to avoid recycling operations, and good mechanical properties to allow operation at high flow rates, thus providing high reaction productivities. Operating at high flow rates could be achieved by using immobilization supports consisting of methacrylic polymer matrices since the pressure drop produced by the bed is very low. Concerning the immobilization protocol, it should avoid enzyme leaching and preserve enzyme catalytic activity, while allowing high thermo-stability. Multipoint covalent immobilization on glyoxyl-functionalized agarose supports has been extensively described to deal effectively with these criteria.

With the aim of increasing process productivity of continuous flow reaction of xylan hydrolysis for XOS production in a PBR, different immobilized Xys1Δ biocatalysts were developed. These biocatalysts were achieved by multipoint covalent attachment on different methacrylic polymeric matrices. For this purpose, different commercial methacrylic matrices were firstly functionalized with glyoxyl groups. These glyoxyl-functionalized methacrylic based supports were physically characterized in order to determine the optimal support, in terms of area BET and pore size distribution. Immobilization of Xys1Δ enzyme onto these supports was then carried out, and the resulting biocatalysts were evaluated in terms of maximum protein loading and thermo-stability. A PBR was developed with the optimal biocatalyst, and was operated for continuous flow reaction of corncob xylan hydrolysis at different flow rates. For each one, xylan conversion yield to XOS and reaction volumetric and specific productivities were determined to optimise its operational design. Finally, effects of biocatalyst design on continuous flow operation of PBRs was assessed: protein loading onto support.

5.4.1. Synthesis of enzyme immobilization supports based on methacrylic polymer functionalized with glyoxyl groups

To allow multipoint covalent immobilization of Xys1Δ on different methacrylic polymer matrices, these were firstly functionalized with glyoxyl groups. For this purpose, three commercially available methacrylic supports previously activated with epoxy groups were selected. The reason behind is that epoxy groups can be chemically modified to glyoxyl groups by two simple reactions, and glyoxyl groups display high reactivity towards primary amino group of enzyme lysine residues while providing high values of stability (Mateo et al., 2013). In contrast, epoxy groups are reported to be scarcely reactive towards proteins even under slightly alkaline conditions (Mateo et al., 2007a). Relizyme™ EP403/S (termed R403S), Purolite® ECR8204F (termed P8204F) and Purolite® ECR8215F (termed P8215F) were functionalized with glyoxyl groups by two simple reactions: epoxy groups were firstly hydrolyzed with H_2SO_4 (Mateo et al., 2013) and resulting glyceryl groups were oxidised with $NaIO_4$ (Guisán, 1988). Resulting glyoxyl-functionalized methacrylic supports, R403S-G, P8204F-G and P8215F-G, yielded respectively 105.22; 101.6; and 25.7 $\mu mol_{glyoxyl\ groups}/g_{\ support}$ basing on $NaIO_4$ consumption (Nevell, 1963). According to results from SEM (**Figure 9A, 9B and 9C**) these supports beads displayed spherical morphology.

5.4.2. Physical characterization of different enzyme immobilization supports based on methacrylic polymer functionalized with glyoxyl groups

Physical characterization of these glyoxyl-functionalized methacrylic supports was carried out by Mercury Intrusion Porosimetry (MIP) and Adsorption Isotherm (AI). According to results (**Table 6**), the lowest value of area BET, 69.5 m^2/g, was provided by R403S-G support. This value was lower than total surface area reported for 10% crosslinked-agarose, 94 m^2/g (Molina-Rosell, 1993). However, values of area BET for G-P8204F and G-P8215F supports were considerably higher than total surface area obtained for 10% crosslinked-agarose. In addition, pore size distribution of R403S-G support reveals a pore diameter size range of 40 – 100 nm, being 80 nm the maximum peak value, and also, a very narrow pore size distribution was observed (**Figure 10A and 10B**). The absence of micropores and the low content of mesopores were confirmed by AI (**Figure 9D**). Pore size diameter estimated by MIP for G-P8204F and G-P8215F supports ranged from 20 to 100 nm (**Figure 10C and 10D**) and 80 to 300 nm (**Figure 10E and 10F**), respectively. In addition, G-P8215F seemed to contain a considerably higher proportion of micropore (**Figure 9F**). The high content of micropore of G-P8215F support could be also explained by the relatively high difference between the values of area BET (by

AI) and total pore area (by MIP), as MIP does not allow determination of the micropore fraction (**Table 6**).

Figure 9.SEM images (**A, B and C**) and Adsorption Isotherm (AI) result of pore size distribution (**D, E and F**) of different methacrylic polymer based supports functionalized with glyoxyl groups (short-arm aliphatic aldehyde groups): (**A, D**) Relizyme™ EP403/S (termed R403S-G); (**B, E**) Purolite® ECR8204F (termed P8204F-G); and (**C, F**) Purolite® ECR8215F (termed P8215F-G).

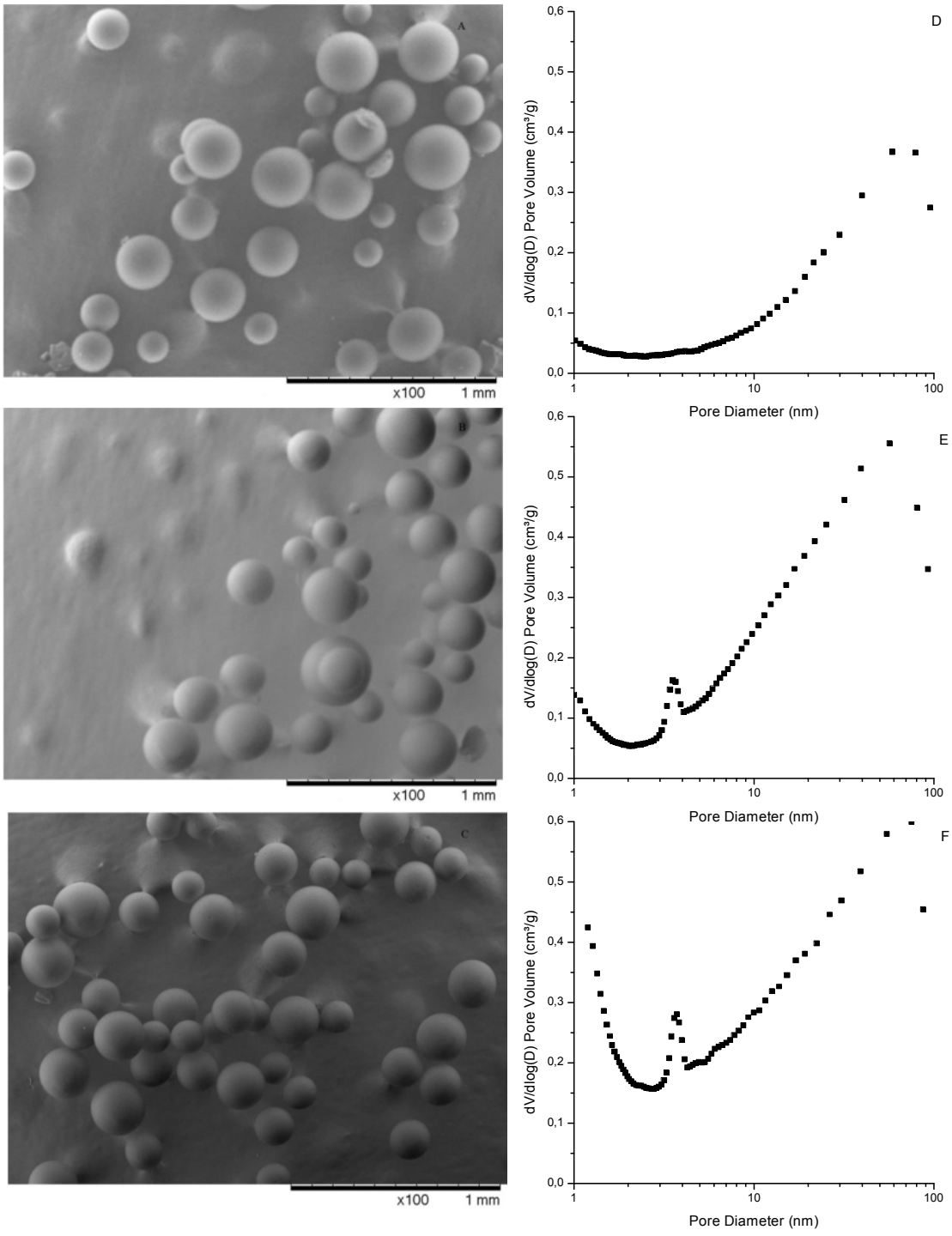

Figure 10. Mercury Intrusion Porosimetry (MIP) result of pore size distribution of different methacrylic supports functionalized with glyoxyl groups (short-arm aliphatic aldehyde groups) with (**A, C, E**) or without (**B, D, F**) inter-particle volume consideration: (**A, B**) Relizyme™ EP403/S (termed R403S-G); (**C, D**) Purolite® ECR8204F (termed P8204F-G); and (**E, F**) Purolite® ECR8215F (termed P8215F-G).

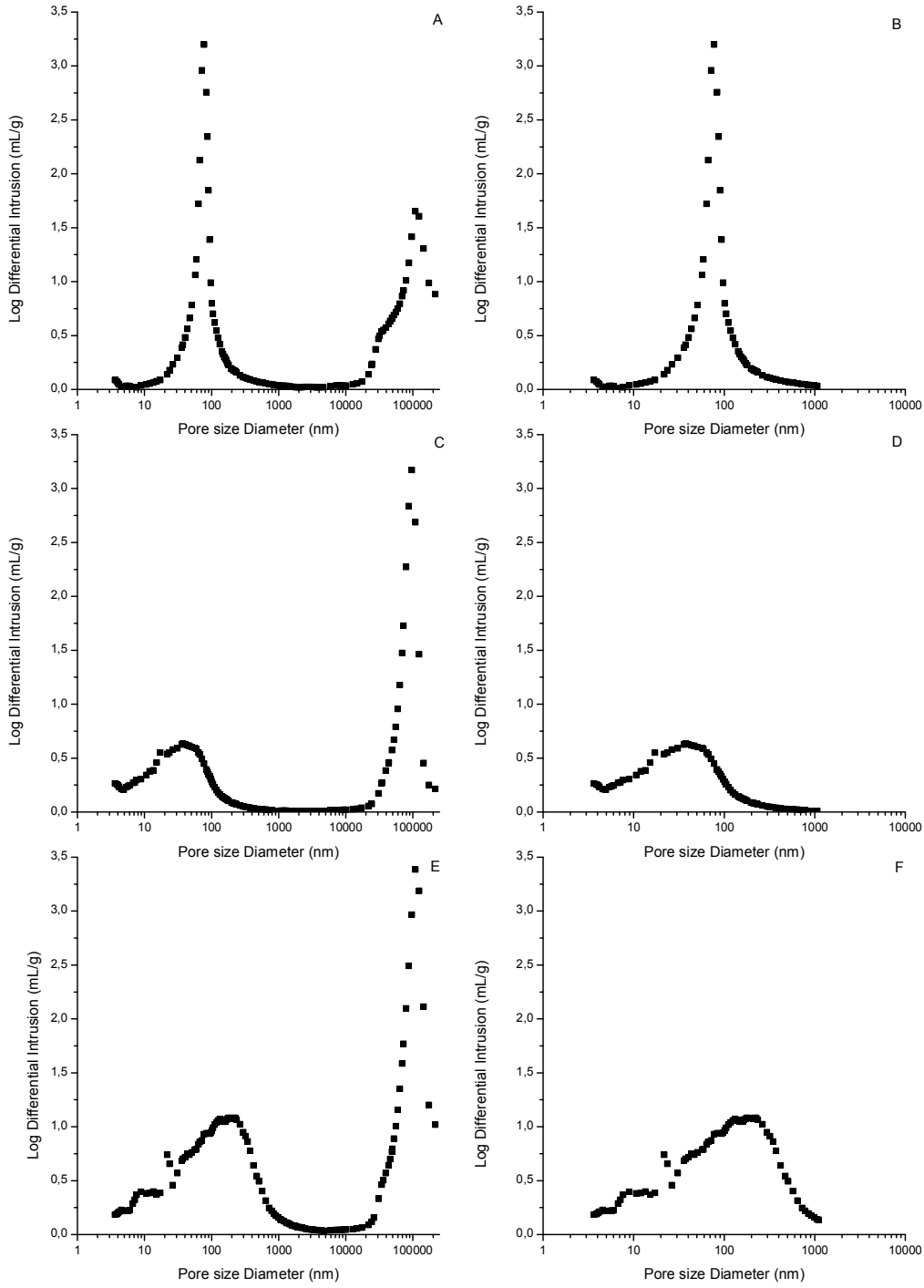

5.4.3. Immobilization of the Xys1Δ enzyme on enzymatic supports based on methacrylic polymer functionalized with glyoxyl groups

An immobilized Xys1Δ biocatalyst with maximum protein loading was then developed on each of these supports. The aim was to develop immobilized enzyme biocatalysts for continuously operating PBRs with one of the previously stated criteria, i.e. high enzyme loading onto support surface. Values of maximum protein loading will lead to determination of the optimal methacrylic support to develop a PBR for this reaction.

Figure 11. Time-course of Xys1Δ immobilziation (0.5 mg protein /g support) on Relizyme™ EP403/S support functionalized with glyoxyl groups (termed R403S-G) at pH 10 under different conditions: **A**) 50% (w/v) glycerol and 4 ºC; **B**) 0% (w/v) glycerol and 4 ºC; **C**) 50% (w/v) glycerol and 25 ºC; and **D**) 0% (w/v) glycerol and 25 ºC**.**

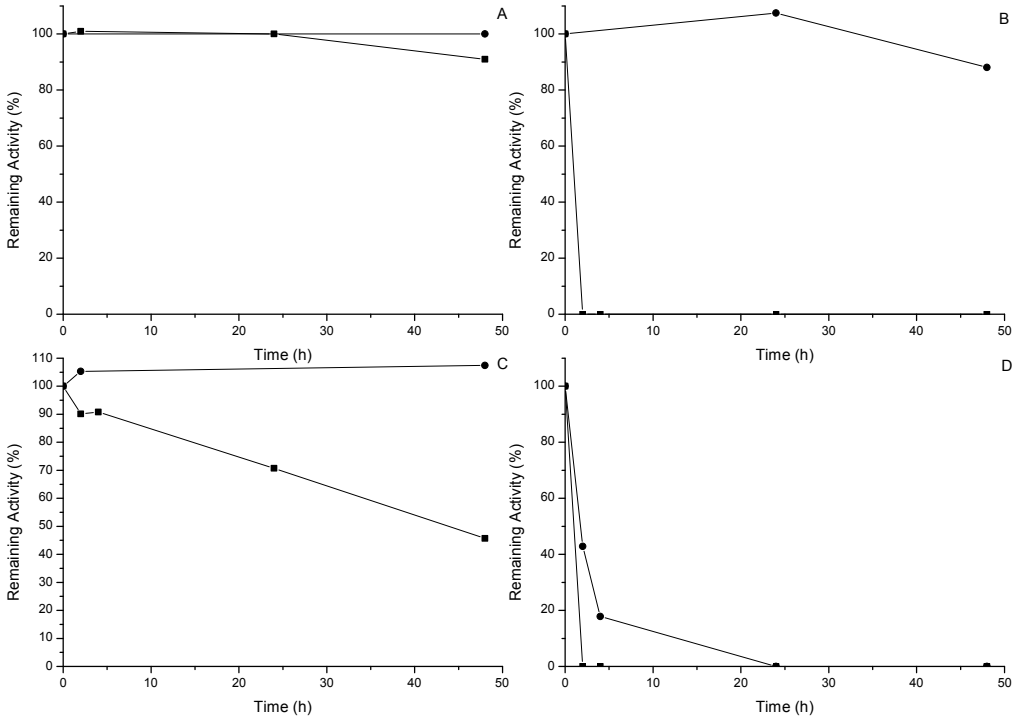

5.4.3.1. Determination of optimal immobilization condition for each glyoxyl-functionalized methacrylic support

Optimal immobilization conditions for immobilization of this enzyme on each support were firstly evaluated. For this purpose, the effect of two parameters on the immobilization yield was analyzed: temperature and the presence of glycerol in the immobilization medium. The immobilization procedure of the Xys1Δ enzyme on Ag-G at pH 10 was previously optimised to obtain high protein loading (20 mg/g support) and high recovered activity. It was achieved by using an immobilization medium consisting of 50% glycerol (w/v) and an immobilization temperature of 4 ºC, both of which allowed preservation of remaining enzyme activity during the immobilization process.

Figure 12. Time-course of Xys1Δ immobilziation (0.5 mg protein /g support) on Purolite® ECR8204F support functionalized with glyoxyl groups (termed P8204F-G) at pH 10 under different conditions: **A**) 50% (w/v) glycerol and 4 ºC; **B**) 0% (w/v) glycerol and 4 ºC; **C**) 50% (w/v) glycerol and 25 ºC; and **D**) 0% (w/v) glycerol and 25 ºC.

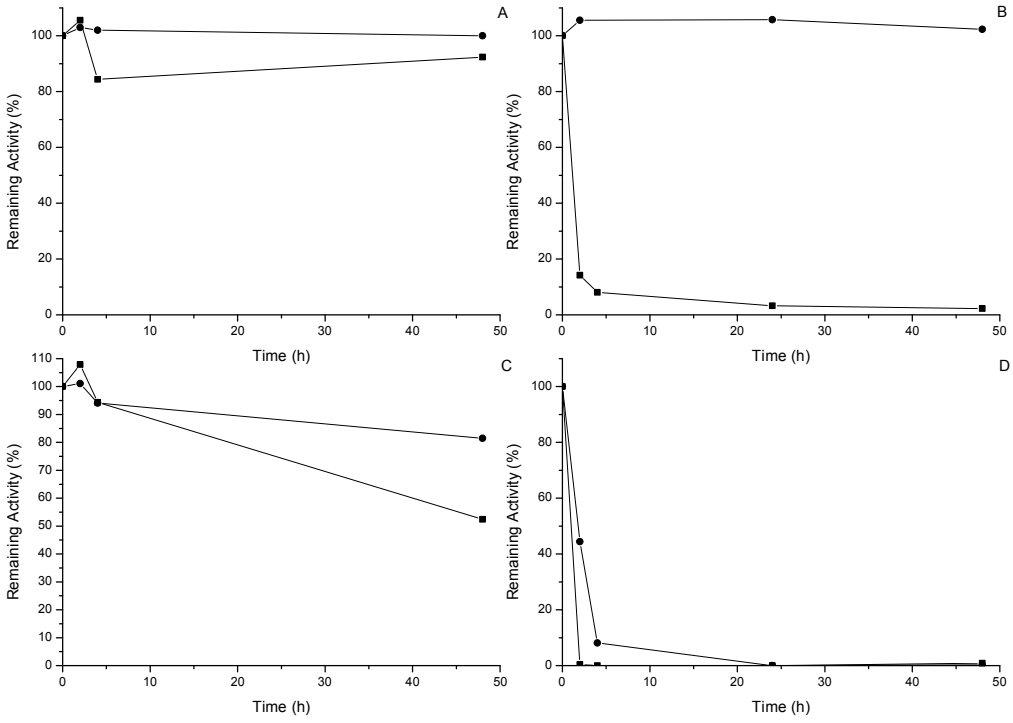

Results from immobilization prcedures of Xys1Δ on R403S-G (**Figure 11**), P8204F-G (**Figure 12**) and P8215F-G (**Figure 13**) supports pointed out that when both preserving conditions were used, the immobilization yield was very low, although the activity was completely preserved during the immobilization process (**Figures 11A, 12A and 13A**). Under opposite conditions (25

ºC and 0% glycerol), this enzyme was unstable (**Figures 11D, 12D and 13D**). In contrast, when this process was developed at 25 ºC in the presence of glycerol, almost all initial protein activity was preserved and the immobilization yield was around 50% (**Figures 11C, 12C and 13C**). In addition, decreasing temperature to 4 ºC and eliminating the use of glycerol drove to the highest immobilization yield (100% approximately) while remaining Xys1Δ enzyme activity was maintained (**Figures 11B, 12B and 13B**). Consequently, multipoint covalent immobilization of the Xys1Δ enzyme on glyoxyl-functionalized methacrylic supports was developed at pH 10 and 4 ºC for 96 h (without the use of any other preservative), before Schiff bases reduction (Guisán, 1988). These immobilization conditions were expected to provide an immobilized biocatalyst with a relatively high degree of heterogeneity of protein distribution on support surface since immobilization rates were considerably high, as previously described in literature (Bolivar et al., 2011).

Figure 13. Time-course of Xys1Δ immobilziation (0.5 mg protein /g support) on Purolite® ECR8215F support functionalized with glyoxyl groups (termed P8215F-G) at pH 10 under different conditions: **A**) 50% (w/v) glycerol and 4 ºC; **B**) 0% (w/v) glycerol and 4 ºC; **C**) 50% (w/v) glycerol and 25 ºC; and **D**) 0% (w/v) glycerol and 25 ºC.

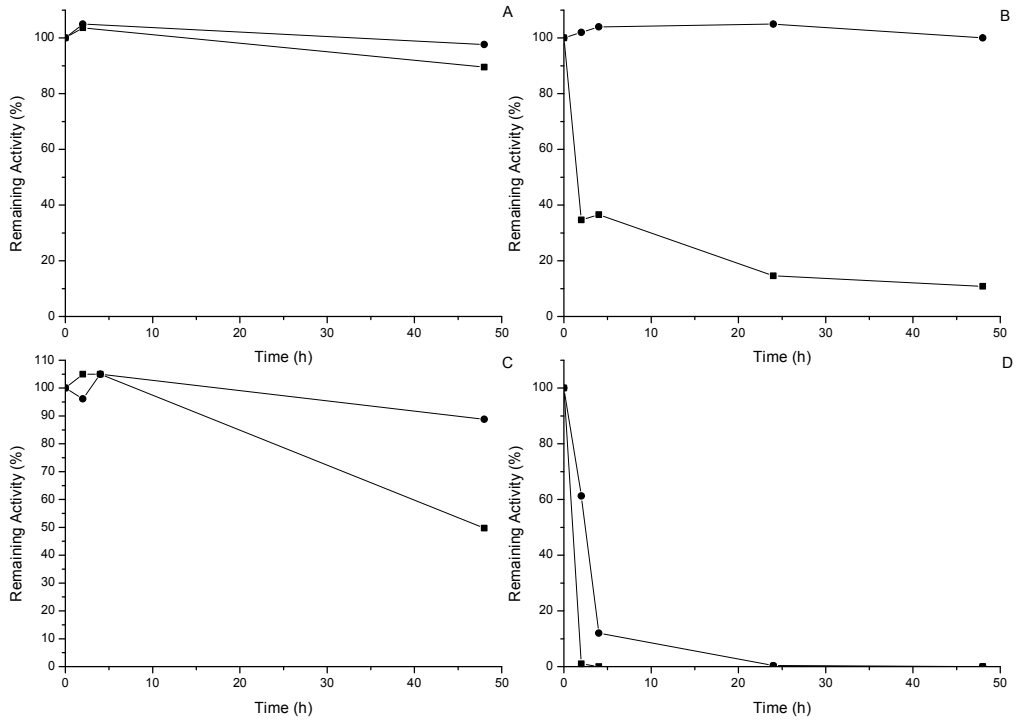

5.4.3.2. Determination of protein loading capacity for the Xys1Δ enzyme of each glyoxyl-functionalized methacrylic support

Three different immobilized Xys1Δ biocatalysts with maximum protein loading were carried out at the immobilization conditions specified above. The maximum immobilized protein loading value, 40 mg/g support, was achieved by Ag-G (**Figure 14A**). This value was considerably higher than the ones obtained for the three glyoxyl-functionalized methacrylic supports. Maximum protein loading values obtained for R403S-G, P8204F-G and P8215F-G were, respectively, 20, 20 and 10 mg/g support (**Figure 14A**). The same immobilization trend was observed with remaining xylanase activity (**Figure 14B**). Resulting immobilized Xys1Δ biocatalysts with maximum protein loading on Ag-G, R403S-G, P8204F-G, and P8215F-G were respectively termed Ag-G-Xys1Δ-40-HT; R403S-G -Xys1Δ-20-HT; P8204F-G-Xys1Δ-20-HT; and P8215F-G-Xys1Δ-10-HT biocatalysts. They displayed values of expressed activity of 62.64 U/g; 54.78 U/g; 59.36 U/g; and 20.96 U/g, respectively.

Figure 14. Time course of total immobilized protein (A) and total immobilized xylanase activity (B) during immobilization of Xys1Δ enzyme on different supports: Ag-G (closed triangle); R403S-G (closed square); P8204F-G (closed circle); and P8215F-G (closed diamond).

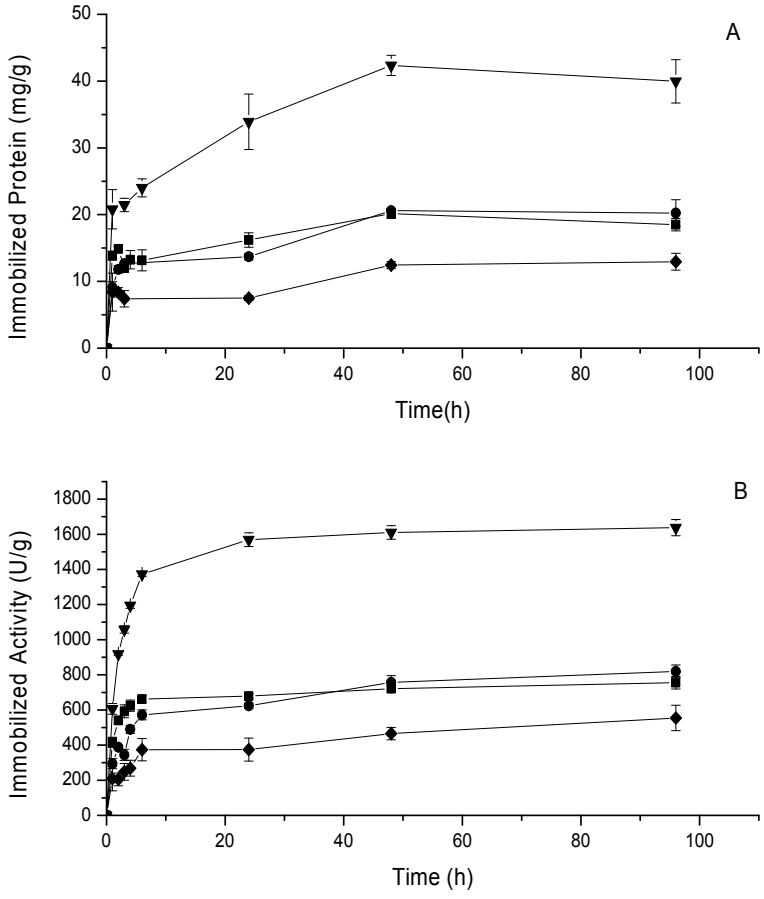

5.4.4. Thermal stability of different immobilized Xys1Δ biocatalysts

With the aim to determine the optimal Xys1Δ immobilized biocatalyst on methacrylic supports to develop a PBR for this continuous flow reaction, thermo-stability of different obtained biocatalysts was also evaluated. According to results from thermal inactivation (**Figure 15**), a different extent of thermo-stability was achieved by each immobilized biocatalyst. The immobilized biocatalyst on Ag-G (Ag-G-Xys1Δ-40-HT) presented the highest thermo-stability degree, followed by the immobilized biocatalyst on R403S-G (R403S-G -Xys1Δ-20-HT). The latter presented a considerably higher thermo-stability value than the ones immobilized on Purolite® supports (P8204F-G-Xys1Δ-20-HT and P8215F-G-Xys1Δ-10-HT).

Figure 15. Time course of thermal inactivation at 65ºC pH 5 of different immobilized Xys1Δ biocatalysts: Ag-G-Xys1Δ-40-HT (closed square), R403S-G-Xys1Δ-20-HT (closed circle), P8204F-G-Xys1Δ-20-HT (closed triangle) and P8215F-G-Xys1Δ-10-HT (star).

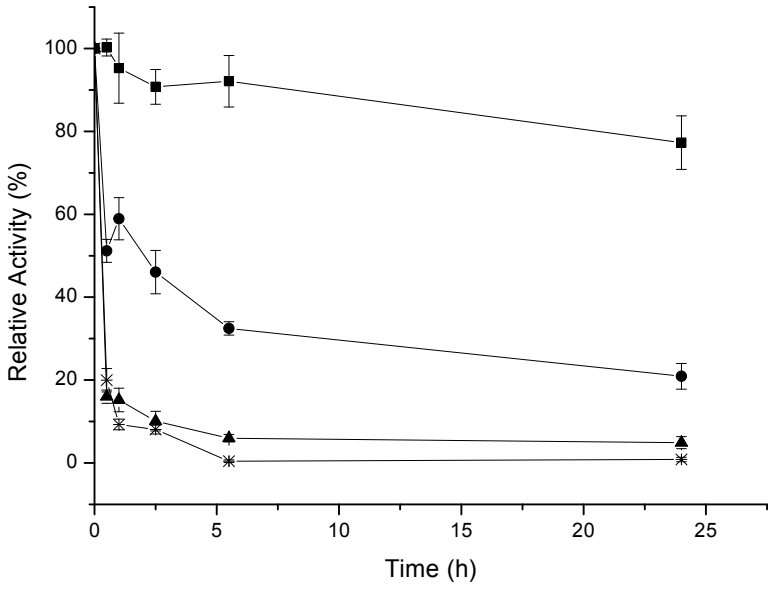

5.4.5. Continuous production of XOS in PBRs at different flow rates

To evaluate the small-scale feasibility of continuous flow operation of xylan hydrolysis for XOS production in a PBR, two different reactors were designed and constructed. They consisted of 8 mL FPLC columns which were packed with two immobilized biocatalysts: the optimal biocatalyst on glyoxyl-functionalized methacrylic support; and the immobilized biocatalyst on Ag-G (Ag-G-Xys1Δ-40-HT), which was used as reference. The former one was selected in terms of more adequate area BET and pore size distribution, maximum protein loading and thermo-stability, and was the R403S-G-Xys1Δ-20-HT biocatalyst. A flow stream of 4% corncob xylan (w/v) in 50 mM sodium acetate buffer pH 5 was pumped through the packed-bed columns at different flow rates.

The PBR implemented with the R403S-G-Xys1Δ-20-HT biocatalyst was operated at flow rates ranging from 0.1 mL/min to 10 mL /min to obtain residence times from 32.4 s to 54 min. In addition, the PBR implemented with the Ag-G-Xys1Δ-40-HT biocatalyst was operated at flow rates ranging from 0.1 mL/min to 3.5 mL/min. As stated by manufacturers, the latter upper range value was the maximum flow rate allowed for agarose beads based supports.

Analysis of exit flow stream from operating these two PBRs at different flow rates is shown in **Figures 16A and 16B**. At 0.5 mL/min flow rate, the maximum reaction yield was reached. Maximum reaction yield was achieved when xylan conversion yields to xylose and to xylobiose were 50% and 50%, respectively, according to batch reaction results from hydrolysis of corncob xylan (**Figure 4E**). At 24 h of this batch reaction course, corncob xylan conversion yields to xylose and to xylobiose were 50% and 50%, respectively, and they did not increase with longer reaction times (**Figure 4E**). Xylanase molecules exert their catalytic action by randomly cleaving β-(1→4)-linked xylose units from the homopolymeric backbone structure of xylan, thus releasing xylan molecules with different DP. These molecules are then cleaved again driving to generation of XOS with lower DP (Moreira and Filho, 2016). Therefore, a higher observed reaction rate leads to a higher proportion of XOS with lower DP in the reaction product. Accordingly, a lower observed reaction rate was achieved for both PBRs at a lower flow rate (0.1 mL/min). At flow rates higher than 0.5 mL/min, the observed reaction rate seemed to decrease with the flow rate for both PBRs (**Figures 16A and 16B**).

Figure 16. Effect of flow rate on continuous flow reaction of 4% (w/v) corncob xylan hydrolysis in 50 mM sodium acetate buffer at pH 5 and 30 ºC using different PBRs. **16A and 16C**) A PBR packed with a covalently immobilized Xys1Δ biocatalyst on methacrylic support functionalized with glyoxyl groups (R403S-G-Xys1Δ-20-HM biocatalyst). **16B and 16D**) A PBR packed with a covalently immobilized Xys1Δ biocatalyst on agarose-based support functionalized with glyoxyl groups by the same immobilization protocol (Ag-G-Xys1Δ-40-HT biocatalyst). **16A and 16B**) Effect of flow rate on xylan conversion yield to different reaction products in exit flow stream: xylose (white bars); xylobiose (light grey bars); xylotriose (grey bars); and xylotreose (dark grey bars). **16C and 16D**) Effect of flow rate on xylan conversion yield to xylose (white bars) and to XOS (striped grey bars).

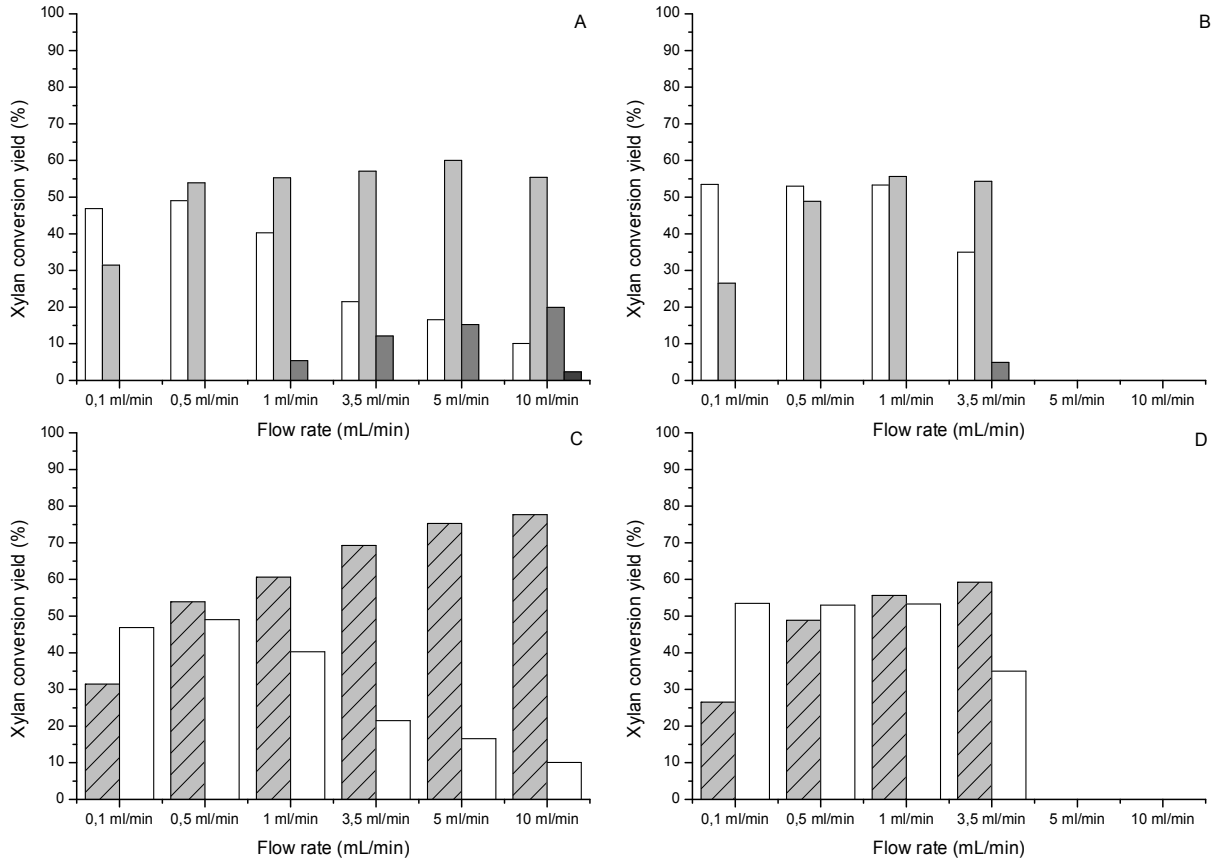

Total xylan conversion yields achieved at each flow rate for these two PBRs were calculated to quantify the previous observation, and are shown in **Figure 17**. For this purpose, 100% xylan conversion yield was considered to be 100% xylan converted to xylose; and so, 100% xylan converted to xylobiose was assumed to be 50% xylan conversion yield; 100% xylan converted to xylotriose was assumed to be 33% xylan conversion yield; and 100% xylan converted to xylotreose was assumed to be 25% xylan conversion yield. Under this theoretical assumption, xylan conversion yield was observed to linearly increase with residence time up to 5.4 min (1 mL/min flow rate).

Figure 17. Effect of residence time on total xylan conversion yield of continuous flow reaction of 4% (w/v) corncob xylan hydrolysis in 50 mM sodium acetate buffer at pH 5 and 30 ºC using a PBRs packed with a covalently immobilized Xys1Δ biocatalyst on methacrylic support functionalized with glyoxyl groups (R403S-G-Xys1Δ-20-HM biocatalyst).

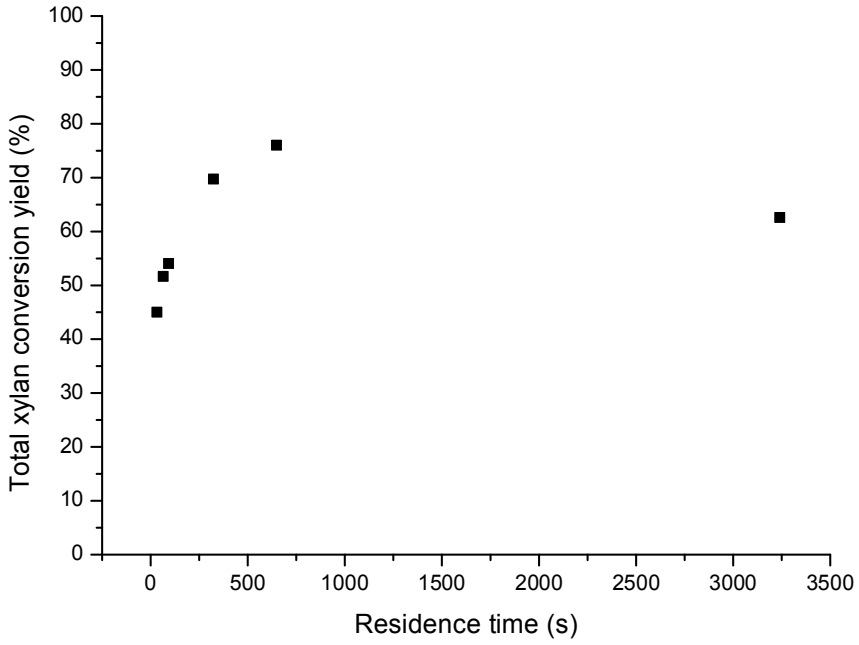

Concerning XOS production, the highest volumetric productivity for XOS (3,453 $g_{XOS}\ L^{-1}h^{-1}$) in continuous flow operation with these two PBRs was obtained at the highest flow rate, 10 mL/min. At this flow rate, only the immobilized biocatalyst on methacrylic support could be operated (**Figure 18A**). The highest specific productivity value was also reached with the PBR implemented with R403S-G-Xys1Δ-20-HT biocatalyst at the highest flow rate: 196.28 $g_{XOS}\ g_{enyme}^{-1}\ h^{-1}$ (**Figure 18B**).

Figure 18. **18A**) Effect of flow rate on volumetric productivity (rp) and **18B**) effect of flow rate on specific productivity (qp), for XOS of continuous flow reaction of 4% (w/v) corncob xylan hydrolysis in 50 mM sodium acetate buffer at pH 5 and 30 ºC using two PBRs packed with covalently immobilized Xys1Δ biocatalysts on different supports : on methacrylic support functionalized with glyoxyl groups (R403S-G-Xys1Δ-20-HM; closed square); on agarose-based support functionalized with glyoxyl groups by the same immobilization protocol (Ag-G-Xys1Δ-40-HT; closed circle).

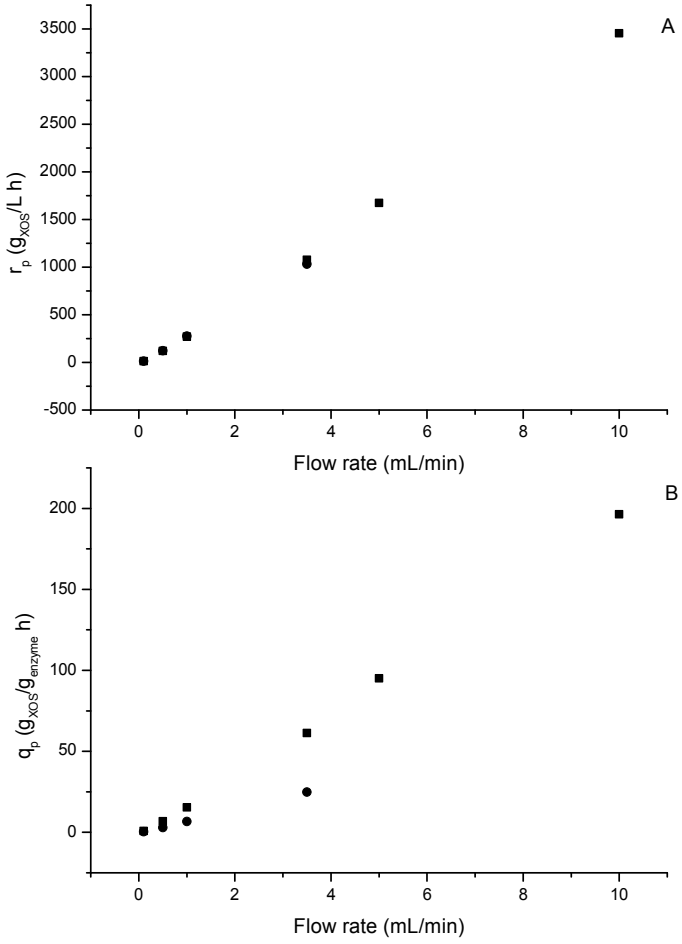

5.4.6. Effect of biocatalyst protein loading on continuous flow reactions in PBRs

The observed reaction rate increased with residence time with a PBR implemented with the R403S-G-Xys1Δ-20-HT biocatalyst up to 10.8 min, which corresponds to 0.5 mL/min flow rate. One possible explanation should be that residence time was shorter than reaction time up to 10.8 min, and so residence time was limiting the reaction. According to this hypothesis, at a residence time value of 54 min, the rate of substrate transport from bulk fluid to biocatalyst surface was lower than reaction rate, and so, external transport time was limiting the reaction. To confirm it, an experimental procedure has been followed. This experimental procedure has been proposed by Madon and Boudart and consists of a simple experimental criterion to determine the absence of artifacts in the measurement of rates of heterogeneous catalytic reactions (Madon and Boudart, 1982). The experiment involves different rate measurements on catalysts in which the concentration of active material has been purposely changed. In the absence of artifacts from transport limitations, the reaction rate is directly proportional to the active material. Basing on that, four different PBRs were developed with Xys1Δ immobilized biocatalysts on R403S-G with protein loading of 15 mg/g; 10 mg/g; 5 mg/g and 1 mg/g, respectively, and operated at 10 mL/min.

Results (**Figure 19A**) indicated that, at this flow rate, the observed reaction rate seemed to decrease for decreasing protein loading values. To confirm it, total xylan conversion yields were also calculated following the same theoretical assumption as above (**Figure 19B).** Volumetric and specific productivities for XOS were calculated, and shown in **Figure 20A and 20B, respectively**. The maximum specific productivity at 10 mL/min flow rate was achieved with a PBR consisting of Xys1Δ immobilized biocatalysts on R403S-G with protein loading of 1 mg/mg (R403S-G-Xys1Δ-1-HT biocatalyst). This was to 3,277 $g_{XOS}\ g_{enzyme}^{-1}\ h^{-1}$, 20-fold increased with respect to the one obtained with a protein loading value of 20 mg/g (196 $g_{XOS}\ g_{enzyme}^{-1}\ h^{-1}$) (**Figure 20B**).

Figure 19. Effect of protein loading of a PBR packed with a covalently immobilized Xys1Δ biocatalyst on methacrylic support functionalized with glyoxyl groups (R403S-G-Xys1Δ-20-HM biocatalyst) in a continuous flow reaction of 4% (w/v) corncob xylan hydrolysis in 50 mM sodium acetate buffer at pH 5 and 30 ºC. **19A**) Effect of protein loading on xylan conversion yield to different reaction products in exit flow stream: xylose (white bars); xylobiose (light grey bars); xylotriose (grey bars); and xylotreose (dark grey bars). **19B**) Effect of protein loading on volumetric productivity (rp) for XOS. **18C**) Effect of protein loading of this PBR on specific productivity (q_p) for XOS.

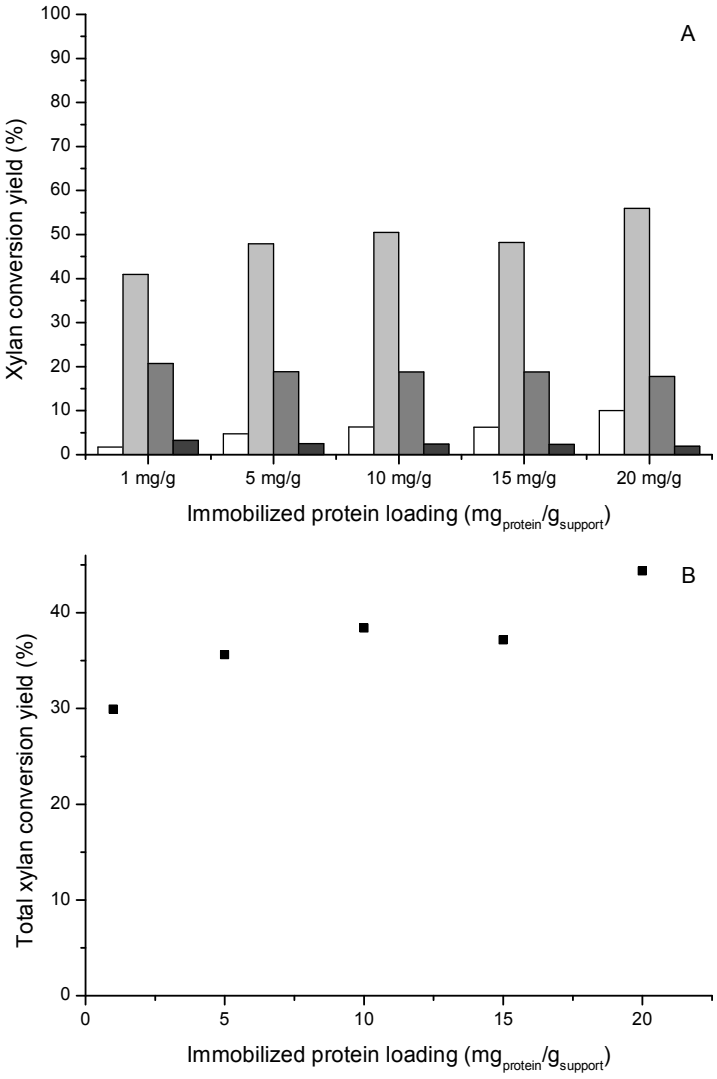

Figure 20. Effect of protein loading of a PBR packed with a covalently immobilized Xys1Δ biocatalyst on methacrylic support functionalized with glyoxyl groups (R403S-G-Xys1Δ-20-HM biocatalyst) in a continuous flow reaction of 4% (w/v) corncob xylan hydrolysis in 50 mM sodium acetate buffer at pH 5 and 30 ºC. **20A**) Effect of protein loading on volumetric productivity (r_p) for XOS. **20B)** Effect of protein loading on specific productivity (q_p) for XOS.

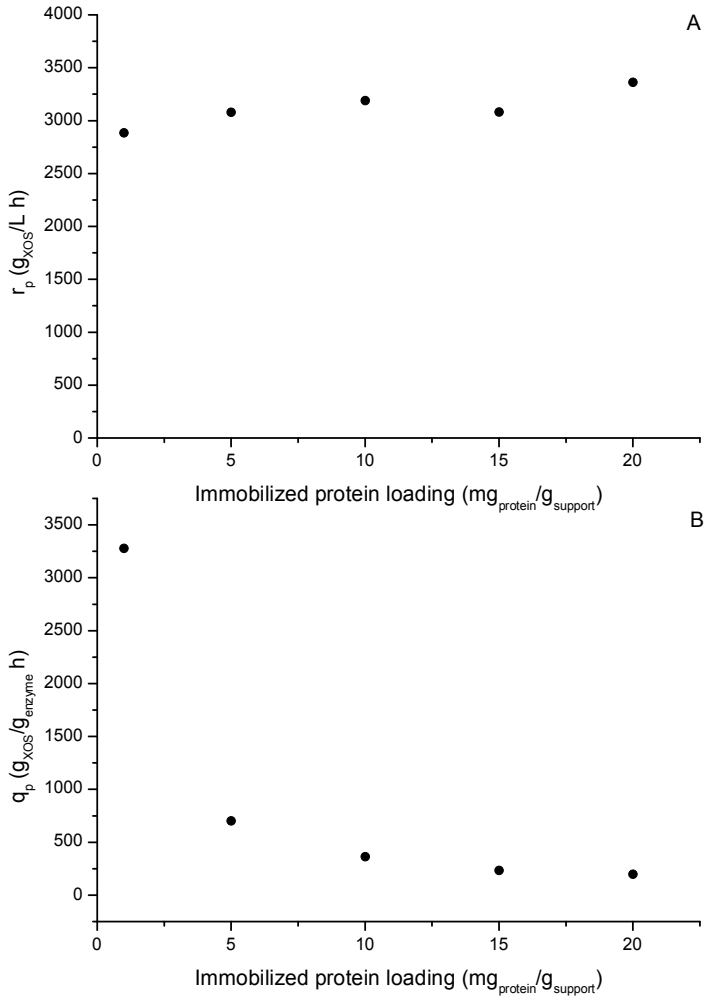

5.4.7. Comparative evaluation of continuous and discontinuous operation with the immobilized Xys1Δ biocatalyst on methacrylic support

Finally, the outcome from the hydrolysis reaction of corncob xylan for XOS production in continuous mode was compared to that of the one obtained in batch mode. For this purpose, this reaction was developed under the same conditions in a batch reactor using the R403S-G-Xys1Δ-5-HT biocatalyst. Results from analysis of reaction products at different time points of reaction

course are shown in **Figure 21**. Xylan conversion yields to xylose and to XOS at 2 h of reaction course were similar to those from continuous flow reaction at 10 mL/min with the R403S-G-Xys1Δ-1-HT biocatalyst.

Figure 21. Time-course of 4% corncob xylan hydrolysis reaction in 50 mM sodium acetate buffer at pH 5 and 30 ºC in batch mode using 1% (w/v) of a covalently immobilized Xys1Δ biocatalyst on methacrylic support functionalized with glyoxyl groups with a protein loading value of 5 mg/g (R403S-G-Xys1Δ-5-HT biocatalyst). **21A**) Xylan conversion yield to xylose (white bars); xylobiose (light grey bars); xylotriose (grey bars); and xylotreose (dark grey bars). **21B**) xylan conversion yield to xylose (white bars) and XOS (striped grey bars).

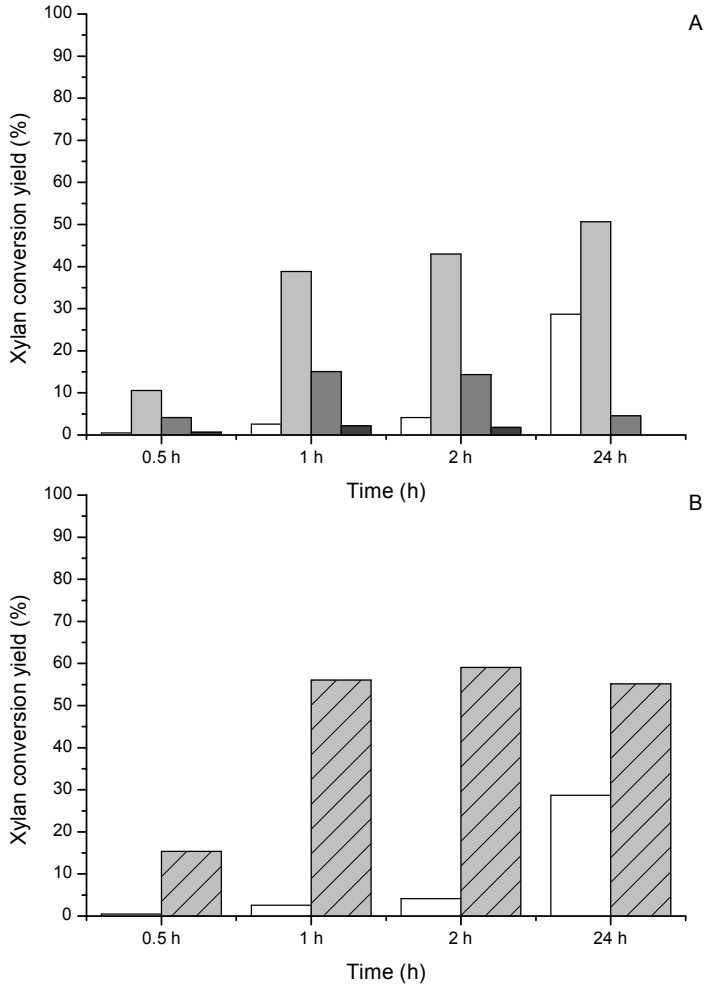

6. Tables

Table 1. List of plasmids used.

Plasmid	Description	Reference
pXHis1	pIJ2925 derivative containing the XYSA gene, which encodes the catalitic domain of the xylanase Xys1Δ, with a tag of six histidine residues, under the control of *xysA* promoter and flanked by the terminator of the methylenomycin resistance gene (T1) and the terminator of phage *fd* (T2)	(Adham et al., 2002)
pXHis1-R58K	pXHis1 derivative carrying Arg58Lys residue replacement	This work
pXHis1-R201K-R204K	pXHis1 derivative carrying Arg201Lys and Arg204Lys residue replacements	This work
pXHis1-R201K-R204K-R239K	pXHis1 derivative carrying Arg201Lys, Arg204Lys and Arg239Lys residue replacements	This work
pXHis1- R58K-R201K-R204K-R239K	pXHis1 derivative carrying Arg201Lys, Arg204Lys, Arg239Lys and Arg58Lys residue replacements	This work
pNX4	pN702GEM3 derivative containing the XYSA gene, which encodes the catalitic domain of the xylanase Xys1Δ, with a tag of six histidine residues, under the control of XYSA promoter and flanked by the terminator of the methylenomycin resistance gene (T1) and the terminator of phage fd (T2)	(Rodríguez et al., 2005)
pTX4	pN702GEM3 derivative in which the 2,1 Kb BglII fragment from plasmid pXHis1 has been cloned into the BglII site of Streptomyces multicopy vector. This BglII fragment contains the XYSA gene under the control of its own promoter (*xysA)* between the mmrt (T1) and fdt (T2) transcriptional terminators	This work
pNX4-R58K	pNX4 derivative carrying Arg58Lys residue replacement	This work
pNX4-R201K-R204K	pNX4 derivative carrying Arg201Lys and Arg204Lys residue replacements	This work
pNX4-R201K-R204K-R239K	pNX4 derivative carrying Arg201Lys, Arg204Lys and Arg239Lys residue replacements	This work
pNX4-R58K-R201K-R204K-R239K	pNX4 derivative carrying Arg201Lys, Arg204Lys, Arg239Lys and Arg58Lys residue replacements	This work

Table 2. List of primers used

Primer	Amino acid replacement	Sequence (5' - 3')
Arg58Lys5	Arg58Lys	GGTGACGCCGCGGCTGCCAAGGGAAAATACTTCGG CGCGGCGGTCGCCG
Arg58Lys3	Arg58Lys	CGGCGACCGCCGCGCCGAAGTATTTTCCCTTGGCAG CCGCGGCGTCACC
Arg201204Lys5	Arg201Lys, Arg204Lys	CTTCATCGAGGAGGCGTTCAAGACCGCAAAAACGG TCGATGCCGACGCG
Arg201204Lys3	Arg201Lys, Arg204Lys	CGCGTCGGCATCGACCGTTTTTGCGGTCTTGAACGC CTCCTCGATGAAG
Arg239Lys5	Arg239Lys	CGAGATGGTGAAGGACTTCAAGCAGAAAGGTGTCC CCATCGACTGCGTG
Arg239Lys3	Arg239Lys	CACGCAGTCGATGGGGACACCTTTCTGCTTGAAGTC CTTCACCATCTCG

Table 3. Description of different immobilized Xys1Δ biocatalysts. Description of different immobilized Xys1Δ biocatalysts and their optimal chemical modifications by surface coating with one or two layers of different polymers at different ratios.

Biocatalyst	Initial biocatalyst	Chemical modification of the first layer	Chemical modification of the second layer
Ag-CB- Xys1Δ-L[a]	Ag-CB- Xys1Δ-L	None	None
Ag-G-Xys1Δ-L[b]	Ag-G-Xys1Δ-L	None	None
Ag-G-Xys1Δ-L+Dex20-80	Ag-G-Xys1Δ-L	Dex20-80 at a ratio of 0.15 g dextran/g biocatalyst, by covalent binding	None
Ag-G-Xys1Δ-L+PEI	Ag-G-Xys1Δ-L	25,000 Da PEI at a ratio of 0.1 g PEI/g biocatalyst, by ionic exchange binding	None
Ag-G-Xys1Δ-L+ Dex20-80+PEI	Ag-G-Xys1Δ-L	Dex20-80 at a ratio of 0.15 g dextran/g biocatalyst, by covalent binding	25,000 Da PEI at a ratio of 0.1 g PEI/g biocatalyst, by ionic exchange binding
Ag-G-Xys1Δ-L+PEI+Dex20-80	Ag-G-Xys1Δ-L	25,000 Da PEI at a ratio of 0.1 g PEI/g biocatalyst, by ionic exchange binding	Dex20-80 at a ratio of 0.15 g dextran/g biocatalyst, by covalent binding
Ag-G-Xys1Δ-H[c]	Ag-G-Xys1Δ-H	None	None
Ag-G-Xys1Δ-H+Dex20-80	Ag-G-Xys1Δ-H	Dex20-80 at a ratio of 0.15 g dextran/g biocatalyst, by covalent binding	None
Ag-G-Xys1Δ-H+PEI	Ag-G-Xys1Δ-H	25,000 Da PEI at a ratio of 1 g PEI/g biocatalyst, by ionic exchange binding	None
Ag-G-Xys1Δ-H+ Dex20-80+PEI	Ag-G-Xys1Δ-H	Dex20-80 at a ratio of 0.15 g dextran/g biocatalyst, by covalent binding	25,000 Da PEI at a ratio of 1 g PEI/g biocatalyst, by ionic exchange binding

[a] Ag-CB-Xys1Δ-L biocatalyst, Xys1Δ immobilized on Ag-CB with low protein loading. [b] Ag-G-Xys1Δ-L biocatalyst, Xys1Δ immobilized on Ag-G with low protein loading. [c] Ag-G-Xys1Δ-H biocatalyst, Xys1Δ immobilized on Ag-G with high protein loading.

Table 4. Thermal inactivation results. Results from thermal inactivation of immobilized Xys1Δ-L and Xys1Δ-H biocatalysts chemically modified by surface coating with a first layer of different polymers at different ratios, at 70 ºC and pH 7, with respect to the unmodified biocatalysts.

Biocatalyst	Type of binding	Polymer	Ratio (g polymer/g biocatalyst)	Stabilization Factor[a]
Ag-CB-Xys1Δ-L	-	-	-	1
Ag-G-Xys1Δ-L	-	-	-	62
Ag-G-Xys1Δ-L	Covalent binding	Dex100	0.15	12
			0.8	17
			4	30
		Dex20	0.15	18
			0.8	16
			4	12
		Dex20-80	0.15	305
			0.8	160
			4	71
	Ionic exchange binding	1,300 Da PEI	0.01	188
			0.1	203
			1	315
			2	267
			10	265
		25,000 Da PEI	0.1	285
			1	251
			2	262
		10,000 Da PEI	1	246
		70,000 Da PEI	1	267
Ag-G-Xys1Δ-H	Covalent binding	Dex20-80	0.15	245
			0.8	224
	Ionic exchange binding	25,000 Da PEI	0.1	88
			1	255
			2	230

[a] Stabilization factors were calculated by dividing $t_{1/2}$ of this enzyme at each condition into $t_{1/2}$ of the control.

Table 5. Kinetic parameters and specific activity values. Kinetic parameters and specific activity values of the native Xys1Δ and the four different Xys1Δ enzyme variants, each one displaying a different number of arginine residues replacements: arginine residue 58 by a lysine residue (Xys1Δ-R58K); arginine residues 201 and 204 by lysine residues (Xys1Δ-R201K-R204K); arginine residues 201, 204 and 239 by lysine residues (Xys1Δ-R201K-R204K-R239K); arginine residues 58, 201, 204, and 239 by lysine residues (Xys1Δ-R58K-R201K-R204K-R239K).

Kinetic parameters	**Xys1Δ**	**Xys1Δ-R58K**	**Xys1Δ-R201K-R204K**	**Xys1Δ-R201K-R204K-R239K**	**Xys1Δ-R58K-R201K-R204K-R239K**
V_{max} (U/mL $_{protein}$)	0.814	0.678	0.791	0.702	0.751
K_M (mg/mL)	1.233	1.232	1.901	1.936	1.885
K_{cat} (s^{-1})	0.041	0.034	0.040	0.035	0.038
$K_{cat}/_{KM}$ (mg/(mL s))	0.033	0.028	0.021	0.018	0.020
Specific activity (U/mg $_{protein}$)	82.428	72.162	74.275	65.972	68.539

Table 6. **Physical characterization by Mercury Intrusion Porosimetry (MIP) and Adsorption Isotherm (AI).** Physical characterization by Mercury Intrusion Porosimetry (MIP) and Adsorption Isotherm (AI) of commercial enzyme supports based on methacrylic polymer functionalized with glyoxyl groups: P8204F-G (Purolite® ECR8204F); P8215F-G (Purolite® ECR8215F); and R403S-G (Relizyme™ EP403/S).

	AI	**MIP**			
Glyoxyl-functionalized methacrylic supports	Area BET (m^2/g)	Total Pore Area (m^2/g)	Bulk Density at 1.01 psia (g/mL)	Apparent (skeletal) Density (g/mL)	Porosity (%)
G-R403S	69.5487	68.373	0.3640	1.1232	67.5873
G-P8204F	161.4177	153.653	0.3975	1.2037	66.9753
G-P8215F	220.5116	175.006	0.2524	1.0286	75.4605

Table 7. Thermal inactivation parameters. Thermal inactivation parameters of different immobilized Xys1Δ-L and biocatalysts Xys1Δ-H chemically modified by surface coating with layers of different polymers, at 70 ºC and pH 7. Inactivation parameters were determined from the best-fit inactivation model of the experimental data as previously reported.

Biocatalyst	k_{D1} (h^{-1})	k_{D2} (h^{-1})	$t_{1/2}$ (h)	Stabilization factor[a]
Ag-G-Xys1Δ-L	4.43	0.307	0.36	62
Ag-G-Xys1Δ-L+PEI	9.33	0.275	1.66	285
Ag-G-Xys1Δ-L+Dex20-80	6.26	0.178	1.77	305
Ag-G-Xys1Δ-L+PEI+Dex20-80	6.21	0.178	2.75	471
Ag-G-Xys1Δ-L+Dex20-80+PEI	5.11	0.163	2.98	506
Ag-G-Xys1Δ-H	3.98	0.214	0.49	82
Ag-G-Xys1Δ-H+PEI	2.64	0.165	1.48	250
Ag-G-Xys1Δ-H+Dex20-80	7.27	0.189	1.42	240
Ag-G-Xys1Δ-H+Dex20-80+PEI	0.22	-	3.28	550

[a]Stabilization factors were calculated by dividing $t_{1/2}$ of this enzyme at each condition by $t_{1/2}$ of the control (Ag-CB-Xys1Δ-L).

7. Discussion

7.1. Increasing thermo-stability of the immobilized Xys1Δ biocatalyst by post-immobilization techniques

With the aim to further increase thermo-stability of the previously immobilized Xys1Δ biocatalyst, a strategy based on surface coating with a multilayer of polymers was developed.

First of all, immobilization of this enzyme was optimised to obtain an immobilized Xys1Δ biocatalyst with higher recovered activity. This was achieved by addition of 50% (w/v) glycerol to the immobilization medium. This medium allowed preservation of remaining enzyme activity at immobilization conditions. Expressed activity was 28.24 U/g support, being 81.54% of total offered activity. This expressed activity is 15% higher than the one obtained for an immobilization procedure without the use of any additive for enzyme activity preservation, as shown in a previous work (Aragon et al., 2013a).

The surface of this biocatalyst, Ag-G-Xys1Δ-L, was then modified by covalent coating with a first layer of derived dextran polymers (Dex100; Dex20; and Dex20-80) at different coating degrees. Interestingly, the effect of this covalent surface modification on biocatalyst activity and thermo-stability was very different depending on the chemical group pattern displayed by each derived dextran polymer, and on the coating degree used for each one.

On the one hand, when the surface of this biocatalyst was coated with a first layer of Dex100, the recovered activity was reduced by approximately 75%. The effect was the same regardless the surface coating degree. The almost complete loss of activity is due to the structure distortion effect promoted by covalent binding, which in this case is caused, by surface coating with the 100% of dextran macromolecule transformed into poly-aldehyde. Aldehyde groups formed covalent bonds with enzyme amino groups. Some other authors have reported similar results with surface coating with dextran polymers transformed into poly-aldehyde macromolecules (Betancor et al., 2004, Bolivar et al., 2012, Fernandez-Lorente et al., 2010). However, when the enzyme surface was coated with a first layer of Dex20 or Dex20-80 (both with the 20% of dextran macromolecule modified to poly-aldehyde), almost all the immobilized activity was retained with all degrees of surface coating. This should indicate that the more covalent bonds are formed, the higher distortion effect is produced, and so, the lower recovered activity is obtained.

On the other hand, from thermal inactivation results of all these chemically modified biocatalysts, it was observed that only when the surface of the immobilized Ag-G-Xys1Δ-L biocatalyst was coated with Dex20-80, there was a thermo-stabilization effect with the lowest coating degree, and higher degrees of polymer coating did not cause any further stabilizing effect. This thermo-stabilization factor was 5 with respect to the unmodified Ag-G-Xys1Δ-L biocatalyst at 70ºC and pH 7, and 305 in regard to Ag-CB-Xys1Δ-L. In light of these results, this stabilizing effect is due to the poly-hydroxyl region harbored by Dex20-80 (**Figure 2**).

Sugars and polyols have been extensively described in literature to display enzyme stabilizing properties (Chong et al., 2014, Lozano et al., 1994). Addition of glycerol, sucrose, mannitol, sorbitol, and starch increased the half-life of an alkaline protease from *Bacillus mojavensis* at 60ºC by 2 – 2.2 fold (Beg and Gupta, 2003). Addition of 3 M sorbitol also improved the thermal stability of *B. cereus* BG1 alkaline protease at 60ºC by 2-fold (Ghorbel et al., 2003). Some authors have reported that under thermal stress, their stabilizing effects are exerted by the maintenance of both, hydrophobic interactions with groups which are now exposed, which are essential for the enzyme native structure, and water shell around the enzyme molecule as these additives form hydrogen bonds with water molecules (Chong et al., 2014, Lozano et al., 1994). As a consequence, these additives, such as sugars and polyols, can alter the microenvironment of enzyme molecules by changing the properties of water shell, driving to important effects on enzyme structure and thermal stability. Although the precise molecular mechanism responsible for the structural stabilization of enzymes in solution by polyols and sugars is not well understood yet, the concept of preferential exclusion has increasingly gained acceptance (Liu et al., 2010, Politi and Harries, 2010, Kumar et al., 2011, Barbiroli et al., 2017). Water molecules preferentially interact with the surface of the protein in the presence of polyols and sugars. This hinders the interaction of other solutes with hydrophobic regions of the enzyme (which are exposed to the solvent under thermal stress) (Iyer and Ananthanarayan, 2008, Kumar et al., 2012). According to this hypothesis, these additives change the microenvironment surrounding the molecules of the enzyme, which leads to a preferential hydration layer of the enzyme. This fact promotes the compaction and increase the stability of the enzyme.The extent to which any additive interacts with water molecules depends upon its molecular structure (Barbiroli et al., 2017). Due to this fact, different thermo-stabilizing effects are promoted with coating with derived dextran polymers containing different patterns of chemical groups.

Moreover, chemical surface modification of the immobilized Ag-G-Xys1Δ-L biocatalyst with the cationic polymer PEI did not affect activity and had a positive effect on thermo-stability, regardless both, size and coating degree of PEI. When the surface of this biocatalyst was chemically modified, via ionic binding, with a first layer of PEI of different molecular weigth

(1,300-70,000 Da) and at different coating degrees (0.01-10 g/g biocatalyst), no loss of activity was observed for any of these modifications . This result is in agreement with previous works (Bolivar et al., 2012, Cabrera et al., 2010, Bolivar et al., 2009).

Furthermore, although surface coating of this biocatalyst with PEI of different molecular weight, and at any coating degree, drove to thermo-stabilizing effects, resulting thermo-stabilization factors were variable depending upon these chemical modifications. The highest one was obtained by surface coating with 25,000 Da PEI at a ratio of 0.1 g/g biocatalyst. As described in literature, PEI is an anionic polymer which provides a positively charged microenvironment around enzyme surface, which is responsible for the hydrophilic conditions around it, and in consequence, for thermo-stabilizing effects (Padilla-Martinez et al., 2015, Velasco-Lozano et al., 2014). In addition, this microenvironment drives to conformational changes in the enzyme structure, and so, different PEI molecular weights and different PEI coating degrees would have different effects upon structural changes resulting in different extents of thermo-stabilization (Velasco-Lozano et al., 2014). The highest thermo-stabilization factor was obtained with 25 KDa PEI at 0.1 g/g biocatalyst ratio. This thermo-stabilization factor was 4.5 with respect to the unmodified Ag-G-Xys1Δ-L biocatalyst at 70ºC and pH 7, and 285 in regard to Ag-CB-Xys1Δ-L.

Afterwards, to further increase the thermo-stability of these two optimised Ag-G-Xys1Δ-L biocatalysts (the Ag-G-Xys1Δ-L+Dex20-80 and Ag-G-Xys1Δ-L+PEI biocatalysts), their surfaces were chemically modified by coating with a second layer of the other polymer, Dex20-80 or PEI in each case. Thermal inactivation results indicated that surface coating of the Ag-G-Xys1Δ-L biocatalyst with a bilayer of polymers promoted a higher thermo-stabilizing effect than the ones obtained with any of the two monolayers. Also, they showed that the bilayer formed by a first layer of Dex20-80 and a second layer of PEI (Ag-G-Xys1Δ-L+Dex20-80+PEI) seemed to promote a slightly higher stabilization effect.

As described above, different polyols based polymers (e.g. dextran) and ionic charged polymers (e.g. PEI), have been extensively used as enzyme stabilizers, since they form a layer on enzyme surface which is capable to maintain both, hydrophobic interactions with groups which are exposed as a result of thermal stress, and water shell around enzyme molecule (Chong et al., 2014, Lozano et al., 1994). However, the use of a multilayer of different polymers for coating immobilized enzymes surfaces has not been extensively described in literature up to date. This strategy relies on the fact a multilayer of polymers would promote an even higher thermo-stabilization effect than a monolayer, since more and different molecular interactions would be created between these polymers and enzyme hydrophobic groups which are exposed due to

thermal stress, and water shell molecules. In light of results presented here, thermal protective effects exerted by surface coating with these two layers of polymers are additive, since coating with a bilayer promotes higher stabilization factors than coating with any of the two monolayers, and so, the number and/or the strength of these surface molecular interactions is increased when using a bilayer of polymers.

Furthermore, these optimal modifications obtained for Ag-G-Xys1Δ-L biocatalyst, were also applied to an immobilized Xys1Δ biocatalyst with high protein loading (Ag-G-Xys1Δ-H) to increase its thermo-stability. So, the surface of the Ag-G-Xys1Δ-H biocatalyst was coated by covalent binding with Dex20-80 polymer at the same coating degrees as before. In this case, stabilization factors obtained for each coating degree were very similar to those achieved for the Ag-G-Xys1Δ-L biocatalyst. The lowest coating degree promoted higher stabilizing effects, and higher coating degrees did not allow significantly higher stabilization factors. This indicates that the same amount of macromolecules of these modified dextran polymer contain enough quantity of aldehyde groups (in the poly-aldehyde region) to stablish covalent bonds with a higher quantity of immobilzied enzyme. However, when the surface of Ag-G-Xys1Δ-H biocatalyst was coated with PEI of 25000 Da molecular weight by ionic exchange at different coating degrees, a 10-fold higher coating degree of PEI is required to obtain the highest thermo-stabilization factor. This seems to point out that a higher amount of PEI is required to interact with a higher quantity of immobilized enzyme. This result could be explained by the fact that the surface of Xys1Δ is rich in residues containg carboxylic groups on lateral chains, such as aspartic and glutamic acids. These groups will form ionic interactions with primary amino groups from PEI, which represent the 25% of the PEI macromolecule.

Finally, to further increase the thermo-stability of the immobilized biocatalyst with high protein loading, the surface of the Ag-G-Xys1Δ-H+Dex20-80 biocatalyst was modified with a second layer of PEI of 25,000 Da molecular weight (resulting in the Ag-G-Xys1Δ-H+Dex20-80+PEI biocatalyst). As in the case of the immobilized biocatalyst with lower protein loading, the thermo-stabilization factor achieved with surface coating with a bilayer of Dex20-80 and PEI (Ag-G-Xys1Δ-H+Dex20-80+PEI) was higher than the one obtained with any of the two monolayers (thermo-stabilization factor of 7.7 with respect to Ag-G-Xys1Δ-H biocatalyst at pH 7 and 70 ºC; and at least 550 with respect to Ag-CB-Xys1Δ-L biocatalyst at pH 7 and 70 ºC). And so, this optimised biocatalyst in terms of thermo-stability with high protein loading was then used for hydrolysis reactions of xylan from different sources for XOS production in batch reactors, and to develop consecutive cyles of this hydrolysis reaction.

7.2. Increasing operational stability of the optimised immobilized Xys1Δ biocatalyst for xylan hydrolysis reaction to produce XOS at high temperatures in batch mode

Taking into account the positive effects that surface coating with this bilayer of polymers (Dex20-80 and PEI) had on the immobilized Xys1Δ biocatalyst thermo-stability, possible effects of this chemical modification on catalytic activity were also evaluated.

With this aim, hydrolysis reactions of different sourced xylans were accomplished with the optimised biocatalyst (Ag-G-Xys1Δ-H+Dex20-80+PEI) and with the unmodified biocatalyst (Ag-G-Xys1Δ-H), in batch reactors at moderately high temperature (50 ºC), and XOS production was analyzed in each case. Three different sourced xylans, beechwood xylan, corncob xylan and wheat arabinoxylan, were used as reaction substrates. These xylan substrates were used as the plant tissue determines the proportion and the type of side chain residues which are substituting xylose residues on the main backbone (Dodd and Cann, 2009). So, possible effects of this chemical modification on catalytic activity of the Xys1Δ biocatalyst were evaluated with different xylan chemical structures towards which this biocatalyst displays different degrees of specificity.

Beechwood xylan was shown to contain a lower soluble fraction (85.37%) than corncob xylan and wheat arabinoxylan (100%, respectively). This result confirmed a different degree of polymerization and/or substitutions, since branch points are responsible for solubility, viscosity and other physicochemical properties of xylan, as reported in literature (Moreira and Filho, 2016).

Results from analysis of reaction products indicated that there was no significant difference between these two biocatalysts in terms of reaction yields at any reaction time point for any of the three xylan substrates. The same XOS production profile between reactions developed by these two biocatalysts was also observed, being xylobiose the major reaction product when the three xylan types were used as reaction substrates. In light of these results, it can be concluded that product specificity towards these three xylan susbtrates with different compositions of the unmodified biocatalyst is the same as the one of the modified biocatalyst. Accordingly, chemical modification by surface coating with a bilayer of polymers (Dex20-80 and PEI) of this this immobilized biocatalyst did not seem to significantly alter the pattern of residues interactions responsible for the configuration of the catalytic cleft of this xylanase enzyme, and did not involve any residue directly implicated in molecular catalysis.

To confirm it, K_M and V_{max} kinetic parameters were calculated for these two biocatalysts using beechwood xylan as substrate. Values of V_{max} were very similar; while values of K_M were slightly different for the unmodified and the modified biocatalysts, respectively. This should indicate that this modification by surface coating with a bilayer of polymers modified the immobilized enzyme affinity to some extent. This is probably due to a slightly different structural conformation of substrate binding site cleft caused by this chemical modification of biocatalyst surface.

When beechwood xylan was hydrolyzed in a batch reactor by these two biocatalysts, the maximum xylan conversion yield was 93% and was achieved at 4h. Longer reaction times did not allow a higher conversion reaction yield. This result apparently indicated that there was a small fraction of this soluble beechwood xylan substrate (7% approx.) which cannot be hydrolyzed by this immobilized Xys1Δ biocatalyst. According to supplier, beechwood xylan consists of 4-O-methyl-glucuronoxylan (xylose 81.3% and glucoronic acid 13.0%; *Supplier information*). The Xys1Δ xylanase, as a member of the GH10 family, is expected to be able to cleave xylan chains when 4-O-methyl glucuronic acid is linked to xylose at the +1 subsite (Dodd and Cann, 2009). As described in *Introduction* section, binding sites for xylose residues in xylanases are termed subsites with bond cleaving occurring between xylose residues at -1 subsite and the +1 subsite (Dodd and Cann, 2009). This apparently not convertible fraction of xylan into XOS could be due to the presence of this substituent at a different subsite. Another possible explanation could be related to the fact that XOS which harbor 4-O-methyl glucuronic acid substituents on the main backbone cannot be detected by the analytical method used (HPAEC-PAD; see *Methods* section). In latter case, xylan hydrolysis would be 100%, but xylan conversion into XOS would be 93%. In addition, after 4 h of reaction, product mixture consisted only of xylose and xylobiose, representing, respectively, the 35 % and the 64% of reaction product.

Concerning the hydrolysis reaction of wheat arabinoxylan, the maximum xylan conversion yield was achieved at 5h of reaction course and did not increase after this time point. However, this conversion degree was only 44%, considerably lower than the one obtained for beechwood xylan. According to supplier, wheat arabinoxylan displays an arabinose to xylose ratio of 38 to 62. This result suggests that the high number of arabinose residues substituting xylose residues on the main xylan backbone, could negatively affect the catalytic performance of this xylanase. This can be confirmed by literature (Dodd and Cann, 2009), where the hydrolysis reaction of the same xylan was developed by different family GH10 xylanase enzymes, together with the hydrolysis of acid debranched wheat arabinoxylan. In this case, arabinose residues had been released from xylan main backbone. Results showed that the more highly substituted

arabinoxylan was hydrolyzed to a lesser extent than the less substituted acid debranched arabinoxylan, thus confirming that arabinose substituents hinder xylan cleavage by family G10 xylanases. Moreover, as in case of beechwood xylan hydrolysis, there could be a fraction of wheat arabinoxylan which is being converted into arabinoxylo-oligosaccharides and is not being accounted for. Indeed, it has been extensively described in literature that, on hydrolysis of wheat arabinoxylan, xylanases from family GH10 are able to produce short chain arabinoxylo-oligosaccharides (McCleary et al., 2015).

In case of the hydrolysis reaction of corncob xylan, a total xylan conversion yield of 100% was observed at 1h of reaction course. This should indicate the absence of substitutions on the main backbone. The fact that this degree of conversion was reached in a shorter period of time could also be explained by this xylan composition, which would consist of xylan molecules with a lower DP, i.e. lower number of β-(1→4)-linked xylose residues, and/or branching points.

Taking into account the composition of the product mixture from these three xylans hydrolysis reactions in batch reactors, the catalytic mechanism of this Xys1Δ xylanase could be established. At 1h of reaction course of corncob xylan hydrolysis, XOS mixture represented the 76%, with xylobiose concentration of 66%, while xylose and xylotriose accounted for 24% and 10%, respectively. However, at 24h of reaction course, only xylose (44%) and xylobiose (56%) could be observed in the product mixture. The same trend was observed in hydrolysis reactions of beechwood xylan and wheat arabinoxylan: as reaction progressed, the proportion of XOS with lower DP increased. This result suggets that this enzyme exerts its catalytic action by randomly cleaving β-(1→4)-linked xylose units from the homopolymeric backbone structure of xylan, thus releasing xylan molecules with different degrees of polymerization. These molecules are then cleaved again driving to generation of more sites for subsequent enzyme hydrolysis, ending up in higher proportions of XOS with lower DP, as previously reported in literature (Moreira and Filho, 2016).

In addition, analysis of reaction products at longer times of reactions courses reveals that the highest DP of produced XOS was xylobiose, meaning that minimum substrate length to cleavage by this GH10 xylanase was found to be xylotriose. This could drive to the conclusion that the catalytic cleft which constitutes the binding site for substrate xylan polymers displays a substrate recognition area composed by subsites -I to -II with strong and specific substrate interactions. The subsites -I, -II and -III accommodates xylose rings from xylose (subsite -I), xylobiose (subsites -I and -II), and xylotriose (subsites -I, -II and -III), with their reducing ends in H-bonding contact with the proton donor, as previously described in literature (Schmidt et al., 1999). However, in view of the variation of XOS composition of reaction product over reaction

time course, it should be proposed that binding to subsite +I (in the product release area) is still more energetically favorable than binding to subsite -III, and for this reason xylotriose appears to be cleaved, as it has been previously reported with the hydrolysis of xylotetraose by a family GH10 xylanase (Schmidt et al., 1999). Contrary to xylotriose, xylobiose is present in high proportions in XOS mixtures in reaction products, meaning that binding to subsite -II was more efficient that to subsite +I, and as a consequence, Xys1Δ xylanase will probably present both a low k_M and a low k_{cat} values towards xylobiose, thus indicating appreciable binding but almost no catalysis.

Taking into account the positive effects that surface coating with this bilayer of polymers (Dex20-80 and PEI) had on immobilized Xys1Δ biocatalyst thermo-stability, and the negligible effects of this chemical modification on catalytic activity, the possible effects on operational stability were also analyzed. Results showed that xylan conversion yield into different XOS was maintained for at least 15 consecutive cycles of hydrolysis reactions of beechwood xylan in batch reactors with the Ag-G-Xys1Δ-H+Dex20-80+PEI biocatalyst. This result suggests that not only the thermo-stability of this immobilized biocatalyst was improved by surface coating with a bilayer of polymers, but also its operational stability was increased. According to these results, 10 mg/ml of xylobiose and 7 mg/ml of xylose could be produced in 3h of reaction with only 1% (w/v) of this optimised biocatalyst (with respect to reaction volume) in a batch reactor, and this biocatalyst could be subsequently re-used for 15 cycles of batch reactions. This means that in 3h of reaction, 10 g of xylobiose would be produced from 40 g of beechwood xylan in batch operation mode using only 1 g of Ag-G-Xys1ΔH biocatalyst (with a protein loading value of 20 mg of Xys1Δ protein/g), and it would be repeated for, at least, 15 consecutive cycles.

In line with our results, several authors have recently reported some other efficient procedures for XOS production from xylan in batch operation mode using different immobilized xylanase systems. Milessi et al. (Milessi, Kopp et al. 2016) carried out the hydrolysis reaction of soluble birchwood xylan, from an initial solution of 4% (w/v), using 1.95 UI (0.22 mg of XynA/g approximately) of a recombinant xylanase (XynA) from Bacillus subtilis immobilized on glyoxyl-agarose, at pH 5.5 and 50ºC. This xylan also belongs to the class of glucuronoxylans, as beechwood xylan, and so, results are comparable to those obtained with beechwood xylan. At 24h of the reaction course, they observed a maximum XOS production of 23.5% (3.2 mg/ml) and a reaction yield for xylobiose of 50% (1.6 mg/ml). After 10 consecutive cycles of 3h, in which a conversion of 20% of XOS was reached (2.8 mg/ml), hydrolysis conversion and XOS production remained essentially constant. So, in 3 h of reaction, 2.9 g of XOS (composed by xylobiose, xylotriose and xylotetraose) would be produced from 40 g of birchwood xylan using approximately 0.043 g of biocatalyst (harboring 0.22 mg of XynA protein/g), and this

biocatalyst can be re-used for 10 reaction cycles. In this system a lower xylan conversion into XOS was achieved but with a lower quantity of enzyme.

Moreover, Liu et al. (Liu, Huo et al. 2015) reported beechwood xylan hydrolysis by an immobilized bifunctional xylanase on carbon-coated chitosan nanoparticles, at pH 7 and 55ºC. After 15 min of reaction, 53.7% of the total hydrolysis product was xylobiose with a concentration value of 2.19 mg/ml. This immobilized derivative retained 82.6% xylanase activity after 7 successive reactions. In this beechwood xylan hydrolysis reaction the major product was also xylobiose, and xylan conversion yield into xylobiose was similar to the one obtained in the present wotk.

In addition, Driss et al. (Driss, Haddar et al. 2014) developed the hydrolysis reaction of 20 g/l corncob xylan with a xylanase from Penicillium occitanis, PoXyn2, immobilized on nickel-chelate Eupergit C, at ph 3 and 50ºC. At the end of 24-h reaction, XOS yield was 67.7% and the fraction composed of xylobiose and xylotriose in the product mixture was 21.3%. The immobilized enzyme exhibited approximately 50% of the initial catalytic activity after 5 cycles of use. Lin et al. (Lin, Tseng et al. 2011) also carried out the hydrolysis of 20 g/l corncob xylan with a xylanase from Bacillus halodurans immobilized onto an anionic exchange resin, at pH 8 and 50ºC. At the end of a 24h reaction, XOS mixture contained a total 22.5% of xylobiose and xylotriose (4.5 mg/ml) and XOS conversion yield was 80.9%. The immobilized enzyme retained about 71% of its original activity after reuse of 5 cycles.

7.3. Increasing thermo-stability of immobilized Xys1Δ biocatalyst by enhancement of multipoint covalent attachment via site-directed mutagenesis

Multipoint covalent attachment on glyoxyl-agarose based supports allows high values of stabilization against distortion agents such as high temperatures due to rigidification of enzyme structure. Consequently, a strategy based on intensification of rigidification of the enzyme surface region involved in multipoint covalent attachment was developed in order to further increase these thermo-stabilization effects. Accordingly, four arginine residues located on the same region as other eight lysine residues were replaced by lysine residues via conservative site-directed mutagenesis: arginine residues 58, 201, 204, and 239. These eight lysine residues were presumably participating in multipoint covalent attachment to the support.

So, four different Xys1Δ enzyme variants were constructed, each one displaying a different number of arginine residues replacements: arginine residue 58 (Xys1Δ-R58K); arginine residues 201 and 204 (Xys1Δ-R201K-R204K); arginine residues 201, 204 and 239 (Xys1Δ-R201K-R204K-R239K); and arginine residues 58, 201, 204, and 239 (Xys1Δ-R58K-R201K-R204K-R239K).

Kinetic parameters of all resulting enzyme variants were compared to those of the Xys1Δ wild type enzyme. The catalytic efficiency (K_{cat}/K_M) of different Xys1Δ variants was lower when compared to the wild type Xys1Δ. This decrease was principally due to the increase of the K_M, suggesting a negative contribution of all these residues replacements to the affinity towards substrate. Also, it should be observed that substrate affinity decreased with the number of lysine residues replacements. These results indicated that the more changes in this enzyme native structure resulted in lower substrate affinity, and so, these changes contributed to differences in catalytic efficiency of this xylanase enzyme.

In addition, thermo-stability of resulting immobilized Xys1Δ biocatalysts indicated that the 1-4 additional covalent bonds formed between enzyme and immobilization support, if formed, did not provided further thermo-stabilizing effects. This could lead to the conclusion that these additional covalent bonds did not seem to promote more intense rigidification of the enzyme surface region involved in multipoint covalent attachment, probably due to the fact that rigidification of this surface area was already achieved by the other eight lysine residues already present in this area. One possible solution should be to develop semi-conservative site directed mutagenesis by substituting other residues located on the same surface area.

7.4. Increasing process productivity of continuous flow reaction of xylan hydrolysis to produce XOS by multipoint covalent immobilization of the Xys1Δ enzyme onto different methacrylic polymeric based supports

With the aim of increasing process productivity of continuous flow reaction of xylan hydrolysis for XOS production in PBRs, different immobilized Xys1Δ biocatalysts were developed. This was achieved by multipoint covalent immobilization of this enzyme on different commercial methacrylic matrices. For this purpose, these matrices were firstly functionalized with glyoxyl groups. Resulting glyoxyl-functionalized methacrylic supports, R403S-G, P8204F-G and P8215F-G, yielded respectively 105.22; 101.6; and 25.7 $\mu mol_{\ glyoxyl\ groups}/g_{\ support.}$ These values

were considerably lower than the one achieved for 10% crosslinked agarose (Ag-G): 200 μmol $_{\text{glyoxyl groups}}$/g $_{\text{support}}$ (Guisán et al., 1997).

Immobilization of Xys1Δ xylanase on these resulting supports, along with Ag-G, was carried out in order to obtain four different immobilized Xys1Δ biocatalysts with maximum protein loading. Immobilization procedure was developed at immobilization conditions which allowed maximum immobilization yield: pH 10 and 4 ºC for 96 h (without the use of any another preservative), before Schiff bases reduction (Guisán, 1988). The maximum value of immobilized protein was 40 mg/g $_{\text{support}}$, and it was achieved by Ag-G. Remarkably, this value was almost the double of the one obtained with the previous immobilization procedure carried out with an immobilization medium consisting of 50% glycerol (w/v) and at an immobilization temperature of 4 ºC (targeting Ag-G-Xys1Δ-H biocatalyst). The difference of maximum protein loading values between immobilization procedures is probably due to the lower immobilization rate which was achieved with the former one. In order to immobilize the same amount of protein with a lower immobilization rate, a longer immobilization process (>96 h) would probably be required. However, a longer immobilization process would presumably end in denaturation of remaining protein at required alkaline conditions for immobilization.

The maximum value of immobilized protein loading achieved by Ag-G was also considerably higher than the ones obtained for the three glyoxyl-functionalized methacrylic supports. These values should be explained by both the total surface area, and the size of the enzyme to be immobilized. According to results obtained from MIP and AI, R403S-G, P8204F-G and P8215F-G supports displayed area BET values of 69.5 m^2/g; 161.4 m^2/g; and 220.5 m^2/g, respectively, while the calculated value of surface area for Ag-G has been reported to be 94 m^2/g (Molina-Rosell, 1993). For determination of enzyme size, the same Stokes radius as the one estimated for trypsin could be assumed: 22 Å (Blanco et al., 1989), as Xys1Δ enzyme displays a similar molecular weight (approximately 33.7 KDa (Canals et al., 2003)), to that of trypsin (25 KDa) and trypsin has been extensively used for modelling immobilization mechanisms. Under this assumption, the minimum pore size diameter should be 4.4 nm to allow immobilization of Xys1Δ. This threshold would be even higher than 4.4 nm since Xys1Δ molecular weight is slightly larger than trypsin one. This assumption would be in agreement with literature, since it has been described that a laccase enzyme appeared to be immobilized mainly at sites with pore width greater than 3 nm (Nguyen et al., 2016).

Taking into account this minimum size of pore diameter, an important fraction of total surface cannot be used for immobilization of Xys1Δ in case of P8215F-G support, and in a lower extent, in case of P8204F. This surface proportion corresponds to micropores harbouring a

diameter value below 4.4 nm. Consequently, this proportion of surface area could be defined as "not accessible" for enzyme immobilization. In contrast, R403S-G showed a pore size distribution above this threshold value, driving to the conclusion that total surface area (69.5 m^2/g) is "accessible" for immobilization of Xys1Δ enzyme. Accordingly, although P8204F-G and P8215F-G supports present higher values of total surface areas, they display "inaccessible" surface fractions, which would explain the identity of maximum protein loading values for P8204F-and R403S-G in spite of different total surface areas. It would also explain the lower value of maximum protein loading achieved by P8215F-G in comparison with R403S-G. The presence of a surface area fraction which is not being accessible for enzyme immobilization agrees with literature (Nguyen et al., 2016). These authors reported that even at saturation coverage, laccase only occupy 36% of support surface, leading to the conclusion that enzymatic porous supports with high values of total surface area are not necessarily required for enzyme immobilization since pore size distribution should be also taken into consideration.

Moreover, a different extent of thermo-stability was achieved by each immobilized biocatalyst. The immobilized biocatalyst on Ag-G (Ag-G-Xys1Δ-40-HT) presented the highest thermo-stability degree. Among biocatalysts immobilized on glyoxyl-functionalized methacrylic supports, R403S-G-Xys1Δ-20-HT displayed the highest thermo-stability degree, while the ones immobilized on Purolite® (P8204F-G-Xys1Δ-20-HT and P8215F-G-Xys1Δ-10-HT) presented approximately the same thermo-stability degree. On the one hand, these differences in thermo-stability could be explained by the chemical and physical characteristics displayed by each support. If a homogeneous initial epoxy group density on supports surface and the absence of any diffusional limitation for $NaIO_4$ throughout these supports structures are assumed, an homogeneous distribution of glyoxyl groups all over total surface area would be resulted from support functionalization. Under this assumption, R403S-G, P8204F-G and P8215F-G supports would display values of glyoxyl group density of 1.51 μmol glyoxyl/m^2; 0.63 μmol glyoxyl/m^2 and 0.12 μmol glyoxyl/m^2, respectively, while 10% crosslinked-agarose would present a value of glyoxyl group density of 2.12 μmol glyoxyl/m^2 according to literature (Guisán et al., 1997). Differences in thermo-stability are then concluded to be due to differences among these values of glyoxyl group density, as it has been described that there is a correspondence between the density of glyoxyl groups onto support surface and the extent of thermo-stabilization achieved by the resulting biocatalyst (Blanco et al., 1989, Pedroche et al., 2007).

On the other hand, other factors affecting thermo-stability of different biocatalysts should be taken into account. One of these factors could be the hydrophobicity pattern displayed by each support (Basso et al., 2016). All these supports consisted of methacrylic polymer matrices manufactured by suspension polymerization (Basso et al., 2016). Apart from their chemical

composition, it has been described that a number of variables resulting from the suspension polymerization process affect several physical properties of the ending methacrylic polymer product, such as pore volume, pore-size distribution, surface area, and bead diameter (Beneš et al., 2005). As a conclusion, these supports could possibly display differences in hydrophobicity in spite of presenting the same chemical composition, which could drive to differences in thermo-stability, and so indicating the reason why almost the same degree of thermo-stability was achieved by two supports with different glyoxyl group densities onto their surfaces (P8204F-G and P8215F-G).

The optimal biocatalyst on glyoxyl-functionalized methacrylic supports was selected in terms of more adequate area BET and pore size distribution, the maximum protein loading and the highest thermo-stability, to meet the previously stated industrial requirements. Therefore, continuous flow reaction of xylan hydrolysis for XOS production was developed at different flow rates with a PBR consisting of a column packed with the R403S-G-Xys1Δ-20-HT biocatalyst, along with a PBR implemented with the Ag-G-Xys1Δ-40-HT biocatalyst. At 0.5 mL/min flow rate, the maximum reaction yield was reached for these two PBRs. According to results from batch hydrolysis reactions of the same xylan, the maximum reaction yield is achieved when xylan conversion yields to xylose and to xylobiose are 50% and 50%, respectively, due to the catalytic mechanism of these enzymes: xylanase molecules exert their catalytic action by randomly cleaving β-(1→4)-linked xylose units from the homopolymeric backbone structure of xylan, thus releasing xylan molecules which are cleaved again driving to generation of XOS with lower DP (Moreira and Filho, 2016). Consequently, a higher observed reaction rate is translated into a higher proportion of XOS with lower DP in the reaction product. At 0.5 mL/min flow rate, the maximum reaction yield was reached, and a lower observed reaction rate was achieved at a lower flow rate (0.1 mL/min) for both PBRs. At flow rates higher than 0.5 mL/min, the observed reaction rate seemed to decrease with the flow rate for both PBRs.

Assuming that 100% xylan conversion yield would be translated into 100% xylan conversion yield to xylose, total xylan conversion yield was observed to increase linearly with residence time up to 5.4 min (1 mL/min flow rate) for the PBR implemented with the R403S-G-Xys1Δ-20-HT biocatalyst. One possible explanation to these results should be that residence time is limiting reaction rate up to 5.4 min. In other words, residence time is shorter than reaction time up to 5.4 min, and so, this system could be thought to be reaction-limited: the rate of substrate transport from bulk fluid to biocatalyst surface is higher than the reaction rate (Sen et al., 2016). In contrast, at longer residence times (54 min), this linearity does not seem to be followed, and so, this system could be diffusion-limited: the rate of substrate transport from bulk fluid to

biocatalyst surface is lower than the reaction rate (Sen et al., 2016). This hypothesis would agree to general knowledge about effects of transport limitations on rates of solid-catalyzed reaction, which establishes that increasing the fluid velocity (and so decreasing residence time) can significantly increase the mass-transfer coefficients (Davis and Davis, 2003).

A balance between the reaction rate and transport phenomena is frequently considered the most effective mean of operating a catalytic reaction (Davis and Davis, 2003). Nevertheless, the main industrial interest of this reaction is XOS production, and so, xylose production should be avoided. As a result, the balance between the reaction rate and the rate of substrate transport from bulk fluid to the biocatalyst surface is not pursued, since it would end in a higher proportion of XOS with lower DP in the reaction product. For this reason, PBRs implemented with immobilized Xys1Δ biocatalysts on methacrylic polymeric supports were proved to be a powerful tool for continuous production of XOS. Higher flow rates allow shorter residence times, and the latter limit the reaction which favours XOS production. As a consequence, the highest volumetric productivity for XOS (3,453 g_{XOS} $L^{-1}h^{-1}$) in continuous flow operation with these two PBRs was obtained at the highest flow rate, 10 mL/min, at which only the immobilized biocatalyst on methacrylic support could be operated.

To confirm the hypothesis that residence time was limiting the reaction at shorter residence times, the experimental procedure proposed by Madon and Boudart was followed (Madon and Boudart, 1982). This experimental procedure states that the reaction rate is directly proportional to the active material in the absence of artifacts from transport limitations. This means that the intrinsic turnover frequency should be independent of the concentration of active material in a catalyst. Four different PBRs were developed with Xys1Δ immobilized biocatalysts on R403S-G with protein loading values of 15 mg/g; 10 mg/g; 5 mg/g and 1 mg/g, respectively, and operated at 10 mL/min. At this flow rate, the observed reaction rate seemed to decrease for decreasing protein loading values from 20 mg/g to 1 mg/g. In addition, theoretically calculated total xylan conversion yields were linearly proportional to the concentration of active material. This confirmed the previous hypothesis: residence time is shorter than reaction time at this flow rate (10 mL/min), and so, the system should be reaction-limited (Sen et al., 2016). Accordingly, the specific productivity for XOS at 10 mL/min was 20-fold increased, from 196 g_{XOS} g_{enzyme}^{-1} h^{-1} to 3,277 g_{XOS} g_{enzyme}^{-1} h^{-1}, with a PBR consisting of Xys1Δ immobilized biocatalysts on R403S-G with protein loading of 1 mg/mg (R403S-G-Xys1Δ-1-HT biocatalyst).

In addition, another transport process may offer resistance to the reaction, apart from fluid film resistance (external transport process): pore diffusion resistance or internal transport process (Sen et al., 2016). This transport process refers to diffusion of substrate molecules from

biocatalyst surface through the pores (Sen et al., 2016). According to the general equation of diffusion over a distance, $x^2 = qiDt$, where "x" is the mean distance from the starting point that a molecule will have diffused in time, "t"; "qi" is numerical constant which depends on dimensionality (1,2 or 3); and "D" is the diffusion coefficient (Doran, 1995), the time required for a substrate molecule to diffuse through spherical particle pores (t) would be $t = r^2/3D$, where "r" is particle mean diameter. Diffusivities of gases and liquids typically have magnitudes that are 10^{-4} and 10^{-9} m^2/s, respectively (Davis and Davis, 2003). Assuming a mean particle diamater of 150 µm, this time would be approxiamtely 0.1875 s for a PBR set up with the R403S-G-Xys1Δ-1-HT biocatalyst. Therefore, this time is lower than the lowest residence time used (32 s), and so, time for internal transport is not limiting the reaction at any studied flow rate with the R403S-G-Xys1Δ-1-HT biocatalyst.

Finally, the outcome from hydrolysis reaction of corncob xylan for XOS production in continuous mode was compared to that of the one obtained in batch mode. Xylan conversion yields to xylose and to XOS at 2 h of time course of the equivalent batch reaction with the R403S-G-Xys1Δ-5-HT biocatalyst, were similar to those from continuous flow reaction at 10 mL/min with the biocatalyst which allowest the maximum specific productivity: R403S-G-Xys1Δ-1-HT. In light of these results, the most suitable performance of corncob xylan hydrolysis reaction for XOS production is continuous mode, as it allows a specific productivity value of 3,277 $g_{XOS}\ g_{enzyme}^{-1}\ h^{-1}$, while the same reaction in batch mode with discontinuous runs of 2 h would end in an analogous specific productivity value of 236.36 g_{XOS}/g_{enz} h (using 1% (w/v) of biocatalyst to reaction medium). So, flow chemistry has been proved as a powerful tool for bioprocess intensification in XOS production using an immobilized xylanase biocatalyst.

8. Conclusiones

1. La xilanasa Xys1Δ de *Streptomyces halstedii* JM8 covalentemente inmovilizada sobre soportes de agarosa (10BCL) funcionalizados con grupos glioxil en presencia de glycerol (50% (p/v)) con una carga proteica de 10 mg/g mantiene el 81,54% de la actividad xilanasa inicial, y proporciona un considerable aumento de su termoestabilidad (stabilization factor of 62).
2. La modificación química de la superficie de este biocatalizador de Xys1Δ inmovilizado mediante el recubrimiento con una monocapa de dextrano modificado al 20% a poli-aldehído, y al 80% a grupos hidroxilo, permite preservar la actividad xilanasa inmovilizada y se aumentar su termoestabilidad (factor de estabilización de 305 con respecto a la enzima soluble). Cuando se recubre electroestáticamente con una monocapa de polímero polietilenimina de 25 KDa (0,1 g polímero/g biocatalizador), se preserva también la actividad xilanasa inmovilizada y se obtiene un incremento en termoestabilidad de 285 veces con respecto a la enzima soluble.
3. La modificación química de la superficie del biocatalizador de Xys1Δ inmovilizado mediante el recubrimiento con una bicapa de estos dos polímeros promueve mayores incrementos de termoestabilidad que cualquiera de las dos correspondientes monocapas: factor de estabilización de 550 con respecto a la enzima soluble.
4. La misma modificación química llevada a cabo sobre la superficie del biocatalizador de Xys1Δ inmovilizado con una mayor carga proteica, 20 mg/g, produce el mismo efecto termoestabilizante. Dicha modificación química no tiene efectos significativos sobre las propiedades catalíticas del biocatalizador de Xys1Δ inmovilizado en la reacción de hidrólisis de diferentes xilanos para la producción de XOS.
5. Dicha modificación permite aumentar la estabilidad operacional de este biocatalizador, al menos, hasta 15 ciclos de reacción de hidrólisis de xilano de haya en un reactor agitado discontinuo a 50 ºC. Los rendimientos totales de reacción de hidrólisis del xilano de haya, de trigo y de maíz son del 93% en 4 h, 44% en 5 h y del 100% en 1 h, respectivamente. A estos tiempos de reacción, la conversión de estos tres xilanos en XOS es del 65 %; 31% y 76%, respectivamente.
6. La adición de 1 – 4 residuos de lisinas, por sustitución de residuos de arginina, en el área de la superficie de la enzima Xys1Δ donde se encuentra el mayor número de estos residuos, no produce un aumento en la termoestabilidad del biocatalizador de Xys1Δ inmovilizado.
7. La enzima Xys1Δ ha sido covalentemente inmovilizada sobre tres soportes basados en polímeros de metacrilato previamente funcionalizados con grupos glioxil: Relizyme™ EP403/S, Purolite® ECR8204F y Purolite® ECR8215F, con densidades de grupos de

glioxil de 105,22; 101,6; y 25,7 μmol $_{\text{grupos glioxil}}$/g $_{\text{soporte}}$, respectivamente. La caracterización física de estos soportes por MIP y AI revela unos valores de área BET de 69,5; 161,4; y 220,5 m^2/g, y unos rangos de distribución de tamaño de poro de 40 – 100; 20 – 100 y 80 – 300 nm, respectivamente. En los soportes Purolite® ECR8204F y Purolite® ECR8215F se han observado fracciones de microporo con un tamaño de diámetro de poro menor a 4.4 nm.

8. La capacidad máxima de proteína Xys1Δ inmovilizada sobre estos soportes es de 20, 10 y 10 mg/g, respectivamente, mientras que el valor obtenido en las mismas condiciones de inmovilización con geles de glioxil-agarosa (10BCL) es de 40 mg/g. El grado de termoestabilidad obtenido para los biocatalizadores de Xys1Δ inmovilizados en estos soportes es mayor en agarosa (10BCL) que en Relizyme™ EP403/S; y éste a su vez es mayor que en Purolite® ECR8204F y Purolite® ECR8215F.
9. La reacción de hidrólisis de xilano de maíz en flujo continuo llevada a cabo en un reactor empaquetado de lecho fijo con el biocatalizador de Xys1Δ inmovilizado en Relizyme™ EP403/S, puede ser realizada a mayores flujos que con el reactor análogo basado en soportes de glioxil-agarosa (>3,5 mL/min). A flujos mayores de 0,5 mL/min, el rendimiento total de reacción disminuye conforme aumenta el flujo, debido a que el tiempo de residencia limita la reacción (régimen delimitado por la reacción), lo cual favorece la producción de XOS debido al mecanismo catalítico de las xilanasas.
10. La mayor productividad volumétrica en cuanto a XOS (3.453 $g_{XOS}\ L^{-1}h^{-1}$)se obtiene a 10 mL/min utilizando un reactor PBR implementado con el biocatalizador de Xys1Δ inmovilizado en Relizyme™ EP403/S con una carga proteica de 1 mg/g. En estas condiciones, la productividad específica para XOS es de 3,277 $g_{XOS}\ g_{enzyme}^{-1}\ h^{-1}$, 14 veces mayor que la más alta de las productividades específicas análogas obtenidas en modo discontinuo bajo las mismas condiciones.

9. Conclusions

1. The xylanase enzyme Xys1Δ from *Streptomyces halstedii* JM8 was covalently immobilized onto agarose based supports (10BCL) functionalized with glyoxyl groups, containing glycerol (50% (p/v)) into the immobilization medium, and with a protein loading value of 10 mg/g. It maintains 81,54% of the initial xylanase activity, and provides a considerable increase of its thermo-stability (stabilization factor of 62).
2. The chemical modification of the Xys1Δ biocatalyst surface by covalent coating with a monolayer of derived dextran (20% modified to a poli-aldehyde, and 80% to poli-hydroxyl), allows preservation of enzyme activity and an increase of its thermo-stability (stabilization factor of 305 with regard to soluble enzyme). When the surface of this biocatalyst is coated by ionic exchange with a monolayer of polyethylenimine of 25 KDa molecular weight (0.1 g polymer/g biocatalyst), xylanase activity is maintained and thermo-stability is increased (stabilization factor of 285 with regard to soluble enzyme).
3. The chemical modification of the Xys1Δ biocatalyst surface by coating with a bilayer of these two polymers allows higher stabilizing effects than any of each monolayer: stabilization factor of 550 with regard to soluble enzyme.
4. The same chemical modification was applied to the Xys1Δ biocatalyst with a higher value of protein loading, 20 mg/g. The same thermo-satbilizing effect is observed, and this modification does not produce significant effects on this enzyme catalytic properties during hydrolysis reactions of xylan from different sources for XOS production.
5. This modification allows an increase of Xys1Δ biocatalyst operation stability: 15 cycles of beechwood xylan hydrolysis reaction in batch mode at 50 ºC. Maximum total xylan conversion yields were 93% at 4 h; 44% at 5 h and 100% at 1 h, for hydrolysis reactions of beechwood, wheat and corncob, respectively. At these time points of reaction course, the three xylans conversion yields to XOS was 65 %; 31% y 76%, respectively.
6. The addition of 1 – 4 lysine residues, by substituting arginine residues, to the region of the Xys1Δ enzyme surface where the highest amount of lysisne residues is found, does not increase immobilized Xys1Δ biocatalyst thermo-stability.
7. The Xys1Δ enzyme was covalently immobilized onto three different supports, which are based on methacrylic polymeric matrix, previously functionalized with glyoxyl groups: Relizyme™ EP403/S, Purolite® ECR8204F y Purolite® ECR8215F. They respectively display values of glyoxyl groups density of 105,22; 101,6; y 25,7 $\mu mol_{\ glyoxyl\ groups}/g_{\ support}$. The physical characterization of these supports by MIP and AI reveals values of area BET 69,5; 161,4; y 220,5 m^2/g, respectively; and ranges of pore size distribution of 40 – 100; 20 – 100 y 80 – 300 nm, respectively. It is observed that Purolite® ECR8204F y Purolite®

ECR8215F display fractions of micropore with a pore size diameter lower than 4.4 nm.

8. Maximum values of immobilized Xys1Δ protein onto these three supports is 20, 10 y 10 mg/g, respectively, whereas the value obtained for 10BCL glyoxyl-agarose gel is 40 mg/g, under the same immobilization conditions. The degree of thermo-stability of immobilized Xys1Δ biocatalyst on 10BCL glyoxyl-agarose is higher than those of immobilized Xys1Δ biocatalysts on methacrylic supports. In addition, the degree of thermo-stability of immobilized Xys1Δ biocatalyst on Relizyme™ EP403/S is higher than those of immobilized Xys1Δ biocatalysts on Purolite® ECR8204F and Purolite® ECR8215F.
9. Continuous flow reaction of corncob xylan hydrolysis carried out in a packed-bed reactor with immobilized Xys1Δ biocatalyst on Relizyme™ EP403/S, can be performed at flow rates higher than those with an equivalent reactor based on agarose support (>3.5 mL/min). At higher flow rates than 0.5 mL/min, the overall observed reaction rate decreases as residence time limits the reaction (reaction-limited regime) which favours XOS production due to the catalytic mechanism of xylanase enzymes.
10. The highest volumetric productivity for XOS (3,453 $g_{XOS}\ L^{-1}h^{-1}$) is obtained at 10 mL/min flow rate using a PBR implemented with an immobilized Xys1Δ biocatalyst on Relizyme™ EP403/S with a protein loading value of 1 mg/g. At these conditions, the specific productivity for XOS is 3,277 $g_{XOS}\ g_{enzyme}^{-1}\ h^{-1}$, which is 14-fold higher than the highest analogous specific productivity value obtained in batch mode under the same conditions.

References

AACHARY, A. A. & PRAPULLA, S. G. 2009. Value addition to corncob: Production and characterization of xylooligosaccharides from alkali pretreated lignin-saccharide complex using *Aspergillus oryzae* MTCC 5154. *Bioresource Technology,* 100**,** 991-995.

ABIAN, O., GRAZÚ, V., HERMOSO, J., GONZÁLEZ, R., GARCÍA, J. L., FERNÁNDEZ-LAFUENTE, R. & GUISÁN, J. M. 2004. Stabilization of Penicillin G Acylase from *Escherichia coli*: Site-Directed Mutagenesis of the Protein Surface to Increase Multipoint Covalent Attachment. *Applied and Environmental Microbiology,* 70**,** 1249-1251.

ABIAN, O., MATEO, C., FERNÁNDEZ-LORENTE, G., PALOMO, J. M., FERNÁNDEZ-LAFUENTE, R. & GUISÁN, J. M. 2001. Stabilization of immobilized enzymes against water-soluble organic cosolvents and generation of hyperhydrophilic micro-environments surrounding enzyme molecules. *Biocatalysis and Biotransformation,* 19**,** 489-503.

ADHAM, S. A., HONRUBIA, P., DÍAZ, M., FERNÁNDEZ-ABALOS, J. M., SANTAMARÍA, R. I. & GIL, J. A. 2002. Expression of the genes coding for the xylanase Xys1 and the cellulase Cel1 from the straw-decomposing *Streptomyces halstedii* JM8 cloned into the amino-acid producer *Brevibacterium lactofermentum* ATCC13869. *Archives of Microbiology,* 177**,** 91-97.

AI, Z., JIANG, Z., LI, L., DENG, W., KUSAKABE, I. & LI, H. 2005. Immobilization of *Streptomyces olivaceoviridis* E-86 xylanase on Eudragit S-100 for xylo-oligosaccharide production. *Process Biochemistry,* 40**,** 2707-2714.

AKPINAR, O., ERDOGAN, K., BAKIR, U. & YILMAZ, L. 2010. Comparison of acid and enzymatic hydrolysis of tobacco stalk xylan for preparation of xylooligosaccharides. *LWT - Food Science and Technology,* 43**,** 119-125.

AKPINAR, O., ERDOGAN, K. & BOSTANCI, S. 2009. Production of xylooligosaccharides by controlled acid hydrolysis of lignocellulosic materials. *Carbohydrate Research,* 344**,** 660-666.

ANNE, J., VRANCKEN, K., VAN MELLAERT, L., VAN IMPE, J. & BERNAERTS, K. 2014. Protein secretion biotechnology in Gram-positive bacteria with special emphasis on *Streptomyces lividans*. *Biochim Biophys Acta,* 1843**,** 1750-61.

ANNÉ, J., VRANCKEN, K., VAN MELLAERT, L., VAN IMPE, J. & BERNAERTS, K. 2014. Protein secretion biotechnology in Gram-positive bacteria with special emphasis on *Streptomyces lividans*. *Biochimica et Biophysica Acta - Molecular Cell Research,* 1843**,** 1750-1761.

ARAGON, C. C., MATEO, C., RUIZ-MATUTE, A. I., CORZO, N., FERNANDEZ-LORENTE, G., SEVILLANO, L., DÍAZ, M., MONTI, R., SANTAMARÍA, R. I. & GUISAN, J. M. 2013a. Production of xylo-oligosaccharides by immobilized-stabilized derivatives of endo-xylanase from *Streptomyces halstedii*. *Process Biochemistry,* 48**,** 478-483.

ARAGON, C. C., SANTOS, A. F., RUIZ-MATUTE, A. I., CORZO, N., GUISAN, J. M., MONTI, R. & MATEO, C. 2013b. Continuous production of xylooligosaccharides in a packed bed reactor with immobilized-stabilized biocatalysts of xylanase from *Aspergillus versicolor*. *Journal of Molecular Catalysis B: Enzymatic,* 98**,** 8-14.

ARMISÉN, P., MATEO, C., CORTÉS, E., BARREDO, J. L., SALTO, F., DIEZ, B., RODÉS, L., GARCÍA, J. L., FERNÁNDEZ-LAFUENTE, R. & GUISÁN, J. M. 1999. Selective adsorption of poly-His tagged glutaryl acylase on tailor-made metal chelate supports. *Journal of Chromatography A,* 848**,** 61-70.

BARBIROLI, A., MARENGO, M., FESSAS, D., RAGG, E., RENZETTI, S., BONOMI, F. & IAMETTI, S. 2017. Stabilization of beta-lactoglobulin by polyols and sugars against temperature-induced denaturation involves diverse and specific structural regions of the protein. *Food Chemistry,* 234**,** 155-162.

BASSO, A., HESSELER, M. & SERBAN, S. 2016. Hydrophobic microenvironment optimization for efficient immobilization of lipases on octadecyl functionalised resins. *Tetrahedron,* 72**,** 7323-7328.

BEG, Q. K. & GUPTA, R. 2003. Purification and characterization of an oxidation-stable, thiol-dependent serine alkaline protease from *Bacillus mojavensis*. *Enzyme and Microbial Technology,* 32**,** 294-304.

BENEŠ, M. J., HORÁK, D. & SVEC, F. 2005. Methacrylate-based chromatographic media. *Journal of Separation Science,* 28**,** 1855-1875.

BETANCOR, L., LOPEZ-GALLEGO, F., HIDALGO, A., ALONSO-MORALES, N., FUENTES, M., FERNANDEZ-LAFUENTE, R. & GUISAN, J. M. 2004. Prevention of interfacial inactivation of enzymes by coating the enzyme surface with dextran-aldehyde. *Journal of Biotechnology,* 110**,** 201-7.

BLANCO, R. M., CALVETE, J. J. & GUISÁN, J. 1989. Immobilization-stabilization of enzymes; variables that control the intensity of the trypsin (amine)-agarose (aldehyde) multipoint attachment. *Enzyme and Microbial Technology,* 11**,** 353-359.

BOLIVAR, J. M., HIDALGO, A., SÁNCHEZ-RUILOBA, L., BERENGUER, J., GUISÁN, J. M. & LÓPEZ-GALLEGO, F. 2011. Modulation of the distribution of small proteins within porous matrixes by smart-control of the immobilization rate. *Journal of Biotechnology,* 155**,** 412-420.

BOLIVAR, J. M., ROCHA-MARTIN, J., MATEO, C., CAVA, F., BERENGUER, J., FERNANDEZ-LAFUENTE, R. & GUISAN, J. M. 2009. Coating of Soluble and Immobilized Enzymes with Ionic Polymers: Full Stabilization of the Quaternary Structure of Multimeric Enzymes. *Biomacromolecules,* 10**,** 742–747.

BOLIVAR, J. M., ROCHA-MARTÍN, J., MATEO, C. & GUISAN, J. M. 2012. Stabilization of a highly active but unstable alcohol dehydrogenase from yeast using immobilization and post-immobilization techniques. *Process Biochemistry,* 47**,** 679-686.

CABRERA, Z., GUTARRA, M. L. E., GUISAN, J. M. & PALOMO, J. M. 2010. Highly enantioselective biocatalysts by coating immobilized lipases with polyethyleneimine. *Catalysis Communications,* 11**,** 964-967.

CAKMAK, U. & SAGLAM ERTUNGA, N. 2017. Gene cloning, expression, immobilization and characterization of endo-xylanase from *Geobacillus* sp. TF16 and investigation of its industrial applications. *Journal of Molecular Catalysis B: Enzymatic,* 133**,** S288 - S298.

CANALS, A., VEGA, M. C., GOMIS-RÜTH, F. X., DÍAZ, M., I.SANTAMARÍA, R. & COLL, M. 2003. Structure of xylanase Xys1D from *Streptomyces halstedii*. *Acta Crystallographica Section D Biological Crystallography,* D59**,** 1447-1453.

CHAUBEY, A., PARSHAD, R., KOUL, S., TANEJA, S. C. & QAZI, G. N. 2006. Enantioselectivity modulation through immobilization of *Arthrobacter* sp. lipase: Kinetic resolution of fluoxetine intermediate. *Journal of Molecular Catalysis B: Enzymatic,* 42**,** 39-44.

CHONG, B. F., HARRISON, M. D. & O'HARA, I. M. 2014. Stability of endoglucanases from mesophilic fungus and thermophilic bacterium in acidified polyols. *Enzyme and Microbial Technology,* 61-62**,** 55-60.

DALL'OGLIO, F., CONTENTE, M. L., CONTI, P., MOLINARI, F., MONFREDI, D., PINTO, A., ROMANO, D., UBIALI, D., TAMBORINI, L. & SERRA, I. 2017. Flow-based stereoselective reduction of ketones using an immobilized ketoreductase/glucose dehydrogenase mixed bed system. *Catalysis Communications,* 93**,** 29-32.

DAMÁSIO, A. R. D. L., SILVA, T. M., ALMEIDA, F. B. D. R., SQUINA, F. M., RIBEIRO, D. A., LEME, A. F. P., SATO, F., PRADE, R. A., JORGE, J. A., TERENZI, H. F. & POLIZELI, M. D. L. T. M. 2011. Heterologous expression of an *Aspergillus niveus* xylanase GH11 in *Aspergillus nidulans* and its characterization and application. *Process Biochemistry,* 46**,** 1236-1242.

DAVIS, M. E. & DAVIS, R. J. 2003. Effects of Transport Limitations on Rates of Solid-Catalyzed Reactions. *In:* CORPORATION, C. (ed.) *Fundamentals of chemical reaction engineering.* New York: McGraw-Hill Higher Education.

DÍAZ, M., RODRIGUEZ, S., FERNÁNDEZ-ABALOS, J. M., DE LAS RIVAS, J., RUIZ-ARRIBAS, A., SHNYROV, V. L. & SANTAMARÍA, R. I. 2004. Single mutations of residues outside the active center of the xylanase Xys1Δ from *Streptomyces halstedii* JM8 affect its activity. *FEMS Microbiology Letters,* 240**,** 237-243.

DODD, D. & CANN, I. K. O. 2009. Enzymatic deconstruction of xylan for biofuel production. *Global change biology. Bioenergy,* 1**,** 2-17.

DORAN, P. M. 1995. 12 - Heterogeneous Reactions. *Bioprocess Engineering Principles.* London: Academic Press.

DRISS, D., HADDAR, A., GHORBEL, R. & CHAABOUNI, S. E. 2014a. Production of xylooligosaccharides by immobilized his-tagged recombinant xylanase from *Penicillium occitanis* on nickel-chelate Eupergit C. *Applied Biochemistry and Biotechnology,* 173**,** 1405-1418.

DRISS, D., ZOUARI-ELLOUZI, S., CHAARI, F., KALLEL, F., GHAZALA, I., BOUAZIZ, F., GHORBEL, R. & CHAABOUNI, S. E. 2014b. Production and in vitro evaluation of xylooligosaccharides generated from corncobs using immobilized *Penicillium occitanis* xylanase. *Journal of Molecular Catalysis B: Enzymatic,* 102**,** 146-153.

ELGHARBI, F., HLIMA, H. B., FARHAT-KHEMAKHEM, A., AYADI-ZOUARI, D., BEJAR, S. & HMIDA-SAYARI, A. 2015. Expression of *A. niger* US368 xylanase in *E. coli*: Purification, characterization and copper activation. *International Journal of Biological Macromolecules,* 74**,** 263-270.

FERNANDEZ-LAFUENTE, R., ROSELL, C. M., CAANAN-HADEN, L., RODES, L. & GUISAN, J. M. 1999. Facile synthesis of artificial enzyme nano-environments via solid-phase chemistry of immobilized derivatives: Dramatic stabilization of penicillin acylase versus organic solvents. *Enzyme and Microbial Technology,* 24**,** 96-103.

FERNÁNDEZ-LORENTE, G., BETANCOR, L., CARRASCOSA, A. V., PALOMO, J. M. & GUISAN, J. M. 2011. Modulation of the Selectivity of Immobilized Lipases by Chemical and Physical Modifications: Release of Omega-3 Fatty Acids from Fish Oil. *Journal of the American Oil Chemists' Society,* 89**,** 97-102.

FERNANDEZ-LORENTE, G., FILICE, M., LOPEZ-VELA, D., PIZARRO, C., WILSON, L., BETANCOR, L., AVILA, Y. & GUISAN, J. M. 2010. Cross-Linking of Lipases Adsorbed on Hydrophobic Supports: Highly Selective Hydrolysis of Fish Oil Catalyzed by RML. *Journal of the American Oil Chemists' Society,* 88**,** 801-807.

GAWANDE, P. V. & KAMAT, M. Y. 1998. Preparation, characterization and application of *Aspergillus* sp. xylanase immobilized on Eudragit S-100. *Journal of Biotechnology,* 66**,** 165-175.

GHORBEL, B., SELLAMI-KAMOUN, A. & NASRI, M. 2003. Stability studies of protease from *Bacillus cereus* BG1. *Enzyme and Microbial Technology,* 32**,** 513-518.

GIANFREDA, L. & SCARFI, M. R. 1991. Enzyme stabilization: state of the art. *Molecular and Cellular Biochemistry,* 100**,** 97-128.

GIBSON, G. R. & ROBERFROID, M. B. 1995. Dietary modulation of the human colonic microbiota: introducing the concept of prebiotics. *The Journal of Nutrition,* 125**,** 1401-1412.

GIBSON, G. R., SCOTT, K. P., RASTALL, R. A., TUOHY, K. M., HOTCHKISS, A., DUBERT-FERRANDON, A., GAREAU, M., MURPHY, E. F., SAULNIER, D., LOH, G., MACFARLANE, S., DELZENNE, N., RINGEL, Y., KOZIANOWSKI, G., DICKMANN, R., LENOIR-WIJNKOOP, I., WALKER, C. & BUDDINGTON, R. 2010. Dietary prebiotics: current status and new definition. *Food Science & Technology Bulletin: Functional Foods,* 7**,** 1-19.

GODOY, C. A., DE LAS RIVAS, B., FILICE, M., FERNÁNDEZ-LORENTE, G., GUISAN, J. M. & PALOMO, J. M. 2010. Enhanced activity of an immobilized lipase promoted by site-directed chemical modification with polymers. *Process Biochemistry,* 45**,** 534-541.

GODOY, C. A., DE LAS RIVAS, B. & GUISÁN, J. M. 2014. Site-directing an intense multipoint covalent attachment (MCA) of mutants of the *Geobacillus thermocatenulatus* lipase 2 (BTL2): Genetic and chemical amination plus immobilization on a tailor-made support. *Process Biochemistry,* 49**,** 1324-1331.

GUISÁN, J. M. 1988. Aldehyde-agarose gels as activated supports for immobilization-stabilization of enzymes. *Enzyme and Microbial Technology,* 10**,** 375-382.

GUISÁN, J. M., POLO, E., AGUADO, J., ROMERO, M. D., ÁLVARO, G. & GUERRA, M. J. 1997. Immobilization-stabilization of thermolysin onto activated agarose gels. *Biocatalysis and Biotransformation,* 15**,** 159-173.

GUISAN, J. M., SABUQUILLO, P., FERNANDEZ-LAFUENTE, R., FERNANDEZ-LORENTE, G., MATEO, C., HALLING, P. J., KENNEDY, D., MIYATA, E. & RE, D. 2001. Preparation of new lipases derivatives with high activity-stability in anhydrous media: Adsorption on hydrophobic supports plus hydrophilization with polyethylenimine. *Journal of Molecular Catalysis - B Enzymatic,* 11**,** 817-824.

GUPTA, M. N. 1991. Thermostabilization of proteins. *Biotechnology and applied biochemistry,* 14**,** 1-11.

GUTARRA, M. L. E., ROMERO, O., ABIAN, O., TORRES, F. A. G., FREIRE, D. M. G., CASTRO, A. M., GUISAN, J. M. & PALOMO, J. M. 2011. Enzyme Surface Glycosylation in the Solid Phase: Improved Activity and Selectivity of *Candida antarctica* Lipase B. *ChemCatChem,* 3**,** 1902-1910.

HAN, X., GAO, J., SHANG, N., HUANG, C. H., KO, T. P., CHEN, C. C., CHAN, H. C., CHENG, Y. S., ZHU, Z., WIEGEL, J., LUO, W., GUO, R. T. & MA, Y. 2013. Structural and functional analyses of catalytic domain of GH10 xylanase from Thermoanaerobacterium saccharolyticum JW/SL-YS485. *Proteins: Structure, Function and Bioinformatics,* 81**,** 1256-1265.

HEINEN, P. R., PEREIRA, M. G., RECHIA, C. G. V., ALMEIDA, P. Z., MONTEIRO, L. M. O., PASIN, T. M., MESSIAS, J. M., CEREIA, M., KADOWAKI, M. K., JORGE, J. A. & POLIZELI, M. L. T. M. 2017. Immobilized endo-xylanase of *Aspergillus tamarii* Kita: an interesting biological tool for production of xylooligosaccharides at high temperatures. *Process Biochemistry,* 53**,** 145-152.

ITABAIANA JR, I., DE MARIZ E MIRANDA, L. S. & DE SOUZA, R. O. M. A. 2013. Towards a continuous flow environment for lipase-catalyzed reactions. *Journal of Molecular Catalysis B: Enzymatic,* 85-86**,** 1-9.

IYER, P. V. & ANANTHANARAYAN, L. 2008. Enzyme stability and stabilization-Aqueous and non-aqueous environment. *Process Biochemistry,* 43**,** 1019-1032.

JIANG, Y., WU, Y. & LI, H. 2015. Immobilization of *Thermomyces lanuginosus* xylanase on aluminum hydroxide particles through adsorption: Characterization of immobilized enzyme. *Journal of Microbiology and Biotechnology,* 25**,** 2016-2023.

JUTURU, V. & WU, J. C. 2012. Microbial xylanases: Engineering, production and industrial applications. *Biotechnology Advances,* 30**,** 1219-1227.

KAPOOR, M. & KUHAD, R. C. 2007. Immobilization of xylanase from *Bacillus pumilus* strain MK001 and its application in production of xylo-oligosaccharides. *Applied Biochemistry and Biotechnology,* 142**,** 125-138.

KATZ, E., THOMPSON, C. J. & HOPWOOD, D. A. 1983. Cloning and expression of tbe tyrosinase gene from *Streptomyces antibioticus* in *Streptomyces lividans*. *Journal of General Microbiology,* 129**,** 2703-2714.

KIESER T, H. D., BIBB JM, CHATER KF, BUTTNER MJ 2000. *Practical Streptomyces genetics,* Norwich, UK, John Innes Foundation.

KLIBANOV, A. M. 1983. Stabilization of Enzymes against Thermal Inactivation. *Advances in Applied Microbiology,* 29**,** 1–28.

KUMAR, A., ATTRI, P. & VENKATESU, P. 2012. Effect of polyols on the native structure of α-chymotrypsin: A comparable study. *Thermochimica Acta,* 536**,** 55-62.

KUMAR, L., NAGAR, S., MITTAL, A., GARG, N. & GUPTA, V. K. 2014. Immobilization of xylanase purified from *Bacillus pumilus* VLK-1 and its application in enrichment of orange and grap juices. *Journal of Food Science and Technology,* 51**,** 1737-1749.

KUMAR, P., GUPTA, A., DHAKATE, S. R., MATHUR, R. B., NAGAR, S. & GUPTA, V. K. 2013. Covalent immobilization of xylanase produced from *Bacillus pumilus* SV-85S on electrospun polymethyl methacrylate nanofiber membrane. *Biotechnology and Applied Biochemistry,* 60**,** 162-169.

KUMAR, S., HAQ, I., PRAKASH, J. & RAJ, A. 2017. Improved enzyme properties upon glutaraldehyde cross-linking of alginate entrapped xylanase from *Bacillus licheniformis*. *International Journal of Biological Macromolecules,* 98**,** 24-33.

KUMAR, V., CHARI, R., SHARMA, V. K. & KALONIA, D. S. 2011. Modulation of the thermodynamic stability of proteins by polyols: Significance of polyol hydrophobicity and impact on the chemical potential of water. *International Journal of Pharmaceutics,* 413**,** 19-28.

LAM, K.-L. & CHI-KEUNG CHEUNG, P. 2013. Non-digestible long chain beta-glucans as novel prebiotics. *Bioactive Carbohydrates and Dietary Fibre,* 2**,** 45-64.

LIU, F. F., JI, L., ZHANG, L., DONG, X. Y. & SUN, Y. 2010. Molecular basis for polyol-induced protein stability revealed by molecular dynamics simulations. *Journal of Chemical Physics,* 132.

LIU, M. Q., DAI, X. J., GUAN, R. F. & XU, X. 2014. Immobilization of Aspergillus niger xylanase A on Fe3O 4-coated chitosan magnetic nanoparticles for xylooligosaccharide preparation. *Catalysis Communications,* 55**,** 6-10.

LIU, M. Q., HUO, W. K., XU, X. & JIN, D. F. 2015. An immobilized bifunctional xylanase on carbon-coated chitosan nanoparticles with a potential application in xylan-rich biomass bioconversion. *Journal of Molecular Catalysis B: Enzymatic,* 120**,** 119-126.

LIU, M. Q., WENG, X. Y., WANG, Q., HUO, W. K. & XU, X. 2017. Recombinant Thermostable *Thermomonospora fusca* TF Endo-xylanase A and Its Immobilization on Modified Mesoporous SiO2 Microspheres for Manufacturing Xylooligosaccharides. *Catalysis Letters,* 147**,** 765-772.

LOZANO, P., COMBES, D. & IBORRA, J. L. 1994. Effect of polyols on α-chymotrypsin thermostability: A mechanistic analysis of the enzyme stabilization. *Journal of Biotechnology,* 35**,** 9-18.

MADON, R. J. & BOUDART, M. 1982. Experimental criterion for the absence of artifacts in the measurement of rates of heterogeneous catalytic reactions. *Industrial & Engineering Chemistry Fundamentals,* 21**,** 438-447.

MANRICH, A., KOMESU, A., ADRIANO, W. S., TARDIOLI, P. W. & GIORDANO, R. L. C. 2010. Immobilization and stabilization of xylanase by multipoint covalent attachment on agarose and on chitosan supports. *Applied Biochemistry and Biotechnology,* 161**,** 455-467.

MARTINEK, K., KLIBANOV, A. M., GOLDMACHER, V. S. & BEREZIN, I. V. 1977. The principles of enzyme stabilization I. Increase in thermostability of enzymes covalently bound to a complementary surface of a polymer support in a multipoint fashion. *BBA - Enzymology,* 485**,** 1-12.

MATEO, C., ABIAN, O., FERNANDEZ-LAFUENTE, R. & GUISAN, J. M. 2000. Reversible Enzyme Immobilization via a Very Strong and Nondistorting Ionic Adsorption on Support–Polyethylenimine Composites. *Biotechnology and Bioengineering,* 68**,** 98-105.

MATEO, C., FERNANDEZ-LORENTE, G., ROCHA-MARTIN, J., BOLIVAR, J. M. & GUISAN, J. M. 2013. Oriented covalent immobilization of enzymes on heterofunctional-glyoxyl supports. *Methods in Molecular Biology.*

MATEO, C., GRAZU, V., PALOMO, J. M., LOPEZ-GALLEGO, F., FERNANDEZ-LAFUENTE, R. & GUISAN, J. M. 2007a. Immobilization of enzymes on heterofunctional epoxy supports. *Nature Protocols,* 2**,** 1022-1033.

MATEO, C., PALOMO, J. M., FERNANDEZ-LORENTE, G., GUISAN, J. M. & FERNANDEZ-LAFUENTE, R. 2007b. Improvement of enzyme activity, stability and selectivity via immobilization techniques. *Enzyme and Microbial Technology,* 40**,** 1451-1463.

MCCLEARY, B. V., MCKIE, V. A., DRAGA, A., ROONEY, E., MANGAN, D. & LARKIN, J. 2015. Hydrolysis of wheat flour arabinoxylan, acid-debranched wheat flour arabinoxylan and arabino-xylo-oligosaccharides by β-xylanase, α-l-arabinofuranosidase and β-xylosidase. *Carbohydrate Research,* 407**,** 79-96.

MILESSI, T. S. S., KOPP, W., ROJAS, M. J., MANRICH, A., BAPTISTA-NETO, A., TARDIOLI, P. W., GIORDANO, R. C., FERNANDEZ-LAFUENTE, R., GUISAN, J. M. & GIORDANO, R. L. C. 2016. Immobilization and stabilization of an endoxylanase from Bacillus subtilis (XynA) for xylooligosaccharides (XOs) production. *Catalysis Today,* 259**,** 130-139.

MILLER, G. L. 1959. Use of dinitrosalicylic acid reagent for determination of reducing sugar. *Analytical Chemistry,* 31**,** 426-428.

MOLINA-ROSELL, C. 1993. *Reacciones de química fina catalizadas por derivados estabilizados de Penicilina G Acilasa.* Doctoral Thesis, Universidad Complutense de Madrid.

MOREIRA, L. R. S. & FILHO, E. X. F. 2016. Insights into the mechanism of enzymatic hydrolysis of xylan. *Applied Microbiology and Biotechnology,* 100**,** 5205-5214.

NETO, W., SCHÜRMANN, M., PANELLA, L., VOGEL, A. & WOODLEY, J. M. 2015. Immobilisation of ω-transaminase for industrial application: Screening and characterisation of

commercial ready to use enzyme carriers. *Journal of Molecular Catalysis B: Enzymatic,* 117**,** 54-61.

NEVELL, T. P. 1963. *Methods in Carbohydrate Chemistry,* New York, Academic Press.

NGUYEN, L. N., HAI, F. I., DOSSETO, A., RICHARDSON, C., PRICE, W. E. & NGHIEM, L. D. 2016. Continuous adsorption and biotransformation of micropollutants by granular activated carbon-bound laccase in a packed-bed enzyme reactor. *Bioresource Technology,* 210**,** 108-116.

NUNES, M. A. P., MARTINS, S., ROSA, M. E., GOIS, P. M. P., FERNANDES, P. C. B. & RIBEIRO, M. H. L. 2015. Improved thermostable polyvinyl alcohol electrospun nanofibers with entangled naringinase used in a novel mini-packed bed reactor. *Bioresource Technology,* 213**,** 208-215.

OTIENO, D. O. & AHRING, B. K. 2012. A thermochemical pretreatment process to produce xylooligosaccharides (XOS), arabinooligosaccharides (AOS) and mannooligosaccharides (MOS) from lignocellulosic biomasses. *Bioresource Technology,* 112**,** 285-292.

PADILLA-MARTINEZ, S. G., MARTINEZ-JOTHAR, L., SAMPEDRO, J. G., TRISTAN, F. & PEREZ, E. 2015. Enhanced thermal stability and pH behavior of glucose oxidase on electrostatic interaction with polyethylenimine. *International Journal of Biological Macromolecules,* 75**,** 453-9.

PALOMO, J. M. 2008. Lipases enantioselectivity alteration by immobilization techniques. *Current Bioactive Compounds,* 4**,** 126-138.

PALOMO, J. M., MUÑOZ, G., FERNÁNDEZ-LORENTE, G., MATEO, C., FUENTES, M., GUISAN, J. M. & FERNÁNDEZ-LAFUENTE, R. 2003. Modulation of *Mucor miehei* lipase properties via directed immobilization on different hetero-functional epoxy resins Hydrolytic resolution of (R,S)-2-butyroyl-2-phenylacetic acid. *Journal of Molecular Catalysis B: Enzymatic* 21**,** 201-210.

PEDROCHE, J., DEL MAR YUST, M., MATEO, C., FERNÁNDEZ-LAFUENTE, R., GIRÓN-CALLE, J., ALAIZ, M., VIOQUE, J., GUISÁN, J. M. & MILLÁN, F. 2007. Effect of the support and experimental conditions in the intensity of the multipoint covalent attachment of proteins on glyoxyl-agarose supports: Correlation between enzyme-support linkages and thermal stability. *Enzyme and Microbial Technology,* 40**,** 1160-1166.

PESSELA, B. C., MATEO, C., FILHO, M., CARRASCOSA, A. V., FERNANDEZ-LAFUENTE, R. & GUISÁN, J. M. 2008. Stabilization of the quaternary structure of a hexameric alpha-galactosidase from *Thermus* sp. T2 by immobilization and post-immobilization techniques. *Process Biochemistry,* 43**,** 193-198.

PINEIRO, M., ASP, N. G., REID, G., MACFARLANE, S., MORELLI, L., BRUNSER, O. & TUOHY, K. 2008. FAO Technical meeting on prebiotics. *Journal of Clinical Gastroenterology,* 42**,** S156-S159.

PLUEN, A., NETTI, P. A., JAIN, R. K. & BERK, D. A. 1999. Diffusion of Macromolecules in Agarose Gels: Comparison of Linear and Globular Configurations. *Biophysical Journal,* 77**,** 542-552.

POLITI, R. & HARRIES, D. 2010. Enthalpically driven peptide stabilization by protective osmolytes. *Chemical Communications,* 46**,** 6449-6451.

ROCHA-MARTIN, J., ACOSTA, A., BERENGUER, J., GUISAN, J. M. & LOPEZ-GALLEGO, F. 2014. Selective oxidation of glycerol to 1,3-dihydroxyacetone by covalently immobilized glycerol dehydrogenases with higher stability and lower product inhibition. *Bioresource Technology,* 170**,** 445-453.

RODRIGUES, R. C., BOLIVAR, J. M., VOLPATO, G., FILICE, M., GODOY, C., FERNANDEZ-LAFUENTE, R. & GUISAN, J. M. 2009. Improved reactivation of immobilized-stabilized lipase from *Thermomyces lanuginosus* by its coating with highly hydrophilic polymers. *Journal of Biotechnology,* 144**,** 113-9.

RODRÍGUEZ, S., SANTAMARÍA, R. I., FERNÁNDEZ-ÁBALOS, J. M. & DÍAZ, M. 2005. Identification of the sequences involved in the glucose-repressed transcription of the *Streptomyces halstedii* JM8 xysA promoter. *Gene,* 351**,** 1-9.

ROMERO, O., GUISÁN, J. M., ILLANES, A. & WILSON, L. 2012. Reactivation of penicillin acylase biocatalysts: Effect of the intensity of enzyme-support attachment and enzyme load. *Journal of Molecular Catalysis B: Enzymatic,* 74**,** 224-229.

SAMANTA, A. K., JAYAPAL, N., JAYARAM, C., ROY, S., KOLTE, A. P., SENANI, S. & SRIDHAR, M. 2015. Xylooligosaccharides as prebiotics from agricultural by-products: Production and applications. *Bioactive Carbohydrates and Dietary Fibre,* 5**,** 62-71.

SAMANTA, A. K., JAYAPAL, N., KOLTE, A. P., SENANI, S., SRIDHAR, M., SURESH, K. P. & SAMPATH, K. T. 2012. Enzymatic production of xylooligosaccharides from alkali solubilized xylan of natural grass (*Sehima nervosum*). *Bioresource Technology,* 112**,** 199-205.

SAMBROOK, J., FRITSCH, E. F. & MANIATIS, T. 1989. *Molecular cloning: a laboratory manual,* Cold Spring Harbor, NY, Cold Spring Harbor Laboratory Press.

SCHMIDT, A., GÜBITZ, G. M. & KRATKY, C. 1999. Xylan binding subsite mapping in the xylanase from *Penicillium simplicissimum* using xylooligosaccharides as cryo-protectant. *Biochemistry,* 38**,** 2403-2412.

SEN, P., NATH, A. & BHATTACHARJEE, C. 2016. Packed-Bed Bioreactor and Its Application in Dairy, Food, and Beverage Industry. *Current Developments in Biotechnology and Bioengineering: Bioprocesses, Bioreactors and Controls.*

SHAARANI, S. M., JAHIM, J. M., RAHMAN, R. A., IDRIS, A., MURAD, A. M. A. & ILLIAS, R. M. 2016. Silanized maghemite for cross-linked enzyme aggregates of recombinant xylanase from *Trichoderma reesei*. *Journal of Molecular Catalysis B: Enzymatic,* 133**,** 65-76.

SINGH, R. D., BANERJEE, J. & ARORA, A. 2015. Prebiotic potential of oligosaccharides: A focus on xylan derived oligosaccharides. *Bioactive Carbohydrates and Dietary Fibre,* 5**,** 19-30.

TACIAS-PASCACIO, V. G., PEIRCE, S., TORRESTIANA-SANCHEZ, B., YATES, M., ROSALES-QUINTERO, A., VIRGEN-ORTÍZ, J. J. & FERNANDEZ-LAFUENTE, R. 2016. Evaluation of

different commercial hydrophobic supports for the immobilization of lipases: Tuning their stability, activity and specificity. *RSC Advances,* 6**,** 100281-100294.

TECHAPUN, C., POOSARAN, N., WATANABE, M. & SASAKI, K. 2003. Thermostable and alkaline-tolerant microbial cellulase-free xylanases produced from agricultural wastes and the properties required for use in pulp bleaching bioprocesses: A review. *Process Biochemistry,* 38**,** 1327-1340.

VELASCO-LOZANO, S., LOPEZ-GALLEGO, F., VAZQUEZ-DUHALT, R., MATEOS-DIAZ, J. C., GUISAN, J. M. & FAVELA-TORRES, E. 2014. Carrier-free immobilization of lipase from *Candida rugosa* with polyethyleneimines by carboxyl-activated cross-linking. *Biomacromolecules,* 15**,** 1896-1903.

WILES, C. & WATTS, P. 2012. Continuous flow reactors: A perspective. *Green Chemistry,* 14**,** 38-54.

YU, H., WU, J. & CHING, C. B. 2004. Enhanced activity and enantioselectivity of *Candida rugosa* lipase immobilized on macroporous adsorptive resins for ibuprofen resolution. *Biotechnology Letters,* 26**,** 629–633.

ZAMBELLI, P., TAMBORINI, L., CAZZAMALLI, S., PINTO, A., ARIOLI, S., BALZARETTI, S., PLOU, F. J., FERNANDEZ-ARROJO, L., MOLINARI, F., CONTI, P. & ROMANO, D. 2016. An efficient continuous flow process for the synthesis of a non-conventional mixture of fructooligosaccharides. *Food Chemistry,* 190**,** 607-613.